Magnesium Based Materials and their Antimicrobial Activity

A DISSERTATION
SUBMITTED TO THE FACULTY OF THE GRADUATE SCHOOL
OF THE UNIVERSITY OF MINNESOTA
BY

Duane Allan Robinson

IN PARTIAL FULFILLMENT OF THE REQUIREMENTS
FOR THE DEGREE OF
DOCTOR OF PHILOSOPHY

Michael G. Conzemius, Advisor

September 2011

Acknowledgements

Looking back at the past 5-6 years it is humbling to think of where I have come and what I have accomplished. What is even more humbling is to think of those that have had faith in me and have helped me get to where I am today. I will do my best to acknowledge you here but to anyone I forget, I apologize and extend to you my heartfelt thanks.

First, I want to thank my advisor, mentor and friend Mike Conzemius. Thank-you for your unwavering support and encouragement, thanks also for believing in me and for giving me the opportunity to complete this work along with a residency. As I move on it feels strange to think that I will not be able to stop by and chat, to go over a case or talk about a project but I am reassured to know you are only a call or email away.

Next, thanks to the members of my Committee: Liz Pluhar, Vicki Wilke and Joanie Bechtold. Your support and guidance, both for this dissertation and my career, have been much appreciated. I hope there will be times in the future where we can work together again.

In completing these projects, there were many without whom I could not have accomplished what I did. Ron Griffith, Linda Zeller and Andrew Waxman were incredibly helpful in figuring out the kinks in the initial steps. Alexa Hart, Anna Tchernatynskaia and Katja Wucherer helped me settle into life in Minnesota and within the college. Barb Wicklund at Excelen, thanks for helping collect bacterial samples. Stacy Meola, Kristina Kiefer, Cory Pinel and Kristin Jacobsen, thanks for your help with the rat project. It was some long and busy days but it was achieved because of your help.

Lisa Hubinger is someone all graduate students within the college come to know and love. She is our biggest cheerleader and is unfaltering in her support and dedication. Without her I do not

know how we would maneuver the red tape or figure out what to do when we miss a deadline. To Lisa, I can never thank you enough for all you do.

Thanks to Michele Martin, my friend and greatest supporter. Perhaps it was fortuitous that we were on a similar journey or perhaps it was just your keen sense of knowing what I needed to hear. Regardless, I can never thank you enough.

To my family, I know it has been a challenge for you to understand what I'm doing and why it seems like I am never going to be done with school. I know it has also been difficult to have me away from home. Thanks for being there, thanks for being supportive and I promise to make it home more often.

Last but not least, thanks to the DVM students, my house officer colleagues and faculty. I quickly became used to the look of disbelief and how many of you thought I was crazy to be taking on both a PhD and Residency but your support and encouragement was also very evident. Whether it was listening to me vent, helping me get away from the hospital to go to class or heading out for a beer I am grateful beyond words.

The rat fracture project was supported in part by the AO North America Resident Research Support Program.

Abstract

The overall goals of this body of work were to characterize the antimicrobial properties of magnesium (Mg) metal and nano-magnesium oxide (nMgO) *in vitro*, to evaluate the *in vitro* cytotoxicity of Mg metal, and to incorporate MgO nanoparticles into a polymeric implant coating and evaluate its *in vitro* antimicrobial properties.

In the course of this work it was found that Mg metal, Mg-mesh, and nMgO have *in vitro* antimicrobial properties that are similar to a bactericidal antibiotic. For Mg metal, the mechanism of this activity appears to be related to an increase in pH (i.e. a more alkaline environment) and not an increase in Mg^{2+}. Given that Mg-mesh is a Mg metal powder, the assumption is that it has the same mechanism of activity as Mg metal. The mechanism of activity for nMgO remains to be elucidated and may be related to a combination of interaction of the nanoparticles with the bacteria and the alkaline pH. It was further demonstrated that supernatants from suspensions of Mg-mesh and nMgO had the same antimicrobial effect as was noted when the particles were used. The supernatant from Mg-mesh and nMgO was also noted to prevent biofilm formation for two *Staphylococcus* strains. Finally, poly-ε-caprolactone (PCL) composites of Mg-mesh (PCL+Mg-mesh) and nMgO (PCL+nMgO) were produced. Coatings applied to screws inhibited growth of *Escherichia coli* and *Pseudomonas aeruginosa* and in thin disc format inhibited the growth of *Staphylococcus aureus* in addition to the *E. coli* and *P. aeruginosa*. Pure Mg metal was noted to have some cytotoxic effect on murine fibroblast and osteoblast cell lines, although this effect needs to be characterized further. To address the need for an *in vivo* model for evaluating implant associated infections, a new closed fracture osteomyelitis model in the femur of the rat was developed.

Magnesium, a readily available and inexpensive metal was shown to have antimicrobial properties that appear to be related to its corrosion products and that nMgO has similar effects. Incorporation of nMgO into a PCL composite was easily achieved and revealed similar, although not identical antimicrobial results. This work has provided a strong foundation and methodology for further evaluation of Mg based materials and their antimicrobial properties.

Table of Contents

List of Tables

List of Figures

Abbreviations

316LSS ..... 316L stainless steel

AFM ..... atomic force microscopy

Al_2O_3 ..... aluminum oxide

ASTM ..... American Society for Testing and Materials

BMP-2 ..... bone morphogenetic protein – 2

CDC ..... Centers for Disease Control and Prevention

CeO_2 ..... cerium oxide

CLSM ..... confocal laser scanning microscopy

CNT ..... carbon nanotubes

CFU ..... colony forming units

CuO ..... copper oxide

EDTA ..... ethylenediaminetetraacetic acid

FBS ..... fetal bovine serum

FDA ..... Food and Drug Administration

HAIs ..... hospital acquired infections

Mg-mesh ..... magnesium metal mesh

$MgCl_2$ ..... magnesium chloride

MgO ..... magnesium oxide

$Mg(OH)_2$ ..... magnesium hydroxide

MH ..... Mueller-Hinton

MTT ..... ((3-(4,5-dimethylthiazol-2-yl)-2,5-diphenyltetrazolium bromide

NaCl ..... sodium chloride

NaOH ..... sodium hydroxide

nMgO ..... nano-magnesium oxide

nZnO ..... nano-zinc oxide

OD ..... optical density

PBS ..... phosphate buffered saline

PCL ..... poly-ε-caprolactone

PE ..... ultrahigh molecular weight polyethylene

PI ..... propidium iodide

PLGA ..... polylactide-co-glycolide

PMMA ..... poly(methyl methacrylate)

ROI ..... region of interest

RPM ..... revolutions per minute

SEM ..... scanning electron microscopy

SSI ..... surgical site infection

TiO_2 ..... titanium oxide

TPLO ..... tibial plateau leveling osteotomy

TSA ..... tryptic soy agar

TSB ..... tryptic soy broth

Chapter 1

Introduction and Literature Review

1.1 Hospital acquired infections

Hospital acquired infections (HAIs) and more specifically, device-associated infections represent a substantial burden to the healthcare industry through increased patient morbidity, mortality and economic consequences. While the reported likelihood is dependent on device design and location (i.e. titanium versus stainless steel and orthopaedic versus cardiovascular) the overall consequences are comparable. A tremendous amount of research is devoted to this problem from the patient, implant and microbial perspective. Although changes in implant design whether through polymeric or metallic coatings, surface modifications or development of biodegradable materials have made significant progress, a definitive solution remains elusive. It seems prudent for any researcher in this field to recognize that although the goal of elimination of device-associated infections is ideal, it is likely unrealistic. Nonetheless, research must continue and a collaborative interdisciplinary approach is essential.

HAIs have become so significant that they are prompting policy reviews by organizations like the Centers for Medicare and Medicaid Services.(1, 2) In this review the Department of Health and Human Services began the task of identifying examples of hospital acquired conditions that could be reasonably "prevented through the application of evidence-based guidelines"(2) with the goal being to reduce the costs incurred by Medicare and Medicaid. It will be interesting to monitor these changes, especially if/when private insurance companies follow suit. In 2009 the Centers for Disease Control and Prevention (CDC) attempted to estimate the annual direct hospital cost of treating HAIs in the United States. To do so, they utilized results from published medical and economic literature and made adjustments to 2007 dollars using two different Consumer Price Index adjustments. The result was a range of $28.4 to $45 billion.(3) Implant associated infections fall under the classification of a surgical site infection (SSI) and are included in the overall HAIs. The CDC classifies an SSI as an infection that occurs in a site where surgery has occurred. They can be superficial or involve deeper tissues or implanted materials.(4) The

incidence varies depending on the time frame and surgical site, but SSIs are thought to represent 14-20% of total HAIs.(1, 5, 6) Economically the impact is quite variable, due in large part to the surgical procedure, length of hospital stay and associated consumables. A more recent trend has been to also consider the impact on utilization of hospital resources in addition to the direct financial costs to the hospital and the payor.(3, 5-9) Dimick *et al.* found that the profit margin for a hospital dropped to 3.4% for patients with surgical complications compared to 23% for surgical patients without complications and that the financial burden of the complication was absorbed by the payor.(8) In a retrospective cohort study Ho *et al.* found that an SSI after kidney transplantation increased the payor outlay by 13% without substantially impacting hospital profits.(7) Finally, Lissovoy *et al.* used hospital stay data from the 2005 Nationwide Inpatient Sample to evaluated SSIs and their impact on hospital utilization and treatment costs. Their analysis found that an SSI increased the mean hospital stay by 9.7-days and increased the mean costs of treatment by $20,842. When extrapolated to the national level the cases of SSIs result in approximately 1-million excess hospitalization days and just below $1.6-billion in additional costs.(6) While there is variation in the overall impact depending on the study design and surgical procedure involved, the overwhelming consistency is that SSIs not only have a significant impact on patient quality of life, they also have a resounding economic impact on hospitals and health-care payors alike.

Even though advances such as improved surgical technique, implant sterilization and infection control protocols have helped decrease the likelihood of implant associated infection, most would argue that bacterial contamination and infection still occur at an unacceptable level. Although there are many factors to consider, major contributors have been the increasing use of implantable medical devices, both temporary and permanent; the growing number of immunocompromised individuals being treated; and the increasing presence of resistant microorganisms.(10, 11) The focus of this discussion will be orthopaedic implants, however, bacterial infections are also an important consideration in many other surgical and medical

procedures where biofilm formation may play a role.(12-15) Examples are dental implants, cardiovascular implants and temporary indwelling devices such as catheters. Catheters, both vascular and urinary, are particularly problematic because they are a major cause of morbidity and mortality with approximately 50% of the cases of nosocomial infections being associated with these indwelling devices.(16)

The development of an infection is multifactorial and has been described in three parts that are referred to as the chain of infection.(11) First is the agent, which, in most SSIs, is a bacterium. Second is transmission, which can be via direct contact, airborne, droplet, a common fomite or a vector. The third is the host and their specific and non-specific responses.(11) A problem with this model is that it does not consider an implanted device. While the goal is to minimize the amount of material implanted, the use of such devices has become essential to the modern healthcare system and thus the role of the implant itself must be considered. When attempting to develop biomaterials aimed at preventing/treating infection, it is essential to understand that the bacterial population of a wound is not static. Instead the complex and dynamic interactions between different species of microorganisms and the physiological changes occurring in the host result in alterations in the population as healing progresses.(17) As with any biological system, the target is ever changing and unfortunately, in this case, the bacteria have a significant advantage.

1.2 Orthopaedic devices

Orthopaedic implants are a striking example of SSIs where implant related infections occur in nearly 112,000 human patients annually and create an estimated $1.8-billion burden to the health care industry.(13) Because there are a variety of orthopaedic devices currently in use it is best to divide them into two broad categories: fracture fixation devices such as plates, pins, screws, and external fixators; and joint prostheses such as in total hip and total knee arthroplasty. This

distinction is important because each of these categories presents unique problems in terms of prevention and treatment of infection. Fracture fixation devices are often used in an emergent situation and as such there is often devitalized tissue present that may or may not have accompanying contaminated wounds, whereas joint arthroplasty is an elective procedure performed under more controlled circumstances. These patient and environmental factors are important because they can help explain the difference in infection rates between these two categories (i.e. 5-10% for fracture fixation versus 1-3% for joint prostheses).(13, 14) The infection rates are important numbers but there are other factors that cannot be ignored. It is obvious from the data that fracture fixation devices are used more commonly and have a higher infection rate, however, an infection in a prosthetic joint will likely have greater clinical significance and is definitely more difficult and expensive to treat.(15)

Unlike fracture fixation devices, components of a joint arthroplasty are implanted as a replacement for a natural joint and removal and/or revision is less than ideal. Another concern is that hip and knee replacements are most often performed in older patients (>65 years of age)(18) that presents a unique set of problems particularly since this group of patients are more likely to have other complicating diseases. With the increasing age of the population the need for total joint arthroplasty, especially of the hip and knee, is projected to increase. In 2005, 209,000 primary (first time) total hip and 450,000 primary total knee arthroplasties were performed in the US and by 2030 the projected numbers are 572,000 and 3,481,000 per year for primary total hip and total knee arthroplasty respectively.(19) When one considers the projected revisions as a result of deep infection, the numbers are even more daunting. In 2005, revisions due to deep infection were 8.4% and 16.8% for total hip and total knee arthroplasties respectively. By 2030 it is projected that the number of revisions due to deep infection will increase to 47.5% and 65.5% for total hip and total knee arthroplasties respectively.(18) Based on these predictions, deep bacterial infections are poised to become the most common cause for total hip and total knee revision arthroplasties, which will not only have a significant economic impact but will also impact

patient well being.(18) The statistics for orthopaedic surgery alone are impressive but become even more so when one considers the recent rise in infections associated with methacillin/oxacillin/vancomycin resistant and/or Gram-negative organisms(20, 21) that respond poorly to traditional therapies. Even though many improvements have helped decrease the likelihood of implant associated osteomyelitis, most would argue that bacterial contamination and infection still occur at an unacceptable level.

SSIs are also an important issue in veterinary medicine where they can result in increased morbidity/mortality, increased client frustration and increased economic burden to the veterinarian or client. That being said there is little published literature that addresses these concerns. Another issue is the lack of a common scheme for classifying SSIs in veterinary patients, a piece of information that is necessary for effective comparisons across studies or institutions. In a review of post-operative infections in orthopaedic patients, Weese suggested using the definitions used by the CDC.(22) Many of the risk factors that have been evaluated on the human side (i.e. patient, infectious agent, surgical technique, concomitant illness) are likely applicable to veterinary patients but in many cases the relative risk is not available.(22) A classification system, similar to that used in humans, that divides surgical wounds into clean, clean-contaminated, contaminated and dirty is used in veterinary surgery and has been evaluated with variable success.(22-25) In general the conclusions were that the classification system may help in predicting the risk of a post-operative infection but the variability within each classification limits the usefulness. In their review in 2008 Weese included data from a number of studies related to the incidence of SSIs in veterinary medicine. The high variability across studies makes it very difficult to compare them but in those that had a variety of cases (i.e. more than one surgical wound classification) the incidence of an SSI was 0.8 to 5.9%.(22) Orthopaedic procedures are frequently performed in veterinary patients and SSI or implant associated infections are not uncommon. One of the most common orthopaedic diseases is a rupture of the anterior cruciate ligament in dogs and one of the most frequent surgeries to treat this disease is the tibial plateau

leveling osteotomy (TPLO). Several studies have evaluated the complications associated with this procedure (including SSI)(26-29) but none have evaluated the economic impact. To address this deficiency a retrospective evaluation of TPLO cases at the Veterinary Medical Center, University of Minnesota from January 1, 2006 until May 3, 2010 was performed. During this time 1,117 TPLO procedures were performed. During the same time period 102 TPLO plates were removed in total, 62 of these because of a clinically apparent or microbiologically confirmed infection. This amounted to a 5.5% infection rate, which is similar to published rates of reoperation and/or infection as a complication.(26, 27) Of perhaps greater interest or importance is the economic aspect of this study. For the 102 TPLO plates removed the average cost to the owner was $1,156.60 (range $320.00 - $3,492.90). In most cases in veterinary medicine there are no insurance companies involved and thus the extra financial burden is borne by the owner. When the initial procedure can cost in excess of $2,500, the financial impact of an SSI is impossible to ignore. Not unlike human medicine, this is an area where many feel there is room for improvement.

1.3 Bacterial Biofilms

Most of the organisms associated with implanted device infections are considered opportunistic pathogens belonging to the *Staphylococcus* genus, however other organisms have been isolated (i.e. *Pseudomonas aeruginosa*, *Enterococcus faecalis*).(10, 30-34) Traumatic wounds are similar in that the predominate bacterial species isolated are coagulase negative *Staphylococcus* spp. (e.g. *Staphylococcus epidermis*)(35, 36), however, resistant Gram-negative organisms (e.g. *Acinetobacter* spp., *Klebsiella pneuomoniae* and *Pseudomonas aeruginosa*) and methicillin resistant *Staphylococcus aureus* have also been isolated.(35-37) When considering device-associated infections it is critical to understand that bacterial-host interactions are complex and multifactorial. Host defense mechanisms (i.e. a competent immune response) are incredibly important in that they are key in prevention of an infection. An excellent illustration of this is the

fact that although colonization of an implant is a prerequisite to infection, not every colonized implant will become infected.(10, 13, 17, 38) Each bacterial organism has specific characteristics that must also be considered. The presence of virulence characteristics (i.e. different adhesins, production of toxins), antimicrobial sensitivity patterns and propensity to form a biofilm are all variables that can determine whether or not an infection develops.(14, 30) Finally, one must realize that a major hurdle in implant associated infections is the diagnostic challenge they present because several criteria must be met before a definitive diagnosis can be made.(13, 39)

Historically, implant related infections have been treated with antimicrobials and/or revision surgery; however this approach is fraught with problems. Most implant related infections have a nosocomial origin with some degree of antimicrobial resistance and are attributable to the presence of biofilms which are more resistant to antimicrobial therapy than their planktonic counterparts.(13, 40, 41) Although the first description was by van Leeuwenhoek when he described “animalcules” in his own dental plaque in the seventeenth century, it was not until 1978 when Costerton *et al.* proposed the concept that has developed into the current theory of bacterial biofilms.(42) “A biofilm is a microbially derived sessile community characterized by cells that are irreversibly attached to a substratum or interface or to each other, are embedded in a matrix of extracellular polymeric substances that they have produced, and exhibit an altered phenotype with respect to growth rate and gene transcription.”(41) In addition, it is widely known that biofilm communities have several documented methods of opposing antimicrobial therapy (e.g. altered growth rate, delayed penetration of the antimicrobial, and variable physiological activity within the biofilm).(13, 40, 41, 43) The development of a biofilm is dependent on several bacterial, substrate and host factors and is a process that initiates with adherence of planktonic organisms.(14, 44) Studies have found that complex molecular pathways and genetic regulation are responsible for biofilm formation.(40, 45, 46) Of paramount consideration in these findings is the importance of quorum sensing and the role of secreted signal molecules (autoinducers).(47, 48) By monitoring the concentration of autoinducers bacteria can monitor inter- and intra-species

population density and alter their genetic expression and phenotypic appearance.(45) These changes in response to population density are critical not only for biofilm formation but are also important in production of many bacterial virulence factors (i.e. exotoxins).

Although the discovery of bacterial biofilms was an important scientific finding representing a survival advantage for the organism, it has become rapidly apparent that the production of a biofilm represents a significant problem in combating device-associated infections.(14, 44, 49)

1.4 Biomaterials

There are several factors that must be considered when attempting to develop the ideal infection resistant implant. Many different bacterial species can cause implant-associated infections and they do not necessarily share the same virulence mechanisms. The environment in which the implant will be placed varies dramatically (i.e. prosthetic cardiac valve compared to an orthopaedic implant) as does the collateral damage to associated tissues, which affects the healing response. The material properties of an implant are important and must also be considered. In particular, the surface properties (i.e. chemistry and topography) are perhaps more important because they play a significant role in the adhesion, or lack thereof, of bacteria and other cellular constituents.(50) These issues demonstrate why research in this field must utilize a multidisciplinary approach.

Topical biomaterials such as wound dressings, hydrogels, dermal graft materials and bandages play a vital role in the treatment of wounds and traumatic injuries and they provide significant benefit, but there remains tremendous room for improvement. One strategy is to utilize surface alterations to prevent contamination/adhesion using different coatings with the goal being to modify the surface such that adhesion is not promoted. For example, an albumin coating on an implant resulted in a greater than 85% rate of inhibition throughout a 20 day *in vitro*

experiment.(51) Similarly, using dynamic force spectroscopy, heparin has been shown to reduce adherence of *Staphylococcus epidermidis* by interfering with the specific binding mechanism between bacterial adhesins and fibronectin.(52) Another approach has involved surface incorporation of antimicrobial agents either directly or dispersed within a coating. Some examples of which are antimicrobial impregnated polymers(53), polymers that degrade into non-steroidal anti-inflammatory drugs(54), non-pathogenic bacteria(55), covalent attachment of hydrophobic polycations (i.e. poly(4-vinyl-*N*-alkylpyridinium bromide))(56) and hydrophilic polymers(57). One final method has focused on modifications to promote the removal of an existing biofilm. Although enzymatic systems have been effective at biofilm removal *in vitro*(58) and various ultrasound treatments have had promising results both *in vitro*(59) and *in vivo*(60) it seems that the results could be organism specific. Carmen *et al.* found that although low-frequency ultrasound for 48 hours virtually eliminated viable *Escherichia coli* it had no significant effect on the viable bacteria in *Pseudomonas aeruginosa* biofilms in an *in vivo* model.(60) Much of the focus has been on modifications to prevent adherence or incorporation of antimicrobial materials thus avoiding the need for implant removal in order to resolve the infection.(13, 40, 41) Thus, the ideal implantable biomaterial would have three important characteristics: (1) it would have a broad spectrum of antibacterial activity in the prevention/treatment of an infection; (2) it would be biocompatible/biostable; and (3) it would not be susceptible to the development of microbial resistance. An additional benefit for permanently implanted devices is that they would be bioabsorbable. Two of the more common areas of focus in this field are polymers(53, 54, 57) and certain metals(61-67). While these approaches have demonstrated some efficacy against particular biofilms, none have realized universal success.

1.5 Polymers

The use of polymers, whether natural or synthetic, provides a unique opportunity to decrease bacterial adhesion to a biomaterial by increasing surface hydrophilicity.(30, 68) The chemical or

physical attachment of poly(ethylene oxide) or poly(ethylene glycol) to surfaces are two examples that have been proposed as a mechanism to create anti-adhesive surfaces. These polymers repel cells and bacteria from the surface by retention of a surrounding hydrous layer.(68) Another reported technique is the incorporation of an antimicrobial substance into a polymeric coating, resulting in a controlled release phenomena.(30, 53, 68) The major advantage of this technique is that it provides antimicrobial effects at the implant site for longer periods and often at higher concentrations than can be achieved with oral or parental administration. Although there has been some success with this process, the selective pressure for antimicrobial resistance created by the prolonged presence of antimicrobial levels that may not be within the therapeutic range is concerning.(30)

Poly(methyl methacrylate) (PMMA) bone cement is commonly used in both orthopaedic and dental applications. Antibiotics are usually added as prophylaxis in total joint arthroplasty and PMMA beads have been used to treat osteomyelitis.(68) PMMA is not a biodegradable polymer thus the antibiotic must elute from the cement and traditionally the release kinetics have been unsatisfactory. As an example, for gentamicin (an aminoglycoside antibiotic), concentrations of the antibiotic were subinhibitory after one day of elution.(69) In another study using gentamicin the elution of the antibiotic decreased the likelihood of biofilm formation, however *Staphylococcus aureus* organisms were still able to grow on the gentamicin-loaded PMMA.(70) The fact that PMMA is not bioabsorbable may be responsible for these inconsistent findings. Polylactide-co-glycolide (PLGA) 80/20 is a bioabsorbable polymer that has been evaluated as an antibiotic carrier. In one study, PLGA alone, PLGA containing ciprofloxacin (a fluoroquinolone antibiotic) and titanium implants were compared in an *in vitro* biofilm model. PLGA with ciprofloxacin was superior to the other materials in terms of preventing biofilm formation and bacterial attachment.(53) The byproducts of polymer biodegradation have also been evaluated for their effects on biofilm formation *in vitro*. In one study, biodegradable salicylate-based poly(anhydride-esters), which are a group of polymers that degrade into the non-steroidal anti-inflammatory drug

salicylic acid, were evaluated.(54) This study found that the adhesion of *Pseudomonas aeruginosa* was inhibited in the short term (47% reduction) and biofilm formation from the same organism was inhibited in the long term when compared to controls.(54) Poly-ε-caprolactone (PCL) is a biodegradable polyester that is degraded under physiologic conditions by hydrolysis of its ester linkages. PCL can also be degraded by microorganisms, which are widely distributed in the environment.(71) Its slow degradation process has lead to development/use in long term implantable devices and in drug delivery systems. It is currently approved by the Food and Drug Administration (FDA) as a component of suture material and other orthopaedic devices (i.e. Artelon® STT spacer).(72)

Nitric oxide (NO) has been identified as a potential antimicrobial agent and is known to play an important role in the cellular immune response.(73, 74) Knowing this, nitric-oxide releasing sol-gels (xerogels) were evaluated *in vitro* as coatings on stainless steel coupons(73) and *in vivo* as coatings on silicone rubber coupons(74). In the *in vitro* study, the NO releasing xerogels reduced adhesion of *Staphylococcus aureus*, *Staphylococcus epidermidis* and *Pseudomonas aeruginosa* organisms compared to bare stainless steel and a xerogel that did not release NO.(73) In the *in vivo* study the number of infected implants was 82% lower with the NO-releasing xerogel coating.(74) The authors suggest that the use of a NO-releasing gel may be a mechanism to augment the normal cellular response which includes NO production.(73, 74) Another group are the poloxamers which are difunctional block copolymer surfactants, are nonionic and bioabsorbable.(75) One particularly interesting property of these polymers is that their sol-gel transition tends to occur just below the normal body temperature.(76, 77) This feature has prompted research into their use as antibiotic carriers in wounds and thermal burns.(76, 78, 79)

The fact that polymers represent a diverse area of biomedical materials makes them ideal candidates in the search for mechanisms to treat and prevent device-associated infections. Although there is tremendous variety in how polymers can be applied to this problem, there

appears to be agreement that bioabsorbable polymers are better than non-absorbable ones, especially where incorporation of an antimicrobial substance is planned.

1.6 Metals

Metals, whether pure or alloyed, play a crucial role in many areas of medicine, although orthopaedics is where they are predominantly used. As a result it is not surprising that they represent a major area of research with respect to device-associated infections. There may be some variability in what characteristics are thought to be important in an ideal metallic implant. However most would agree that good tissue compatibility without allergenic potential and minimal corrosion are of vital importance. Other considerations are minimal bacterial adhesion and adequate tissue adherence.(80) Titanium has increased in use as an orthopaedic implant because of its ability to meet some of these ideal properties. Titanium is also advocated by those who believe that allergenic responses to the components of stainless steel implants increase the susceptibility to bacterial infection.(34) Nonetheless, the ideal metallic implant has yet to be found.

Tantalum is a relatively new orthopaedic implant material, the trabecular formation of which is reportedly advantageous for both soft tissue and osseous attachment.(34) In one study the bacterial adhesion of *Staphylococcus aureus* and *Staphylococcus epidermidis* were compared for pure tantalum, tantalum-coated stainless steel, commercially pure titanium, titanium alloy (Ti-6Al-4V), grit blasted stainless steel and polished stainless steel. Tantalum was associated with lower adhesion of *Staphylococcus aureus* when compared to the other materials and with a similar adhesion of *Staphylococcus epidermidis*.(34) Although tantalum has other clinical benefits, it does not appear to present a clear benefit with respect to prevention of bacterial adhesion. Silver has also been evaluated as a coating in several medical devices and in one *in vivo* model where titanium endoprostheses were coated with silver. This coated device demonstrated a significantly

lower infection rate when compared to the titanium group.(81) The antibacterial activity of silver was first demonstrated in the 19th century and the use of various forms of silver as a topical agent is commonplace.(61) Silver has known biocidal activity against many microorganisms and has been added to many medical devices (i.e. central venous catheters, urinary catheters). The mechanism of action of silver relies on being able to enter the bacterial cell, thus it must be bioavailable in the form of silver ions (Ag^{1+}).(38) Within the cell, the silver ions impair DNA and electron transport functions inhibiting the bacteria's ability to respire and reproduce.(38) Although the use of silver continues to be a viable strategy it has also been shown to have toxic side effects and is especially concerning when used topically as substantial absorption can occur through dermal wounds.(67, 82) When silver is being considered for permanent implantation it is prudent to realize the silver and its corrosion products are not normal components of the human body. They are known to induce giant cell reactions and a chronic inflammatory state resulting from the body attempting to remove them.(67) Copper has also been used for its sanitizing properties for some time and the recognition of its bacteriostatic properties led to its use as a water purifier and in water distribution systems.(83) Not unlike silver, the mechanism of action for copper relies on the ionic form (Cu^{2+}) which has both intra- and extracellular actions.(83) The incorporation of copper fibers into garments, gloves and filters has been advocated as it would potentially provide these materials with biocidal activity.(84) Although the widespread use of copper in water distribution systems may imply relative safety, it does carry the potential for toxicity, especially when used in biomedical applications.

Other modifications to metallic implants have included various coatings or surface modifications. In one study the adhesion of *Staphylococcus aureus* to titanium that had different surface treatments (e.g. unalloyed titanium with gold anodised (TSS), TSS with sodium hyaluronate grafted, chemically polished titanium with gold anodised) aimed at decreasing the coefficient of friction were evaluated.(50) The majority of coatings had no effect on *Staphylococcus aureus* adhesion with the exception of the sodium hyaluronate coating which decreased the density of

bacterial adhesion.(50) With respect to surface modification, one report evaluated the antibacterial activity of zinc oxide by promoting formation of a mixed titanium and zinc oxide surface on a titanium implant.(64) This *in vitro* study demonstrated that zinc modified titanium oxide surfaces reduced the viability of five oral strains of *Streptococcus* organisms.(64)
Metal device-associated infections are particularly problematic because they are often implanted on a permanent basis and infection increases the morbidity and risk of mortality associated with these implants. Total joint arthroplasty, as outlined earlier, is an example where infection has devastating consequences. While bioabsorbable metallic implants are one solution to this problem, application of such devices is currently limited to cardiovascular and other non-load bearing situations.

1.7 Nanoparticles

Nanoparticles and nanomaterials are relative newcomers to the field of biomedical devices. Nanoparticles have generated tremendous scientific interest over many disciplines due in large part to their very high surface area to volume ratio. They also present opportunities for development of unique methodologies to prevent implant colonization via “nano-functionalization” surface techniques(85), and the ability to produce particles of any shape and size contributes to their use as biocides(86). Many metals have been evaluated for antibacterial potential when used on a nanoscale. In some cases these metals are used alone (e.g. silver nanoparticles(87)), as oxides (e.g. ZnO, TiO_2, Al_2O_3, CuO, CeO_2, MgO(86)) and in combination with halogens(85, 88). Although the exact mechanism(s) of observed antimicrobial properties of nanoparticles are largely unknown, studies have shown that nanoparticles are able to attach and penetrate bacterial cells disrupting normal cellular functions.(85) The ability to attach is a property that reportedly stems from the positively charged nanoparticles and their strong interactions with the negatively charged microbial cells.(88, 89) Jones *et al.* demonstrated that a smaller particle size was associated with an increased efficacy. They found that ZnO nanoparticles with a diameter of

8-nm had >95% growth inhibition at a 80-µg/ml concentration compared to 1.2-mg/ml of 50-70-nm particles having 40-50% inhibition.(86) Stiomenov *et al.* used atomic force microscopy (AFM) and transmission electron microscopy to demonstrate that an aerosol prepared MgO nanoparticle adsorbs halogens (chlorine and bromine) and that this nanoparticle mixture disrupts the cell wall of a *Bacillus megaterium* strain and results in an abnormal appearance to the cell wall of an *Escherichia coli* strain.(88) With regards to the metal oxides specifically, some authors believe that their demonstrated antibacterial activities are related to the generation of active oxygen species that are then able to interact with the microbial cells.(90, 91)

In summary, size, surface charge, penetration of cellular membranes and generation of active oxygen species are a few of the proposed mechanisms of antimicrobial activity. As further advances in nanotechnology are made a better understanding of their interaction with microbial and mammalian cells is likely to follow. Until then it is important to remember that nanoparticles in general often behave much differently than their larger counterparts and that this behavior can change with subtle changes in size, shape and surface polarity.(92)

1.8 Summary

Implant associated infections continue to be a significant contributor to patient morbidity and mortality in both elective and emergent procedures. In recent times a more thorough understanding of the pathophysiology of osteomyelitis has lead to changes in surgical techniques, patient preparation and peri-operative protocols. While these changes have helped reduce the incidence of infections, they have not been eliminated. In some cases, the inappropriate use of peri-operative antibiotics for example, one could contend that they have in fact contributed to the development of resistant strains of microbial organisms. Microbial organisms arguably have an adaptive advantage in that they have a short generation time; can exchange genetic information, and therefore resistance genes, with relative ease; and are ubiquitous in the environment. With

this in mind it seems logical that combating microbial infections has, and always will be a medical challenge. In musculoskeletal infections the presence of an implant is often a complicating factor. This is because the implant provides a substrate to which the microbes can attach. Once attached in sufficient numbers biofilm production can occur garnering several protective advantages for the microbes. In some cases, the implant can be removed and although this does increase patient morbidity, the likelihood of elimination of the infection is high. In other cases, the implant function is such that it cannot be removed without significantly affecting patient quality of life (i.e. joint arthroplasty). The final subset of patients are those in which microbial contamination is unavoidable (i.e. traumatic wounds) and the challenge then lies in mitigating the host and microbial factors that predispose to the development of an infection. The success of an anti-fouling device thus relies on a thorough understanding of implant, host/patient and microbial factors that contribute to infection. As research continues in this area it will undoubtedly be necessary to think "outside the box". New biomaterials, the use of nanomaterials, bioabsorbable polymers or other materials are all areas that must be explored. It is equally important to remember that success, if achieved, is unlikely to be long-lived. Thus continued adaptation and new approaches are essential.

1.9 Hypotheses and Specific Aims

The overall goal of this body of work was to characterize the antimicrobial properties of magnesium (Mg) metal and nano-magnesium oxide (nMgO) *in vitro*, to evaluate the *in vitro* cytotoxicity of Mg metal, and to incorporate MgO nanoparticles into a polymeric implant coating and evaluate its *in vitro* antimicrobial properties. In order to facilitate *in vivo* testing, a rat fracture osteomyelitis model was also developed. The long-term goal was to develop a technique that could be commercially applied in the prevention of implant-associated infections and in particular osteomyelitis.

Specific Aim 1: The goals of this aim were three-fold. First, was to characterize the effects of the corrosion products of magnesium on pH and Mg^{2+} concentrations in a microbial culture broth. Second, was to evaluate the effects of the corrosion products on the *in vitro* growth of *Escherichia coli*, *Pseudomonas aeruginosa* and S*taphylococcus aureus*. Lastly, in an effort to identify a mechanism of action for the antibacterial properties of Mg, evaluate the effects of Mg^{2+} alone and pH on bacterial growth.

Hypotheses:

(1) As Mg metal corrodes in culture broth the increase in Mg^{2+} concentration will parallel that of the pH.

(2) When added to the growth media, magnesium corrosion products will inhibit the growth of *Escherichia coli*, *Pseudomonas aeruginosa* and S*taphylococcus aureus*.

(3) The addition of Mg^{2+} alone will not inhibit bacterial growth.

(4) Increasing the alkalinity (i.e. higher pH) will inhibit bacterial growth.

Specific Aim 2: The objective of this aim was to evaluate the cytotoxic effects of pure Mg metal on fibroblast and osteoblast-like cells via an elution test with both an MTT ((3-(4,5-Dimethylthiazol-2-yl)-2,5-diphenyltetrazolium bromide) colorimetric assay and propidium iodide staining flow cytometry viability assay.

Hypothesis: Magnesium metal turnings and their corrosion products will not be toxic to murine fibroblast and osteoblast-like cells.

Specific Aim 3: The goals of this aim were three-fold. First, was to characterize the effects of the addition of nMgO on the pH of a microbial culture broth. Second, was to evaluate the effects of the presence of nMgO on the *in vitro* growth of clinical and laboratory strains of S*taphylococcus aureus*, *Escherichia coli*, *Staphylococcus epidermidis* and *Pseudomonas aeruginosa*. Third, was to evaluate the effect of a supernatant produced from the nanoparticles on *in vitro* bacterial growth and biofilm production.

Hypotheses:

(1) The addition of nMgO to a microbial culture broth will result in an increase in pH (i.e. make it more alkaline) that is similar to that noted when magnesium metal is added. This pH increase will also be greater than that noted with the addition of nZnO.

(2) The addition of nMgO to a culture vial will result in a decrease in the CFU per ml recovered when compared to controls. This effect will be similar across all bacterial strains tested.

(3) The addition of nMgO supernatant to a culture vial will result in a decrease in the CFU per ml recovered when compared to controls. This effect will be similar across all bacterial strains tested.

(4) The addition of nMgO supernatant will result in the prevention of biofilm prevention in an *in vitro* microtiter biofilm model. This effect will be similar across all bacterial strains tested.

Specific Aim 4: The goals of this aim were three-fold. First, was to determine if nMgO and Mg-mesh could be added to a poly-ε-caprolactone (PCL) based polymer. Second, was to determine if this composite could be applied to orthopaedic screws and then evaluate the *in vitro* antimicrobial activity of said coating. Third, was to determine if thin films of the polymer composite could be made and then evaluate the *in vitro* antimicrobial activity of these discs.

Hypotheses:

(1) The addition of nMgO and Mg-mesh to a PCL based polymer will be possible using a chloroform-based emulsion/evaporation process.

(2) The polymer mixture will be applied to orthopaedic screws via a dip-coating process. Once applied to the orthopaedic screws, the nMgO and Mg-mesh coated screws will have less CFU per ml recovered than the uncoated controls.

(3) Thin films will be readily made and the addition of these discs to culture vials will result in a decrease in the CFU per ml recovered when compared to controls.

Specific Aim 5: The objective of this aim was to modify an existing femur fracture model in the rat to one that could be used as a model of osteomyelitis associated with a closed fracture.

Hypothesis: An injection of 10^4 CFU of a clinical isolate of *Staphylococcus aureus*, known to cause osteomyelitis, will result in acute osteomyelitis and impaired fracture healing in a rat femur fracture model.

1.10 Chapter references

2. Eagye KJ, Kim A, Laohavaleeson S, Kuti JL, Nicolau DP. Surgical site infections: does inadequate antibiotic therapy affect patient outcomes? Surg Infect (Larchmt) 2009 Aug;10(4):323-31.
3. Department of Health and Human Services. Medicare Program; Changes to the Hospital Inpatient Prospective Payment Systems and Fiscal Year 2008 Rates. Federal Register 2007 08/22/2007;72(162):47200-18.
4. Scott III RD. The Direct medical costs of Healthcare-Associated Infections in US Hospitals and the Benefits of Prevention. 2009 (http://www.cdc.gov/ncidod/dhqp/pdf/Scott_CostPaper.pdf).
5. Centers for Disease Control and Prevention, National Center for Emerging and Zoonotic Infectious Diseases (NCEZID), Division of Healthcare Quality Promotion (DHQP). Surgical Site Infection (SSI). 2011 (http://www.cdc.gov/HAI/ssi/ssi.html)
6. Sparling KW, Ryckman FC, Schoettker PJ, Byczkowski TL, Helpling A, Mandel K, *et al.* Financial impact of failing to prevent surgical site infections. Qual Manag Health Care 2007 Jul-Sep;16(3):219-25.
7. de Lissovoy G, Fraeman K, Hutchins V, Murphy D, Song D, Vaughn BB. Surgical site infection: incidence and impact on hospital utilization and treatment costs. Am J Infect Control 2009 Jun;37(5):387-97.
8. Ho D, Lynch RJ, Ranney DN, Magar A, Kubus J, Englesbe MJ. Financial impact of surgical site infection after kidney transplantation: implications for quality improvement initiative design. J Am Coll Surg 2010 Jul;211(1):99-104.
9. Dimick JB, Weeks WB, Karia RJ, Das S, Campbell DA Jr. Who pays for poor surgical quality? Building a business case for quality improvement. J Am Coll Surg 2006 Jun;202(6):933-7.
10. Barie PS. No pay for no performance. Surg Infect (Larchmt) 2007 Aug;8(4):421-33.

11. von Eiff C, Arciola CR, Montanaro L, Becker K, Campoccia D. Emerging *Staphylococcus* species as new pathogens in implant infections. Int J Artif Organs 2006 Apr;29(4):360-7.
12. Ostrowsky B. Epidemiology of Healthcare-Assocaited Infections. In: Jarvis WR, editor. Bennett and Brachman's Hosptial Infections. 5th ed. Philadelphia: Wolters Kluwer Health/Lippincott Williams & Wilkins; 2007. p.3.
13. Clutterbuck AL, Cochrane CA, Dolman J, Percival SL. Evaluating antibiotics for use in medicine using a poloxamer biofilm model. Ann Clin Microbiol Antimicrob 2007 Feb 15;6:2.
14. Darouiche RO. Treatment of infections associated with surgical implants. N Engl J Med 2004 Apr 1;350(14):1422-9.
15. Darouiche RO. Device-associated infections: a macroproblem that starts with microadherence. Clin Infect Dis 2001 Nov 1;33(9):1567-72.
16. Darouiche RO. Antimicrobial coating of devices for prevention of infection: principles and protection. Int J Artif Organs 2007 Sep;30(9):820-7.
17. del Pozo JL, Serrera A, Martinez-Cuesta A, Leiva J, Penades J, Lasa I. Biofilm related infections: is there a place for conservative treatment of port-related bloodstream infections? Int J Artif Organs 2006 Apr;29(4):379-86.
18. Ryan TJ. Infection following soft tissue injury: its role in wound healing. Curr Opin Infect Dis 2007 Apr;20(2):124-8.
19. Kurtz SM, Ong KL, Schmier J, Mowat F, Saleh K, Dybvik E, *et al.* Future clinical and economic impact of revision total hip and knee arthroplasty. J Bone Joint Surg Am 2007 Oct;89 Suppl 3:144-51.
20. Kurtz S, Ong K, Lau E, Mowat F, Halpern M. Projections of primary and revision hip and knee arthroplasty in the United States from 2005 to 2030. J Bone Joint Surg Am 2007 Apr;89(4):780-5.
21. Elemam A, Rahimian J, Mandell W. Infection with panresistant *Klebsiella pneumoniae*: a report of 2 cases and a brief review of the literature. Clin Infect Dis 2009 Jul 15;49(2):271-4.

22. Tsioutis C, Kritsotakis EI, Maraki S, Gikas A. Infections by pandrug-resistant gram-negative bacteria: clinical profile, therapeutic management, and outcome in a series of 21 patients. Eur J Clin Microbiol Infect Dis 2010 Mar;29(3):301-5.
23. Weese JS. A review of post-operative infections in veterinary orthopaedic surgery. Vet Comp Orthop Traumatol 2008;21(2):99-105.
24. Vasseur PB, Levy J, Dowd E, Eliot J. Surgical wound infection rates in dogs and cats. Data from a teaching hospital. Vet Surg 1988 Mar-Apr;17(2):60-4.
25. Eugster S, Schawalder P, Gaschen F, Boerlin P. A prospective study of postoperative surgical site infections in dogs and cats. Vet Surg 2004 Sep-Oct;33(5):542-50.
26. Brown DC, Conzemius MG, Shofer F, Swann H. Epidemiologic evaluation of postoperative wound infections in dogs and cats. J Am Vet Med Assoc 1997 May 1;210(9):1302-6.
27. Pacchiana PD, Morris E, Gillings SL, Jessen CR, Lipowitz AJ. Surgical and postoperative complications associated with tibial plateau leveling osteotomy in dogs with cranial cruciate ligament rupture: 397 cases (1998-2001). J Am Vet Med Assoc 2003 Jan 15;222(2):184-93.
28. Priddy NH,2nd, Tomlinson JL, Dodam JR, Hornbostel JE. Complications with and owner assessment of the outcome of tibial plateau leveling osteotomy for treatment of cranial cruciate ligament rupture in dogs: 193 cases (1997-2001). J Am Vet Med Assoc 2003 Jun 15;222(12):1726-32.
29. Stauffer KD, Tuttle TA, Elkins AD, Wehrenberg AP, Character BJ. Complications associated with 696 tibial plateau leveling osteotomies (2001-2003). J Am Anim Hosp Assoc 2006 Jan-Feb;42(1):44-50.
30. Frey TN, Hoelzler MG, Scavelli TD, Fulcher RP, Bastian RP. Risk factors for surgical site infection-inflammation in dogs undergoing surgery for rupture of the cranial cruciate ligament: 902 cases (2005-2006). J Am Vet Med Assoc 2010 Jan 1;236(1):88-94.
31. Arciola CR, Alvi FI, An YH, Campoccia D, Montanaro L. Implant infection and infection resistant materials: a mini review. Int J Artif Organs 2005 Nov;28(11):1119-25.

32. Castelli P, Caronno R, Ferrarese S, Mantovani V, Piffaretti G, Tozzi M, *et al.* New trends in prosthesis infection in cardiovascular surgery. Surg Infect (Larchmt) 2006;7 Suppl 2:S45-7.
33. Mack D, Rohde H, Harris LG, Davies AP, Horstkotte MA, Knobloch JK. Biofilm formation in medical device-related infection. Int J Artif Organs 2006 Apr;29(4):343-59.
34. Isiklar ZU, Darouiche RO, Landon GC, Beck T. Efficacy of antibiotics alone for orthopaedic device related infections. Clin Orthop Relat Res 1996 Nov;(332)(332):184-9.
35. Schildhauer TA, Robie B, Muhr G, Koller M. Bacterial adherence to tantalum versus commonly used orthopedic metallic implant materials. J Orthop Trauma 2006 Jul;20(7):476-84.
36. Murray CK, Roop SA, Hospenthal DR, Dooley DP, Wenner K, Hammock J, *et al.* Bacteriology of war wounds at the time of injury. Mil Med 2006 Sep;171(9):826-9.
37. Yun HC, Murray CK, Roop SA, Hospenthal DR, Gourdine E, Dooley DP. Bacteria recovered from patients admitted to a deployed U.S. military hospital in Baghdad, Iraq. Mil Med 2006 Sep;171(9):821-5.
38. Davis KA, Moran KA, McAllister CK, Gray PJ. Multidrug-resistant *Acinetobacter* extremity infections in soldiers. Emerg Infect Dis 2005 Aug;11(8):1218-24.
39. White RJ, Cutting K, Kingsley A. Topical antimicrobials in the control of wound bioburden. Ostomy Wound Manage 2006 Aug;52(8):26-58.
40. Darouiche RO. Antimicrobial approaches for preventing infections associated with surgical implants. Clin Infect Dis 2003 May 15;36(10):1284-9.
41. Costerton JW, Stewart PS, Greenberg EP. Bacterial biofilms: a common cause of persistent infections. Science 1999 May 21;284(5418):1318-22.
42. Donlan RM, Costerton JW. Biofilms: survival mechanisms of clinically relevant microorganisms. Clin Microbiol Rev 2002 Apr;15(2):167-93.
43. Costerton JW, Geesey GG, Cheng KJ. How bacteria stick. Sci Am 1978 Jan;238(1):86-95.
44. Fux CA, Costerton JW, Stewart PS, Stoodley P. Survival strategies of infectious biofilms. Trends Microbiol 2005 Jan;13(1):34-40.

45. Donlan RM. Biofilms and device-associated infections. Emerg Infect Dis 2001 Mar-Apr;7(2):277-81.
46. Federle MJ, Bassler BL. Interspecies communication in bacteria. J Clin Invest 2003 Nov;112(9):1291-9.
47. Costerton JW, Montanaro L, Arciola CR. Biofilm in implant infections: its production and regulation. Int J Artif Organs 2005 Nov;28(11):1062-8.
48. Reading NC, Sperandio V. Quorum sensing: the many languages of bacteria. FEMS Microbiol Lett 2006 Jan;254(1):1-11.
49. Daniels R, Vanderleyden J, Michiels J. Quorum sensing and swarming migration in bacteria. FEMS Microbiol Rev 2004;28:261-89.
50. Costerton JW. Introduction to biofilm. Int J Antimicrob Agents 1999 May;11(3-4):217,21; discussion 237-9.
51. Harris LG, Richards RG. *Staphylococcus aureus* adhesion to different treated titanium surfaces. J Mater Sci Mater Med 2004 Apr;15(4):311-4.
52. An YH, Stuart GW, McDowell SJ, McDaniel SE, Kang Q, Friedman RJ. Prevention of bacterial adherence to implant surfaces with a crosslinked albumin coating *in vitro*. J Orthop Res 1996 Sep;14(5):846-9.
53. Arciola CR, Bustanji Y, Conti M, Campoccia D, Baldassarri L, Samorì B, *et al.* *Staphylococcus epidermidis*–fibronectin binding and its inhibition by heparin. Biomaterials, 2003 8;24(18):3013-9.
54. Niemela SM, Ikaheimo I, Koskela M, Veiranto M, Suokas E, Tormala P, *et al.* Ciprofloxacin-releasing bioabsorbable polymer is superior to titanium in preventing *Staphylococcus epidermidis* attachment and biofilm formation *in vitro*. J Biomed Mater Res B Appl Biomater 2006 Jan;76(1):8-14.
55. Bryers JD, Jarvis RA, Lebo J, Prudencio A, Kyriakides TR, Uhrich K. Biodegradation of poly(anhydride-esters) into non-steroidal anti-inflammatory drugs and their effect on

Pseudomonas aeruginosa biofilms *in vitro* and on the foreign-body response *in vivo*. Biomaterials 2006 Oct;27(29):5039-48.

56. Curtin JJ, Donlan RM. Using bacteriophages to reduce formation of catheter-associated biofilms by *Staphylococcus epidermidis*. Antimicrob Agents Chemother 2006 Apr;50(4):1268-75.
57. Tiller JC, Liao CJ, Lewis K, Klibanov AM. Designing surfaces that kill bacteria on contact. Proc Natl Acad Sci U S A 2001 May 22;98(11):5981-5.
58. Smith AW. Biofilms and antibiotic therapy: is there a role for combating bacterial resistance by the use of novel drug delivery systems? Adv Drug Deliv Rev 2005 Jul 29;57(10):1539-50.
59. Johansen C, Falholt P, Gram L. Enzymatic removal and disinfection of bacterial biofilms. Appl Environ Microbiol 1997 Sep;63(9):3724-8.
60. Zips A, Schaule G, Flemming HC. Ultrasound as a means of detaching biofilms. Biofouling 1990;2:323-33.
61. Carmen JC, Roeder BL, Nelson JL, Robison Ogilvie RL, Robison RA, Schaalje GB, *et al.* Treatment of biofilm infections on implants with low-frequency ultrasound and antibiotics. American Journal of Infection Control, 2005 3;33(2):78-82.
62. Chopra I. The increasing use of silver-based products as antimicrobial agents: a useful development or a cause for concern? J Antimicrob Chemother 2007 Apr;59(4):587-90.
63. Silver S, Phung le T, Silver G. Silver as biocides in burn and wound dressings and bacterial resistance to silver compounds. J Ind Microbiol Biotechnol 2006 Jul;33(7):627-34.
64. Sheng J, Nguyen PT, Marquis RE. Multi-target antimicrobial actions of zinc against oral anaerobes. Arch Oral Biol 2005 Aug;50(8):747-57.
65. Petrini P, Arciola CR, Pezzali I, Bozzini S, Montanaro L, Tanzi MC, *et al.* Antibacterial activity of zinc modified titanium oxide surface. Int J Artif Organs 2006 Apr;29(4):434-42.
66. Neel EA, Ahmed I, Pratten J, Nazhat SN, Knowles JC. Characterisation of antibacterial copper releasing degradable phosphate glass fibres. Biomaterials 2005 May;26(15):2247-54.

67. Baena MI, Marquez MC, Matres V, Botella J, Ventosa A. Bactericidal activity of copper and niobium-alloyed austenitic stainless steel. Curr Microbiol 2006 Dec;53(6):491-5.
68. Schierholz JM, Lucas LJ, Rump A, Pulverer G. Efficacy of silver-coated medical devices. J Hosp Infect 1998 Dec;40(4):257-62.
69. Qiu Y, Zhang N, An YH, Wen X. Biomaterial strategies to reduce implant-associated infections. Int J Artif Organs 2007 Sep;30(9):828-41.
70. van de Belt H, Neut D, Schenk W, van Horn JR, van der Mei HC, Busscher HJ. Gentamicin release from polymethylmethacrylate bone cements and *Staphylococcus aureus* biofilm formation. Acta Orthop Scand 2000 Dec;71(6):625-9.
71. van de Belt H, Neut D, Schenk W, van Horn JR, van Der Mei HC, Busscher HJ. *Staphylococcus aureus* biofilm formation on different gentamicin-loaded polymethylmethacrylate bone cements. Biomaterials 2001 Jun;22(12):1607-11.
72. Shimao M. Biodegradation of plastics. Curr Opin Biotechnol 2001 Jun;12(3):242-7.
73. Food and Drug Administration. Search term: polycaprolactone. (http://www.fda.gov/default.htm)
74. Nablo BJ, Rothrock AR, Schoenfisch MH. Nitric oxide-releasing sol-gels as antibacterial coatings for orthopedic implants. Biomaterials 2005 Mar;26(8):917-24.
75. Nablo BJ, Prichard HL, Butler RD, Klitzman B, Schoenfisch MH. Inhibition of implant-associated infections via nitric oxide release. Biomaterials 2005 Dec;26(34):6984-90.
76. Sinha VR, Khosla L. Bioabsorbable polymers for implantable therapeutic systems. Drug Dev Ind Pharm 1998 Dec;24(12):1129-38.
77. Schmolka IR. Artificial skin. I. Preparation and properties of pluronic F-127 gels for treatment of burns. J Biomed Mater Res 1972 Nov;6(6):571-82.
78. Oh SH, Kim JK, Song KS, Noh SM, Ghil SH, Yuk SH, *et al.* Prevention of postsurgical tissue adhesion by anti-inflammatory drug-loaded pluronic mixtures with sol-gel transition behavior. J Biomed Mater Res A 2005 Mar 1;72(3):306-16.

79. Nalbandian RM, Henry RL, Wilks HS. Artificial skin. II. Pluronic F-127 Silver nitrate or silver lactate gel in the treatment of thermal burns. J Biomed Mater Res 1972 Nov;6(6):583-90.
80. Faulkner DM, Sutton ST, Hesford JD, Faulkner BC, Major DA, Hellewell TB, *et al.* A new stable pluronic F68 gel carrier for antibiotics in contaminated wound treatment. Am J Emerg Med 1997 Jan;15(1):20-4.
81. Arens S, Schlegel U, Printzen G, Ziegler WJ, Perren SM, Hansis M. Influence of materials for fixation implants on local infection. An experimental study of steel versus titanium DCP in rabbits. J Bone Joint Surg Br 1996 Jul;78(4):647-51.
82. Gosheger G, Hardes J, Ahrens H, Streitburger A, Buerger H, Erren M, *et al.* Silver-coated megaendoprostheses in a rabbit model--an analysis of the infection rate and toxicological side effects. Biomaterials 2004 Nov;25(24):5547-56.
83. Poon VK, Burd A. *In vitro* cytotoxity of silver: implication for clinical wound care. Burns 2004 Mar;30(2):140-7.
84. Borkow G, Gabbay J. Copper as a biocidal tool. Curr Med Chem 2005;12(18):2163-75.
85. Borkow G, Gabbay J. Putting copper into action: copper-impregnated products with potent biocidal activities. FASEB J 2004 Nov;18(14):1728-30.
86. Lellouche J, Kahana E, Elias S, Gedanken A, Banin E. Antibiofilm activity of nanosized magnesium fluoride. Biomaterials 2009 Oct;30(30):5969-78.
87. Jones N, Ray B, Ranjit KT, Manna AC. Antibacterial activity of ZnO nanoparticle suspensions on a broad spectrum of microorganisms. FEMS Microbiol Lett 2008 Feb;279(1):71-6.
88. Jain J, Arora S, Rajwade JM, Omray P, Khandelwal S, Paknikar KM. Silver nanoparticles in therapeutics: development of an antimicrobial gel formulation for topical use. Mol Pharm 2009 Sep-Oct;6(5):1388-401.
89. Stoimenov PK, Klinger RL, Marchin GL, Klabunde KJ. Metal oxide nanoparticles as bactericidal agents. Langmuir 2002 08/01;18(17):6679-86.
90. Huang L, Li DQ, Lin YJ, Wei M, Evans DG, Duan X. Controllable preparation of nano-MgO and investigation of its bactericidal properties. J Inorg Biochem 2005 May;99(5):986-93.

91. Dong C, Cairney J, Sun Q, Maddan O, He G, Deng Y. Investigation of Mg(OH)2 nanoparticles as an antibacterial agent. J Nanopart Res 2009.
92. Sawai J, Kojima H, Igarashi H, Hashimoto A, Shoji S, Sawaki T, *et al.* Antibacterial characteristics of magnesium oxide powder. World Journal of Microbiology and Biotechnology 2000 03/01;16(2):187-94.
93. Lucas E, Decker S, Khaleel A, Seitz A, Fultz S, Ponce A, *et al.* Nanocrystalline metal oxides as unique chemical reagents/sorbents. Chemistry 2001 Jun 18;7(12):2505-10.

Chapter 2

In vitro antibacterial properties of magnesium metal against *Escherichia coli*, *Pseudomonas aeruginosa* and *Staphylococcus aureus*

This chapter has been published as a single manuscript.

Robinson DA, Griffith RW, Shechtman D, Evans RB, Conzemius MG. *In vitro* antibacterial properties of magnesium metal against *Escherichia coli*, *Pseudomonas aeruginosa* and *Staphylococcus aureus*. Acta Biomater 2010 Oct 7;6(5):1869-77.

Bacterial infections are a costly sequela in any wound. The corrosion properties of 0.15, 0.30, 0.45 and 0.60 g of Mg metal were determined in Mueller–Hinton broth by serially measuring the Mg^{2+} concentrations and pH over 72 hours. In addition, the effect of Mg metal, increased Mg^{2+} concentration and alkaline pH on the *in vitro* growth of *Escherichia coli*, *Pseudomonas aeruginosa* and *Staphylococcus aureus* were evaluated in three separate experiments. The primary outcome measure for culture studies was CFU/ml compared to appropriate positive and/or negative controls. Regardless of the mass of Mg added, there was a predictable increase in pH and Mg^{2+} concentration. The addition of Mg and an increase of pH resulted in antibacterial effects similar to the fluoroquinolone antibiotic; however, a simple increase in Mg^{2+} concentration alone had no effect. The results demonstrate an antibacterial effect of Mg on three common aerobic bacterial organisms, the mechanism of which appears to be an alkaline pH.

2.1 Introduction

Regardless of the source or location, bacterial infections represent significant hurdles in the management of both surgical and traumatic wounds and contribute considerably to increased morbidity and mortality. The continued advancement of the field of medicine has emphasized these problems and underscores why the development of biomaterials that prevent and/or treat infection remains a major unsolved medical problem.(1, 2) The significance of this problem is underscored when one considers that orthopaedic implant-related infections occur in nearly 112,000 human patients annually and create a $2 billion burden for the US healthcare industry.(1) Historically, preventative and therapeutic management of wound-related infections has utilized antimicrobials and adherence to aseptic technique; however, this approach is fraught with problems and has had incomplete success.(3, 4)

Bacterial–host interactions are complex and multifactorial. Although host defense mechanisms (i.e. a competent immune response) are important, the virulence characteristics of the bacterial organisms must also be considered. Together these determine whether an organism is merely a contaminant or is able to establish an infection.(3, 4) When attempting to develop biomaterials aimed at preventing/treating infection, it is prudent to understand that the bacterial population of a wound is not static; instead, the complex and dynamic interactions between different species of microorganisms and the physiological changes occurring in the host result in alterations in the population as healing progresses.(3) Thus, some important characteristics of a bioabsorbable anti-fouling device are: (i) it should have a broad spectrum of antibacterial activity in the prevention/treatment of an infection; (ii) it should be nontoxic to the host; and (iii) it should not be susceptible to the development of microbial resistance.

Current biomaterial research in the area of device-associated infection has focused on many diverse areas including polymers(5-7) and metals(8-13). Thus the concept of a metal possessing

antibacterial properties is not new. The antibacterial activity of silver was first demonstrated in the 19th century and the use of various forms of silver as a topical agent is commonplace.(8) Silver has also been evaluated as an antimicrobial coating on both orthopaedic and vascular devices with some success.(9, 14, 15) One significant problem with the use of silver is that it is nonessential to the host and can be toxic.(9, 16, 17) Zinc(10, 11, 18) and copper(12, 13) have reported antibacterial activity; however, while considered essential to normal homeostasis, both have the potential for toxic sequelae.

Magnesium (Mg) is (i) an inexpensive and readily available metal; (ii) an abundant cation (Mg^{2+}) in mammals, most of which is in bone; and (iii) essential to many processes in eukaryotic cells.(19-21) Since its first use in orthopaedic surgery in the early part of the 20th century(20), Mg and Mg alloys have been evaluated for both orthopaedic and cardiovascular applications.(20, 22, 23) When one considers the material properties of orthopaedic implants commonly used, none have physical and mechanical properties that closely resemble those of cortical bone, whereas Mg does.(20) Clinical investigations utilizing Mg and Mg^{2+} have included alloys for cardiovascular stenting(22, 24-26), orthopaedic applications(20, 23, 27), and as an oral therapy in treating disorders such as autism(28), attention deficit hyperactivity disorders(29) and multiple sclerosis(30).

The first objective of this study was to characterize the effects of the corrosion products of Mg on pH and Mg^{2+} concentrations in a microbial culture broth. The second objective was to evaluate the effects of the corrosion products on the *in vitro* growth of *Escherichia coli* (Gram-negative), *Pseudomonas aeruginosa* (Gram-negative) and *Staphylococcus aureus* (Gram-positive). Finally, in an effort to identify a mechanism of action for the antibacterial properties of Mg, the effects of Mg^{2+} alone and pH on bacterial growth were evaluated. The hypotheses were: (i) as Mg metal corrodes in culture broth the increase in Mg^{2+} concentration will parallel that of the pH; (ii) when added to the growth media, Mg corrosion products will inhibit the growth of *E. coli*, *P. aeruginosa*

and *S. aureus*; (iii) the addition of Mg^{2+} alone will not inhibit bacterial growth; and (iv) increasing the alkalinity (i.e. higher pH) will inhibit bacterial growth.

2.2 Materials and methods

2.2.1 Magnesium corrosion

To determine the corrosion properties of Mg metal in bacterial growth media 0.15, 0.30, 0.45 and 0.60 g of Mg metal turnings (Fisher Scientific, Fairlawn, NJ, USA) with an approximate surface area of 816, 1728, 2544 and 3300 mm^2, respectively, were placed into 8.0 ml of sterile Mueller–Hinton (MH) broth (Beckton Dickinson Diagnostic Systems, Sparks, MD, USA) in duplicate. The concentration of Mg^{2+} and the pH of the broth were serially measured over a 72-hour period. The Mg^{2+} concentrations were measured using an automated serum chemistry analyzer (Hitachi 912 Automatic Analyzer, Boehringer Mannheim Roche, Indianapolis, IN, USA) and converted to mmol/l. The measurement of Mg in this automated analyzer is accomplished using a reaction with xylidyl blue. Xylidyl blue forms a purple complex with Mg and the concentration of Mg is then measured by the decrease in absorbance. This test principle is based on the methodology published by Mann and Yoe.(31) The pH was measured using a portable pH meter (Horiba Instruments Inc., Irvine, CA, USA).

2.2.2 Test materials

Magnesium turnings (0.30 g) (Fisher Chemical, Pittsburgh, PA, USA) were used as the source of Mg metal and served as an implant test group. 316L stainless steel intramedullary pins (316LSS) (Imex Veterinary Inc, Longview, TX, USA), 25 mm long and 6.4 mm in diameter, were used as an implant-negative control material. All test materials were sterilized prior to use in the experiments.

Enrofloxacin (Baytril Injectable, Bayer Animal Health, Kansas City, KS, USA) was used as a treatment positive control for a bactericidal agent. A final concentration of enrofloxacin of 10 µg/ml was used in the culture vials.

To increase the Mg^{2+} ion concentration $MgCl_2$ salt (1.7 mg/ml) (Fisher Scientific, Fairlawn, NJ, USA) was added to the MH broth in an attempt to achieve a final concentration of 6.58 mmol/l (16.0 mg/dl) prior to sterilization. To evaluate the effect of adding an ionic salt to the culture broth, the same amount of NaCl (1.7 mg/ml) (Fisher Scientific, Fairlawn, NJ, USA) was added prior to sterilization. After sterilization, a sample of each was collected, the pH was measured and the Mg^{2+} concentration determined.

To adjust the pH of the MH broth, 1 N NaOH (Fisher Scientific, Fairlawn, NJ, USA) was added to achieve a pH of 8.0, 9.0 or 10.0. The pH was verified prior to and after sterilization.

Finally, all bacteria were cultured with no additive to serve as a treatment negative control.

2.2.3 Bacterial cultures

The bacterial inoculum consisted of one of the following organisms: *Escherichia coli* (ATCC 25922), *Pseudomonas aeruginosa* (ATCC 27853) (both of which are Gram-negative organisms) and *Staphylococcus aureus* (ATCC 25923) (which is a Gram-positive organism) (American Type Culture Collection, Manassas, VA, USA). These bacterial strains were chosen to represent a spectrum of organisms encountered and because they are used as control strains in quality control susceptibility testing, for media testing and for susceptibility disc testing. Thus they are well-established cultures and strains in the *in vitro* setting. Pure cultures of *E. coli*, *P. aeruginosa* and *S. aureus* were aerobically cultured for 24 hours at 37°C on bovine blood agar plates. Samples of each of the pure cultures were collected and suspended in 10 ml of sterile MH broth. The cultures were incubated in a waterbath at 37°C with agitation for approximately 10 min and

then in a dry incubator at 37°C with agitation at 220 rpm for 1 h. 4.67×10^5, 5.75×10^5 and 1.95×10^5 CFU of *E. coli*, *P. aeruginosa* and *S. aureus*, respectively, were used to inoculate the culture vials.

2.2.4 Incubation of bacteria with test materials

Culture vials were prepared for each experiment as outlined below. After the addition of bacteria, the optical density was monitored using a control culture vial for each organism starting at approximately 90 min post-inoculation. The optical density (OD) at 590 nm was used to monitor bacterial growth and to determine when samples would be collected for analysis. The goal was to start sampling when the OD was approximately 0.2 and continue until it was $\geq$ 0.6. The number of samples collected was dependent on bacterial growth but sampling was performed a minimum of three separate times.

Magnesium turnings

Culture vials were prepared such that each contained 8 ml of sterile MH broth. Mg turnings, 316LSS or antibiotic (10 µg/ml of enrofloxacin) were added to the culture vials. Culture vials with a 316LSS coupon only were used to monitor the sterilization process. The culture vials were incubated aerobically in a waterbath at 37°C with agitation at 220 rpm for 3.0 h after the addition of test materials. At this time the vials were inoculated with bacterial suspension and returned to the incubator.

Addition of Mg^{2+}

Culture vials were prepared such that each contained 8 ml of sterile MH broth, MH + $MgCl_2$ broth or MH + NaCl broth. The culture vials were incubated aerobically at 37°C for 3.0 h prior to inoculation with bacterial suspension.

Adjustment of pH

Culture vials were prepared such that each contained 8.0-ml of sterile MH broth with a pH of 7.4 (control), 8.0, 9.0 or 10.0. When mixed for normal use, the MH broth has a pH of approximately 7.4. For this experiment the broth was mixed as per the manufacturer's instructions and 1 N NaOH was added to increase the broth pH. The culture vials were incubated aerobically at 37°C for 3 hours prior to inoculation with bacterial suspension.

2.2.5 Microtiter dilution and viable bacterial counts (Figure 2.1)

Microtiter dilutions were performed using a modification of a previously described technique.(32, 33) The number of CFU in each tube was determined in quadruplicate by aseptically collecting a sample from each tube at the desired time point. Tenfold dilutions were made (10^{-1} - 10^{-7}) using phosphate-buffered saline in 96-well round-bottomed microtiter plates. 20 µl was collected from each well and streaked across a tryptic soy agar (TSA) (Beckton Dickinson Diagnostic Systems, Sparks, MD, USA) plate in a uniform manner. The plates were incubated aerobically at 37°C for 24 hours, at which time the number of colonies was counted.

2.2.6 Statistical analysis

Dilutions with up to 30 colonies present were used to calculate the median CFU/ml. Summary statistics were calculated and are presented as the median CFU/ml. The error bars in the figures represent the 25^{th} and 75^{th} percentiles. At each time point the distributions of CFU/ml were compared for each pair of groups using the least-significant difference method to protect against Type I error inflation(34), followed by pairwise Wilcoxon rank sums test for nonparametric data. Statistical significance was set at $P < 0.05$.

2.3 Results

2.3.1 Magnesium corrosion

The concentration of Mg^{2+} rapidly increased within the first 3 hours to an average of 6.64 mmol/l (16.14 mg/dl) regardless of the mass of Mg turnings added. At 24, 48 and 72 hours, the average Mg^{2+} concentration was 6.60 mmol/l (16.05 mg/dl), 6.60 mmol/l (16.05 mg/dl) and 6.96 mmol/l (16.91 mg/dl), respectively.(Figure 2.2) The pH of the broth rapidly increased over the first 3 hours to an average of 9.49 regardless of the mass of Mg turnings added and there was no apparent dose response. At 24, 48 and 72 hours the average pH was 9.94, 10.10 and 10.15, respectively.(Figure 2.3)

2.3.2 Incubation of bacteria with magnesium turnings

All three organisms grew as expected under the experimental growth conditions as indicated by the CFU/ml recovered from the control culture vials. At all time points and for all three organisms no CFU were recovered from any of the culture vials where only 316LSS was added. In addition, no CFU were recovered from any culture where enrofloxacin was added. The median CFU/ml recovered from the control culture vials and those with enrofloxacin, 316LSS and Mg turnings at all sampling points are reported in Figure 2.4. There was a statistically significant difference in the CFU/ml recovered across all treatment groups at all time points. When the CFU/ml in the Mg group was compared independently to the control and 316LSS groups, a statistically significant difference was found at all time points for all three organisms (with the exception of *P. aeruginosa* at the first time point). Similarly, there was an overall trend ($P = 0.05\text{-}1.0$) towards no significant difference between the Mg and Enrofloxacin groups or between the 316LSS and control groups.(Figure 2.4)

Overall, the addition of Mg turnings to the culture broth resulted in a lower number of CFU/ml recovered at all time points for *E. coli*, *P. aeruginosa* and *S. aureus* as compared to the stainless steel and control (no additive) groups.

2.3.3 Incubation of bacteria with $MgCl_2$ and NaCl

The pH of the $MgCl_2$ and NaCl solutions after sterilization was 7.35 and 7.43, respectively. The Mg^{2+} concentration of the $MgCl_2$ and NaCl solutions was 5.95 mmol/l (14.45 mg/dl) and 0.16 mmol/l (0.38-mg/dl), respectively. As indicated by the CFU/ml recovered from the control vials, all three organisms grew as expected. The median CFU/ml recovered from the control, $MgCl_2$ and NaCl vials at all sampling points are reported in Figure 2.5. With the exception of the third time point for *E. coli* and the second time point for *S. aureus* there was no statistically significant difference across all three-treatment groups at the various time points. The overall trend was that the increase in Mg^{2+} concentration, via the addition of $MgCl_2$, did not result in an appreciable effect on the CFU/ml for *E. coli*, *P. aeruginosa* or *S. aureus*. Similarly, there was no statistically significant difference between the $MgCl_2$ and NaCl groups for all three bacteria at all time points (with the exception of the second time point for *S. aureus*). In general, the addition of an ionic salt, in the form of NaCl, also did not have a measurable effect on the CFU/ml.(Figure 2.5)

2.3.4 Incubation of bacteria at various pH

The pH of the four MH groups after sterilization was 7.4, 8.0, 9.0 and 10.0, respectively. All three bacteria grew as expected as indicated by the CFU/ml recovered from the pH 7.4 group (considered the control). The median CFU/ml recovered from all four treatment groups at all time points is reported in Figure 2.6. There was a statistically significant difference in the CFU/ml recovered across all treatment groups at all time points. When the CFU/ml from the pH 7.4 group was compared to the pH 9.0 and 10.0 groups there was a statistically significant difference at all time points for all three bacteria.(Figure 2.6) Thus an increase in pH to $\geq$ 9 resulted in a measurable effect on the CFU/ml recovered in this *in vitro* model.

2.4 Discussion

The results of this study have demonstrated two important characteristics of Mg metal. First, when added to bacterial culture media Mg metal corrodes in a predictable fashion, resulting in both an increase in pH and Mg^{2+} concentrations, a finding that supports our first hypothesis. In a pure aqueous environment, Mg undergoes an electrochemical reaction with water, producing hydrogen gas and magnesium hydroxide.(Figure 2.7a) In the presence of an activating anion (i.e. chloride) both magnesium and magnesium hydroxide can react further, producing a magnesium salt.(Figure 2.7b)(20, 35) Almost immediately after placing the Mg in the broth, gas formation could be observed on the surface of the metal, and by the end of the incubation period a precipitate could be observed in the bottom of the vials. While we did not analyze either of these reaction products, the equations in Figure 2.7 would estimate their occurrence. In general, Mg corrodes very quickly in the normal physiologic environment (i.e. high chloride concentration and pH of 7.4-7.6)(20), resulting in a rapid increase in pH and Mg^{2+} concentration. This susceptibility of Mg to rapid corrosion is not surprising and can be predicted in part by its low position in the galvanic series for seawater.(36, 37) The specific corrosion rate of a Mg implant, however, will also depend on the surface area, temperature, anatomical location and composition of the implant.(20, 23, 27) Within the first 24 hours both the pH and Mg^{2+} concentration reached a plateau. Passivity of Mg is believed to occur via formation of a $Mg(OH)_2$ film which is thought to be stable at a pH $\geq$ 11.(23, 35, 36) With this in mind, the plateau observed in pH and Mg^{2+} concentration is also predictable, especially since this was a closed environment. As the pH of the broth increased further corrosion was prevented by stabilization of the protective $Mg(OH)_2$ film. Although many of the contributing factors to Mg corrosion have been described, any Mg biomaterial should be evaluated by *in vivo* testing as predicted corrosion behavior cannot be based on *in vitro* testing alone.(27)

The second characteristic observed was that when added to a closed *in vitro* culture system, Mg metal has an effect on the CFU of both Gram-negative and Gram-positive bacteria recovered that is similar to those of a bactericidal fluoroquinolone antibiotic (enrofloxacin). The hypothesis was that when added to the growth media, Mg corrosion products would inhibit the growth of *E. coli*, *P. aeruginosa* and *S. aureus*. The results reported here do not provide sufficient data to confirm this hypothesis; however, we would suggest that there is adequate data to support an overall trend toward an inhibitory effect of Mg corrosion products on the growth of these three bacteria.

While the antimicrobial properties of other metals have been reported previously(8-18), to the best of our knowledge this is the first publication to describe and evaluate the antimicrobial properties of Mg.

In an attempt to characterize the mechanism responsible for the effect of Mg on bacterial growth, we undertook two additional experiments. In the first we increased the concentration of Mg^{2+} and did not detect a measurable effect, which supports our hypothesis that the addition of Mg^{2+} alone would not inhibit bacterial growth. It is well known that Mg is important in the normal homeostatic mechanisms of eukaryotic cells(20, 21) and was first identified as an essential requirement for growth of *E. coli* in 1968.(38) Since that time the importance of Mg in prokaryotic metabolism and the molecular mechanisms of Mg regulation have been further characterized.(39, 40) Although it has been reported that the Mg^{2+} concentration affects the virulence of *Salmonella typhimurium*(39) and the susceptibility of some Gram-negative and Gram-positive aerobic bacteria to fluoroquinolone antibiotics(41), it does not appear to have an appreciable effect in our planktonic model.

In the second experiment we increased the alkalinity of the culture broth prior to inoculation with the bacteria. We hypothesized that increasing the alkalinity (i.e. higher pH) would inhibit bacterial growth, which is supported by the finding that there was a decrease in CFU/ml recovered when

the pH was $\geq$ 9 for all three organisms. pH and charge gradients are important in prokaryotic physiology in terms of generating a proton motive force that is then used to do useful work.(42) Nonetheless, most organisms have a pH range in which preferential growth occurs and several sophisticated systems operate that can affect both the intra- and extracellular environment.(42) The ability of a biomaterial to produce an alkaline pH as an antibacterial mechanism has been suggested in previous studies.(43-45) In one study the antibacterial effects of a bioactive glass paste was evaluated. The bioactive glass resulted in a pH of 10.8 and loss of bacterial viability by 60 min post-inoculation.(43) In another series of experiments Allan *et al.* exposed a range of oral bacteria to particulate Bioglass®. The presence of the Bioglass® in the culture media resulted in a pH of 10 or greater after 3 hours and a kill rate of 94% or greater for the majority of bacterial evaluated.(44) Finally, Hu *et al*. demonstrated that increasing concentrations of 45S5 Bioglass® resulted in an increase in aqueous pH (pH of 9.8 and 10.3 at 50 and 100 mg/ml of 45S5 Bioglass®, respectively) and accompanying increase in bactericidal percentage against three pathogenic bacterial species (*S. aureus*, *S. epidermidis* and *E. coli*).(45) Given the results of these and the study reported here it would seem plausible that an alkaline pH as generated by a biomaterial could be responsible for the antibacterial effect observed.

Based on the overall results of our study we would suggest that the alkaline pH, and not the increased Mg^{2+} concentration, is responsible for the effect on CFU/ml found in this closed *in vitro* model.

In considering Mg as an implant, one must also address the possibility of Mg toxicity and the issue of biocompatibility. Although toxicity can occur, hypermagnesiumia is rare. The daily requirements for an adult are between 300 and 400 mg/day(46), and unlike other antimicrobial metals, Mg is efficiently managed by the normal mammalian kidney and gastrointestinal tract.(20, 21) Another determinant with respect to Mg toxicity is the rate of corrosion. As discussed above, the mechanism and determinants of Mg corrosion are multifactorial and require *in vivo* evaluation

when being considered for use in an implant.(27) With respect to biocompatibility, some would suggest that the alkaline pH produced by an Mg-based implant would be detrimental to host cells and tissues. While not evaluated in the study presented here, there are a number of both *in vitro* and *in vivo* studies in the literature that contradict this assumption. For example, L. Li *et al*. found that there was no evidence of morphological changes or inhibition of cell growth by alkali-heat-treated Mg on mouse marrow cells(47) and Z. Li *et al*. found that L929 cells demonstrated better growth in extraction media from an Mg–Ca alloy than in the control media.(48) During *in vivo* evaluation of Mg alloys, Witte *et al*. found that when compared to a polymeric implant, a Mg alloy resulted in enhanced bone formation around an implant that had been placed in a guinea-pig femur.(23) Similarly, Zhang *et al*. evaluated an Mg–Zn–Mn alloy that was implanted in the femur of a rat and found that these implants were associated with new bone production.(49) While the data reported here is intriguing it is prudent to remember that this was an *in vitro* model and the performance of Mg in an *in vivo* model is required before any conclusions can be made regarding the behavior in a biological system. The next step would undoubtedly be *in vivo* analysis whereby the buffering capacity of biological systems is addressed.

Bacterial wound infections represent a substantial burden to the healthcare system in terms of financial costs and effects on patient morbidity and mortality.(3) In 2004 the projected number of infections associated with cardiovascular, orthopaedic, neurosurgical, urological and plastic implants was 149,130 cases with average infection rates ranging from 2% to 40%.(1) These numbers are impressive but become even more so when one considers the recent rise in antimicrobial-resistant infections associated with methacillin/oxacillin-resistant organisms that respond poorly to traditional therapies. Our results demonstrate that in this *in vitro* model, Mg, an inexpensive metal, can reduce the growth of three common aerobic bacteria. Given that the mechanism of action of Mg metal is related to changing local pH, we would argue that Mg could represent an antibacterial agent that is not susceptible to the traditional mechanisms of microbial

resistance (i.e. enzymatic inactivation of the antibacterial agent, modification of the antibacterial target, failure to activate the antibiotic).

2.5 Conclusions

In this *in vitro* study Mg metal was shown to have a predictable corrosion reaction and had an activity that was comparable to a fluoroquinolone antibiotic against *E. coli*, *P. aeruginosa* and *S. aureus*. The growth-limiting property of Mg metal described here is not typical of conventional antibacterial agents and we would suggest that these results add to the body of knowledge in support of the use of Mg as a biomaterial.

Figure 2.1: 96 well microtiter plate dilutions to determine the CFU/ml.

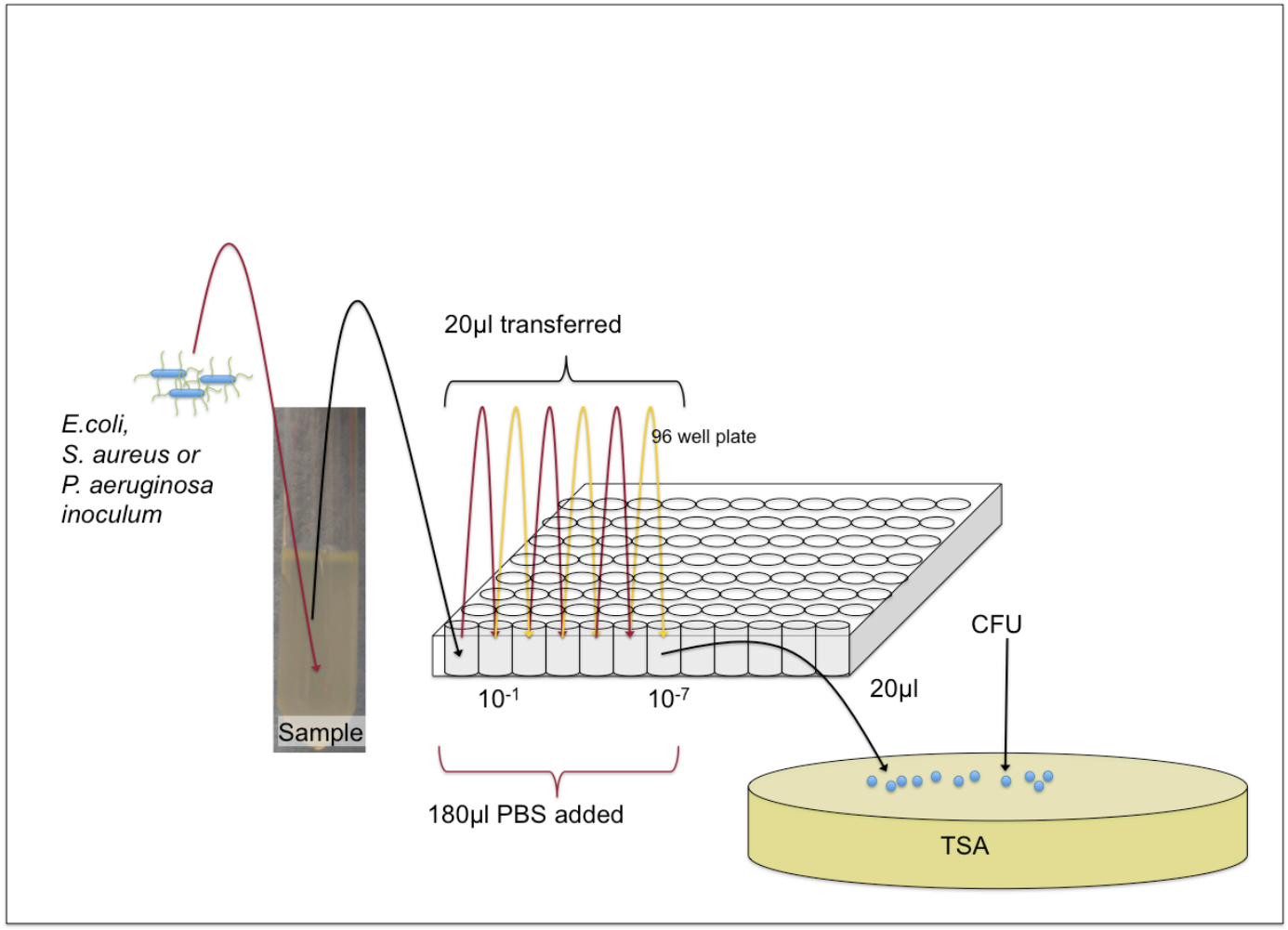

Figure 2.2: Results of pH measurement following the addition of Mg metal turnings to bacterial culture broth.

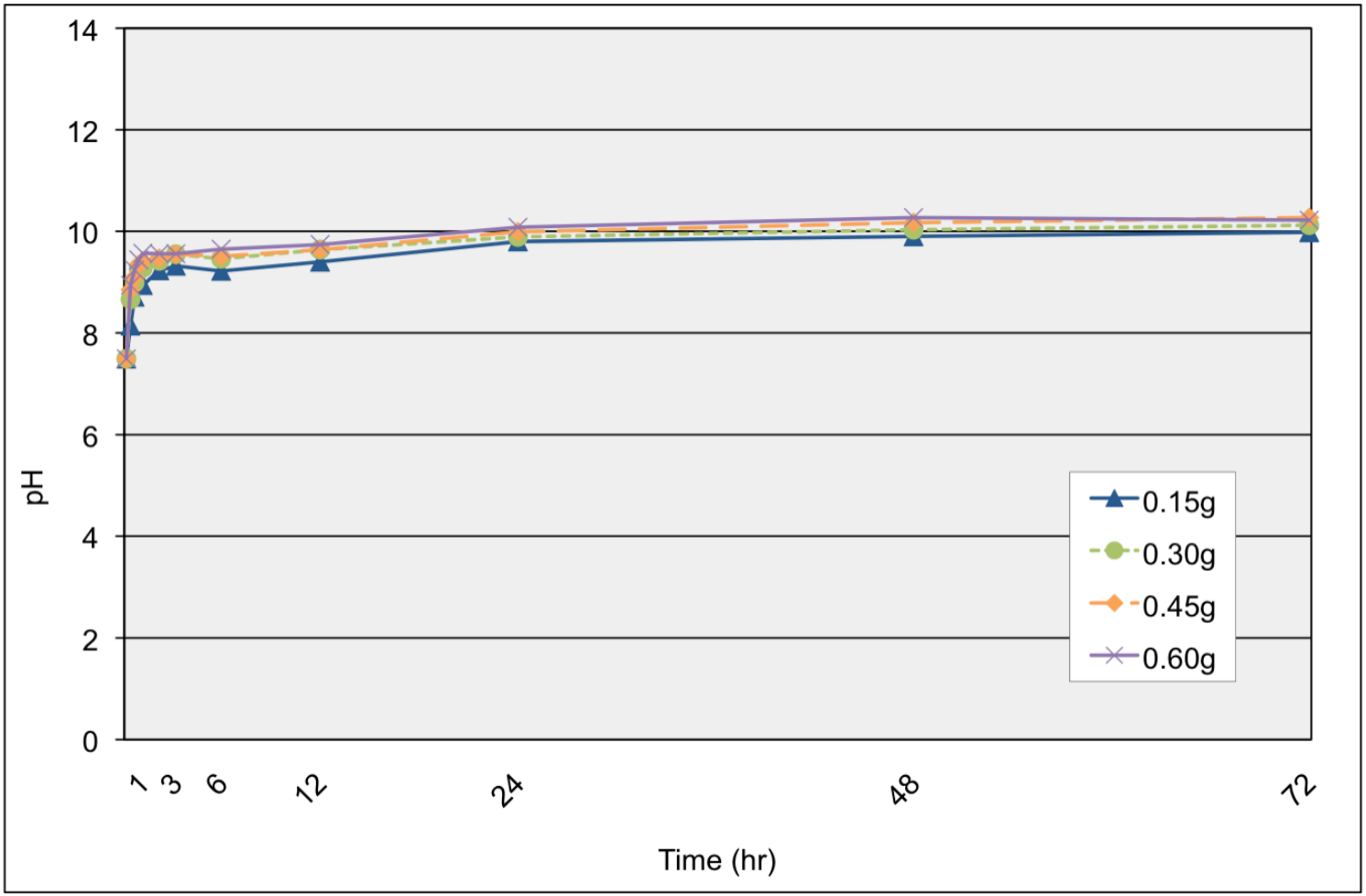

Figure 2.3: Results of Mg^{2+} (mmol/l) measurement following the addition of Mg metal turnings to bacterial culture broth.

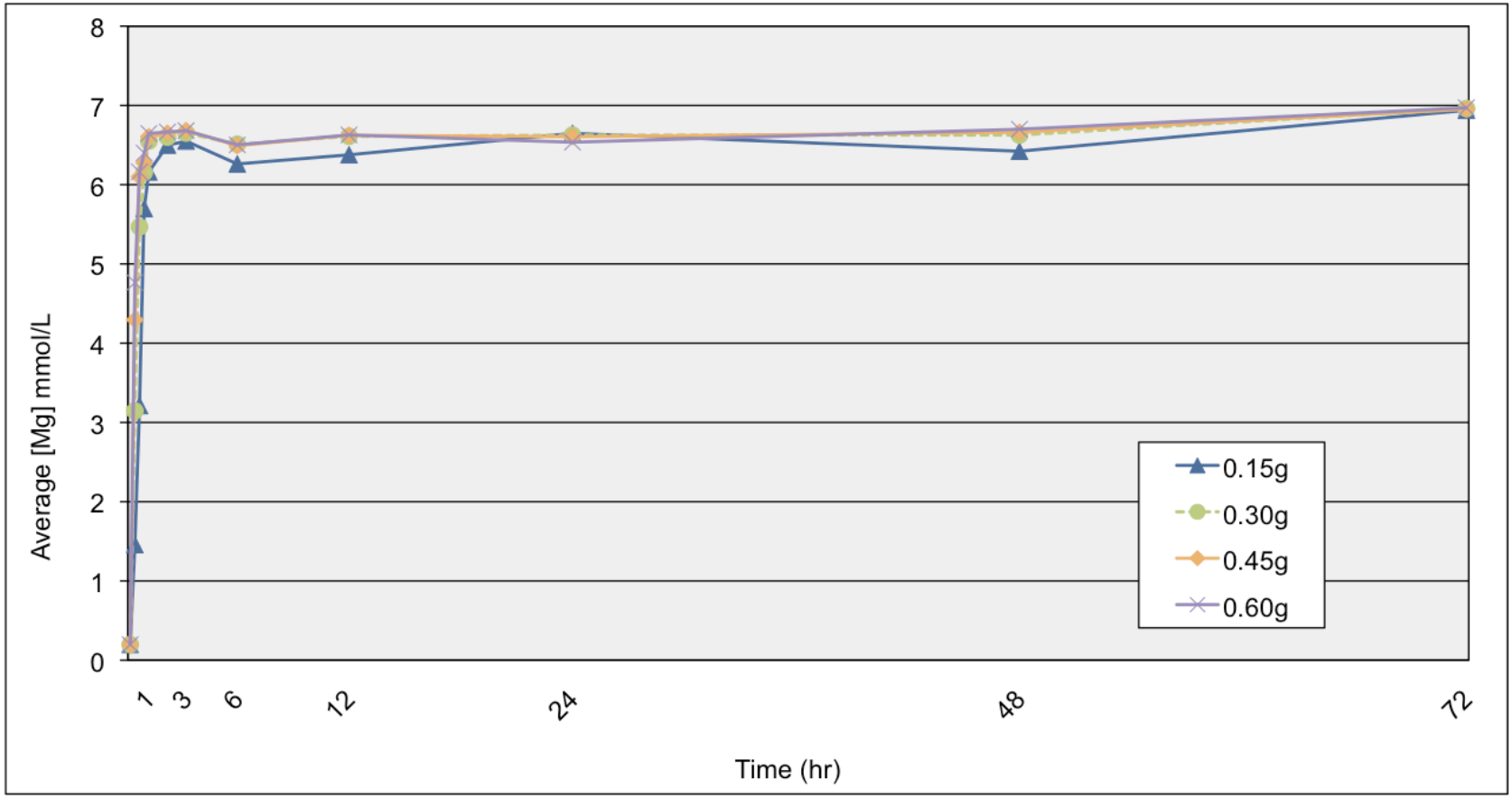

Figure 2.4: Culture plate counts for (a) *Escherichia coli*, (b) *Pseudomonas aeruginosa* and (c) *Staphylococcus aureus* with control, Mg, 316LSS and enrofloxacin treatment groups. Control, no additive; Mg, Mg metal turnings; 316LSS, 316L stainless steel; Enrofloxacin, antibiotic. Data are presented as median CFU/ml with the error bars representing the 25th and 75th percentiles. Columns labeled with the same letter **were not** significantly different (P > 0.05) at the given time point.

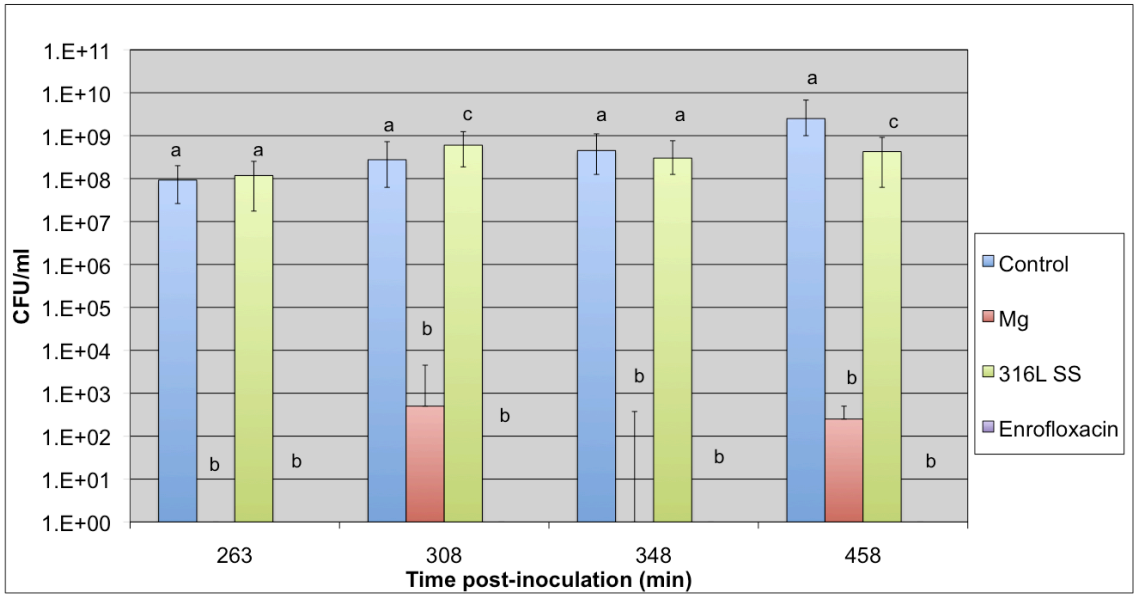

(a) *Escherichia coli*

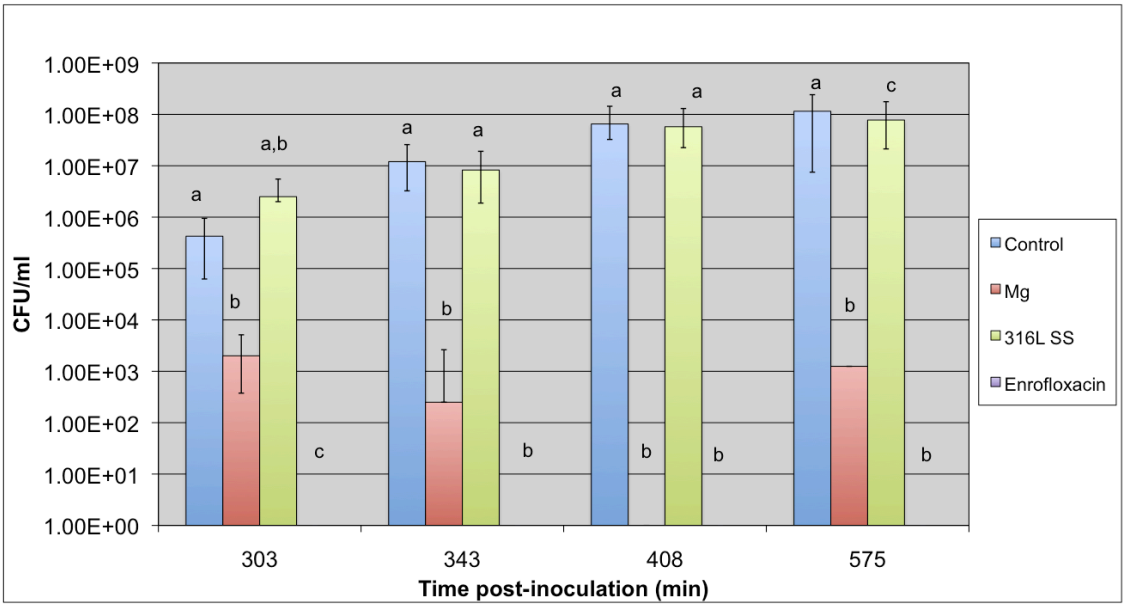

(b) *Pseudomonas aeruginosa*

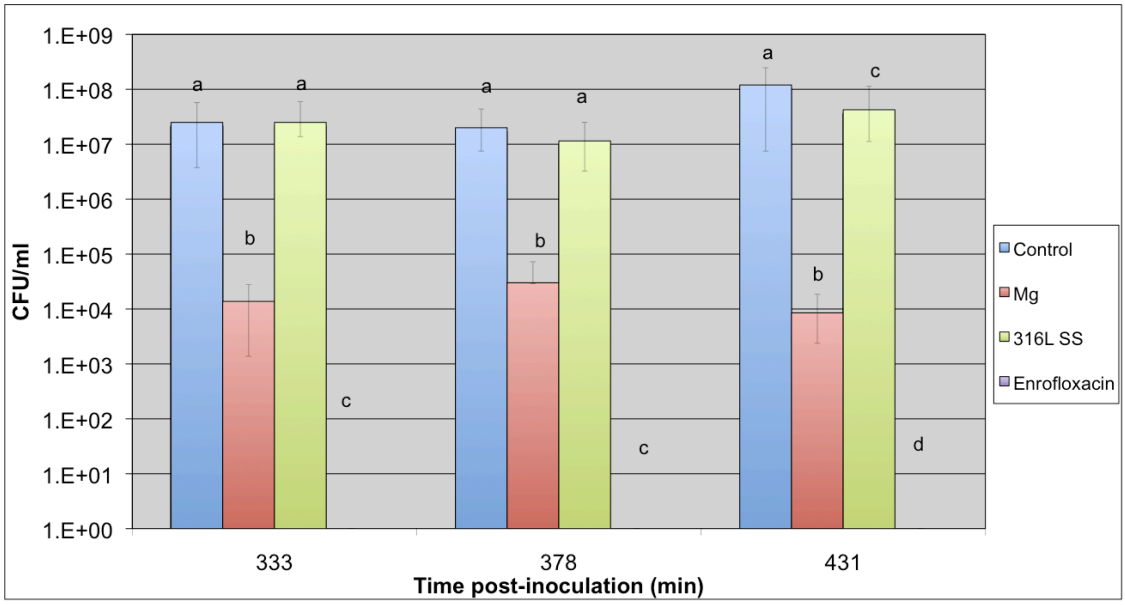

(c) *Staphylococcus aureus*

Figure 2.5: Culture plate counts for (a) *Escherichia coli*, (b) *Pseudomonas aeruginosa* and (c) *Staphylococcus aureus* with control, $MgCl_2$, and NaCl treatment groups. X-axis is the time post inoculation. Data are presented as median CFU/ml with the error bars representing the 25th and 75th percentiles. Columns labeled with the same letter **were** significantly different (P > 0.05) at the given time point.

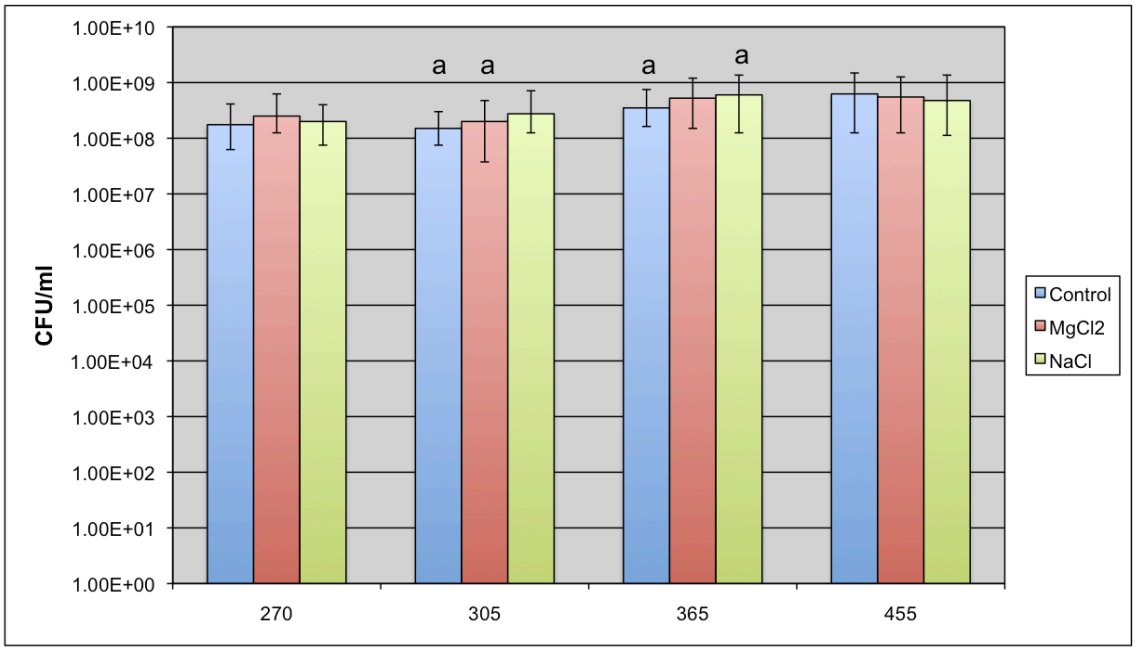

(a) *Escherichia coli*

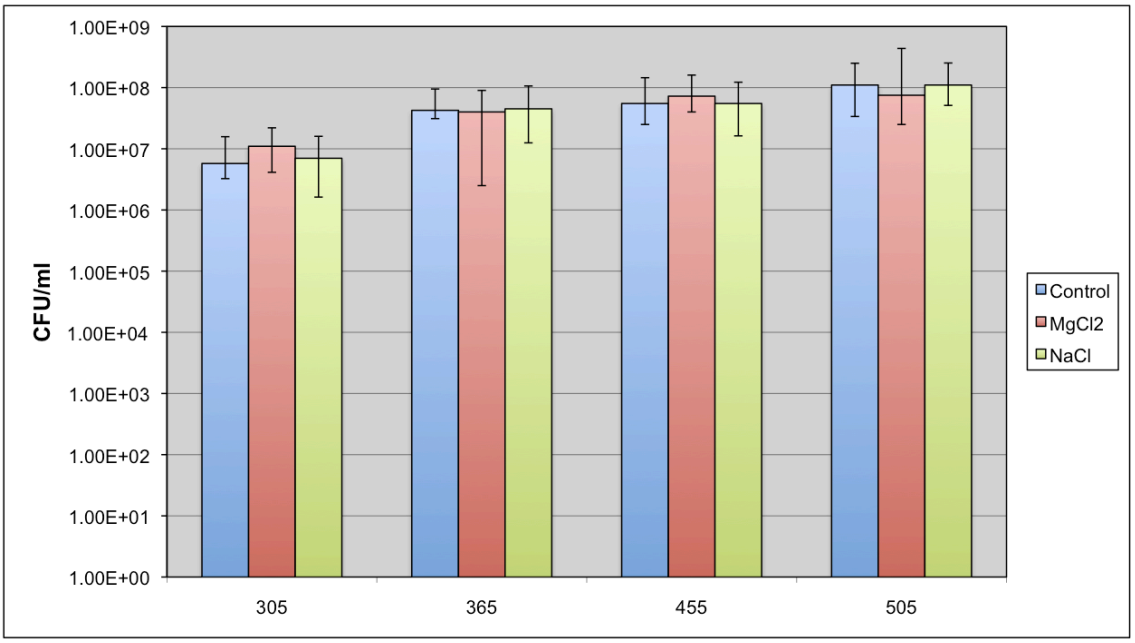

(b) *Pseudomonas aeruginosa*

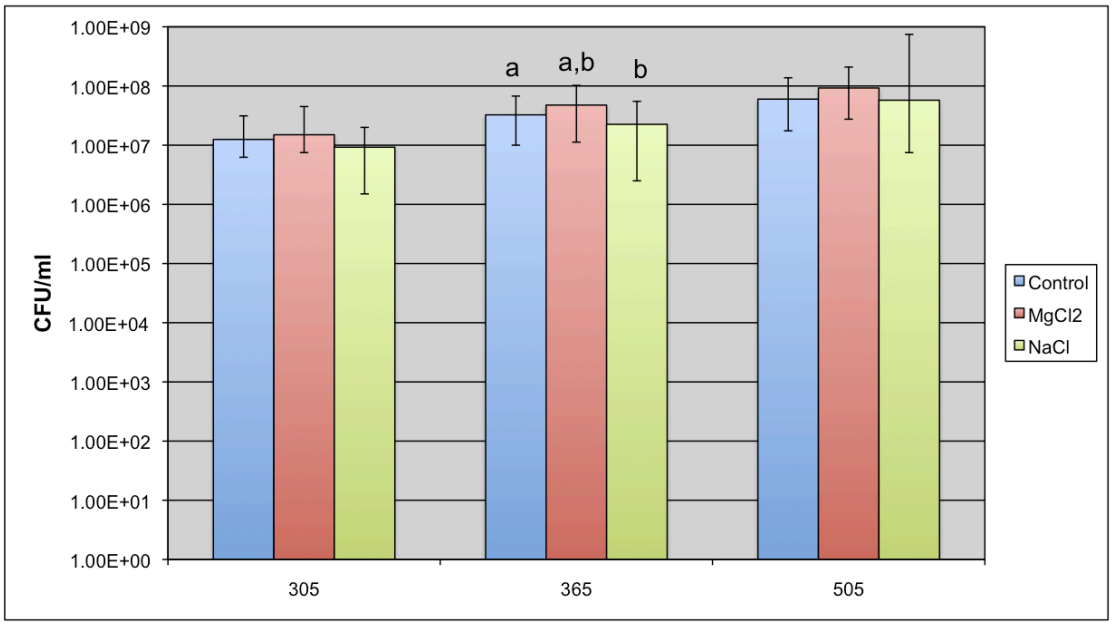

(c) *Staphylococcus aureus*

Figure 2.6: Culture plate counts for (a) *Escherichia coli*, (b) *Pseudomonas aeruginosa* and (c) *Staphylococcus aureus* with pH 7.4 (control), 8, 9 and 10 treatment groups. X-axis is the time post inoculation. Data are presented as median CFU/ml with the error bars representing the 25th and 75th percentiles. Columns labeled with the same letter **were not** significantly different (P > 0.05) at the given time point.

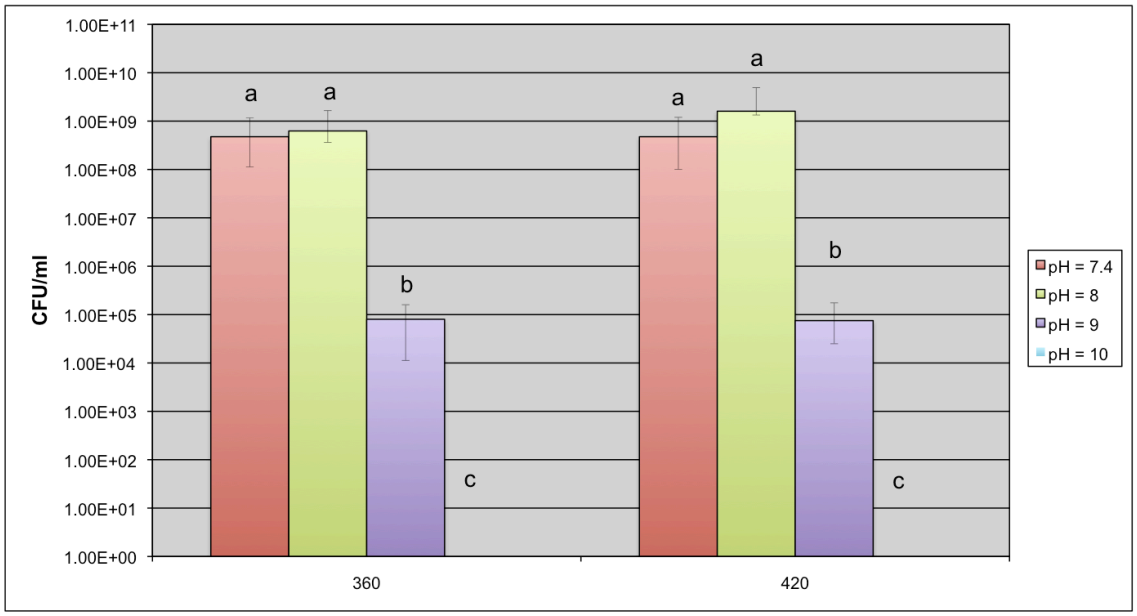

(a) *Escherichia coli*

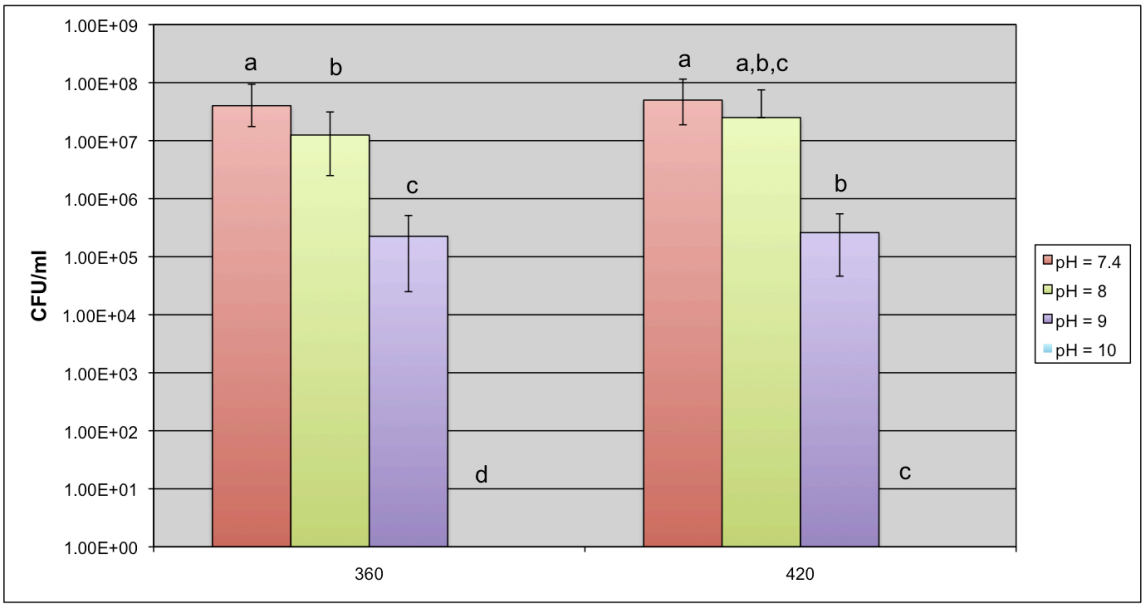

(b) *Pseudomonas aeruginosa*

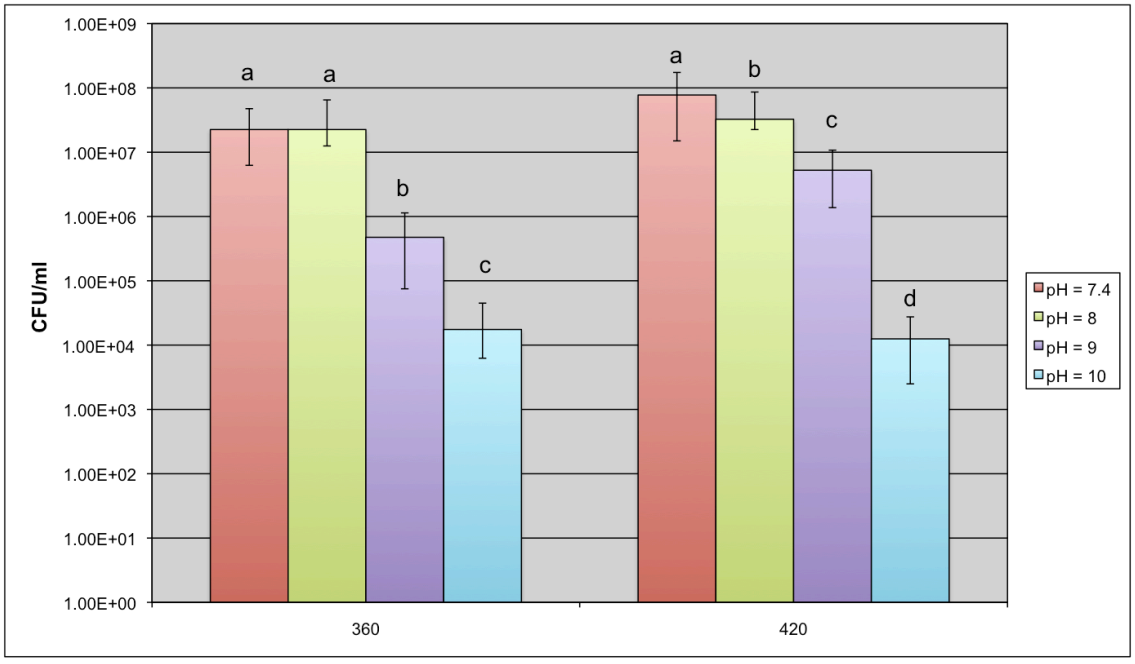

(c) *Staphylococcus aureus*

Figure 2.7: Corrosion reactions for Mg metal (a) in a pure aqueous environment(20, 35) and (b) in the presence of an activating ion (i.e. Cl^-)(20).

(a)	$Mg \rightarrow Mg^{2+} + 2e^-$	(1)
	$2H_2O + 2e^- \rightarrow H_2 + 2(OH^-)$	(2)
(b)	$Mg + 2Cl^- \rightarrow MgCl_2$	(1)

2.6 Chapter references

1. Darouiche RO. Treatment of infections associated with surgical implants. N Engl J Med 2004 Apr 1;350(14):1422-9.
2. Clutterbuck AL, Cochrane CA, Dolman J, Percival SL. Evaluating antibiotics for use in medicine using a poloxamer biofilm model. Ann Clin Microbiol Antimicrob 2007 Feb 15;6:2.
3. Ryan TJ. Infection following soft tissue injury: its role in wound healing. Curr Opin Infect Dis 2007 Apr;20(2):124-8.
4. White RJ, Cutting K, Kingsley A. Topical antimicrobials in the control of wound bioburden. Ostomy Wound Manage 2006 Aug;52(8):26-58.
5. Niemela SM, Ikaheimo I, Koskela M, Veiranto M, Suokas E, Tormala P, et al. Ciprofloxacin-releasing bioabsorbable polymer is superior to titanium in preventing *Staphylococcus epidermidis* attachment and biofilm formation *in vitro*. J Biomed Mater Res B Appl Biomater 2006 Jan;76(1):8-14.
6. Bryers JD, Jarvis RA, Lebo J, Prudencio A, Kyriakides TR, Uhrich K. Biodegradation of poly(anhydride-esters) into non-steroidal anti-inflammatory drugs and their effect on *Pseudomonas aeruginosa* biofilms *in vitro* and on the foreign-body response *in vivo*. Biomaterials 2006 Oct;27(29):5039-48.
7. Smith AW. Biofilms and antibiotic therapy: is there a role for combating bacterial resistance by the use of novel drug delivery systems? Adv Drug Deliv Rev 2005 Jul 29;57(10):1539-50.
8. Chopra I. The increasing use of silver-based products as antimicrobial agents: a useful development or a cause for concern? J Antimicrob Chemother 2007 Apr;59(4):587-90.
9. Silver S, Phung le T, Silver G. Silver as biocides in burn and wound dressings and bacterial resistance to silver compounds. J Ind Microbiol Biotechnol 2006 Jul;33(7):627-34.
10. Sheng J, Nguyen PT, Marquis RE. Multi-target antimicrobial actions of zinc against oral anaerobes. Arch Oral Biol 2005 Aug;50(8):747-57.

11. Petrini P, Arciola CR, Pezzali I, Bozzini S, Montanaro L, Tanzi MC, et al. Antibacterial activity of zinc modified titanium oxide surface. Int J Artif Organs 2006 Apr;29(4):434-42.
12. Neel EA, Ahmed I, Pratten J, Nazhat SN, Knowles JC. Characterisation of antibacterial copper releasing degradable phosphate glass fibres. Biomaterials 2005 May;26(15):2247-54.
13. Baena MI, Marquez MC, Matres V, Botella J, Ventosa A. Bactericidal activity of copper and niobium-alloyed austenitic stainless steel. Curr Microbiol 2006 Dec;53(6):491-5.
14. Gosheger G, Hardes J, Ahrens H, Streitburger A, Buerger H, Erren M, et al. Silver-coated megaendoprostheses in a rabbit model--an analysis of the infection rate and toxicological side effects. Biomaterials 2004 Nov;25(24):5547-56.
15. Ueberrueck T, Zippel R, Tautenhahn J, Gastinger I, Lippert H, Wahlers T. Vascular graft infections: *in vitro* and *in vivo* investigations of a new vascular graft with long-term protection. J Biomed Mater Res B Appl Biomater 2005 Jul;74(1):601-7.
16. Schierholz JM, Lucas LJ, Rump A, Pulverer G. Efficacy of silver-coated medical devices. J Hosp Infect 1998 Dec;40(4):257-62.
17. Poon VK, Burd A. In vitro cytotoxity of silver: implication for clinical wound care. Burns 2004 Mar;30(2):140-7.
18. Cho YH, Lee SJ, Lee JY, Kim SW, Lee CB, Lee WY, et al. Antibacterial effect of intraprostatic zinc injection in a rat model of chronic bacterial prostatitis. Int J Antimicrob Agents 2002 Jun;19(6):576-82.
19. Romani AM, Maguire ME. Hormonal regulation of Mg^{2+} transport and homeostasis in eukaryotic cells. Biometals 2002 Sep;15(3):271-83.
20. Staiger MP, Pietak AM, Huadmai J, Dias G. Magnesium and its alloys as orthopedic biomaterials: a review. Biomaterials 2006 Mar;27(9):1728-34.
21. Saris NL, Mervaala E, Karppanen H, Khawaja JA, Lewenstam A. Magnesium: An update on physiological, clinical and analytical aspects. Clinica Chimica Acta 2000/4;294(1-2):1-26.

22. Waksman R, Pakala R, Kuchulakanti PK, Baffour R, Hellinga D, Seabron R, et al. Safety and efficacy of bioabsorbable magnesium alloy stents in porcine coronary arteries. Catheter Cardiovasc Interv 2006 Oct;68(4):607,17; discussion 618-9.
23. Witte F, Kaese V, Haferkamp H, Switzer E, Meyer-Lindenberg A, Wirth CJ, et al. *In vivo* corrosion of four magnesium alloys and the associated bone response. Biomaterials 2005 Jun;26(17):3557-63.
24. Di Mario C, Griffiths H, Goktekin O, Peeters N, Verbist J, Bosiers M, et al. Drug-eluting bioabsorbable magnesium stent. J Interv Cardiol 2004 Dec;17(6):391-5.
25. Bose D, Eggebrecht H, Erbel R. Absorbable metal stent in human coronary arteries: imaging with intravascular ultrasound. Heart 2006 Jul;92(7):892.
26. Heublein B, Rohde R, Kaese V, Niemeyer M, Hartung W, Haverich A. Biocorrosion of magnesium alloys: a new principle in cardiovascular implant technology? Heart 2003 Jun;89(6):651-6.
27. Witte F, Fischer J, Nellesen J, Crostack HA, Kaese V, Pisch A, et al. *In vitro* and *in vivo* corrosion measurements of magnesium alloys. Biomaterials 2006 Mar;27(7):1013-8.
28. Mousain-Bosc M, Roche M, Polge A, Pradal-Prat D, Rapin J, Bali JP. Improvement of neurobehavioral disorders in children supplemented with magnesium-vitamin B6. II. Pervasive developmental disorder-autism. Magnes Res 2006 Mar;19(1):53-62.
29. Mousain-Bosc M, Roche M, Polge A, Pradal-Prat D, Rapin J, Bali JP. Improvement of neurobehavioral disorders in children supplemented with magnesium-vitamin B6. I. Attention deficit hyperactivity disorders. Magnes Res 2006 Mar;19(1):46-52.
30. Rossier P, van Erven S, Wade DT. The effect of magnesium oral therapy on spasticity in a patient with multiple sclerosis. Eur J Neurol 2000 Nov;7(6):741-4.
31. Mann CK, Yoe JH. Spectrophotometric determination of magnesium with sodium-1-azo-2-hydroxy-3-(2,4-dimethylcarboxanilido)-naphthalene-10 -(2- hydroxybenzene-5-sulfonate). Anal Chem 1956;28:202–5.

32. Cutler SA, Rasmussen MA, Hensley MJ, Wilhelms KW, Griffith RW, Scanes CG. Effects of *Lactobacilli* and lactose on *Salmonella typhimurium* colonisation and microbial fermentation in the crop of the young turkey. Br Poult Sci 2005 Dec;46(6):708-16.
33. Johannsen SA, Griffith RW, Wesley IV, Scanes CG. *Salmonella enterica* serovar *typhimurium* colonization of the crop in the domestic turkey: influence of probiotic and prebiotic treatment (*Lactobacillus acidophilus* and lactose). Avian Dis 2004 Apr-Jun;48(2):279-86.
34. Ramsey F, Schafer DF. The Statistical Sleuth: A Course in Methods of Data Analysis. 2nd ed. Florence, KY: Cengage Learning; 2002.
35. Makar GL, Kruger J. Corrosion of magnesium. Int Mat Rev 1993;38(3):138-53.
36. Ferrando WA. Review of corrosion and corrosion control of magnesium alloys and composites. J Mater Eng 1989;11(4):299-313.
37. Jones D. Galvanic and concentration cell corrosion. In: Principles and prevention of corrosion. Second ed. Upper Sadle River, NJ: Prentice Hall; 1996. p.168-98.
38. Lusk JE, Williams RJP, Kennedy EP. Magnesium and the Growth of *Escherichia coli*. J Biol Chem 1968 May 25;243(10):2618-24.
39. Garcia Vescovi E, Soncini FC, Groisman EA. Mg^{2+} as an extracellular signal: environmental regulation of *Salmonella* virulence. Cell 1996 Jan 12;84(1):165-74.
40. Nelson DL, Kennedy EP. Transport of magnesium by a repressible and a nonrepressible system in *Escherichia coli.* Proc Natl Acad Sci U S A 1972 May;69(5):1091-3.
41. Auckenthaler R, Michea-Hamzehpour M, Pechere JC. *In vitro* activity of newer quinolones against aerobic bacteria. J Antimicrob Chemother 1986 Apr;17 Suppl B:29-39.
42. White D. Membrane Bioenergetics: The Proton Potential. In: The Physiology and Biochemistry of Prokaryotes. 3rd ed. New York: Oxford University Press; 2007. p.83-119.
43. Stoor P, Soderling E, Salonen JI. Antibacterial effects of a bioactive glass paste on oral microorganisms. Acta Odontol Scand 1998 Jun;56(3):161-5.
44. Allan I, Newman H, Wilson M. Antibacterial activity of particulate bioglass against supra- and subgingival bacteria. Biomaterials 2001 Jun;22(12):1683-7.

45. Hu S, Chang J, Liu M, Ning C. Study on antibacterial effect of 45S5 Bioglass. J Mater Sci Mater Med 2009 Jan;20(1):281-6.
46. Yates AA, Schlicker SA, Suitor CW. Dietary Reference Intakes: the new basis for recommendations for calcium and related nutrients, B vitamins, and choline. J Am Diet Assoc 1998 Jun;98(6):699-706.
47. Li L, Gao J, Wand Y. Evaluation of cytotoxicity and corrosion behavior of alkali-heat-treated magnesium in simulated body fluid. Surf Coat Technol 2004;185(1):92-8.
48. Li Z, Gu X, Lou S, Zheng Y. The development of binary Mg-Ca alloys for use as biodegradable materials within bone. Biomaterials 2008 Apr;29(10):1329-44.
49. Zhang E, Xu L, Yu G, Pan F, Yang K. *In vivo* evaluation of biodegradable magnesium alloy bone implant in the first 6 months implantation. J Biomed Mater Res A 2008 Jul 10.

Chapter 3

In vitro cytotoxicity of pure magnesium metal

The physical and mechanical properties of magnesium metal make it an excellent candidate for potential use in the biomedical implant industry. Prior to use as an implant, the issue of biocompatibility must be addressed. The objective of this study was to evaluate the cytotoxic effects of pure Mg metal on murine L929 fibroblasts and MC3T3 osteoblast-like cells via an *in vitro* elution test with a propidium iodide staining flow cytometry viability assay. Elution media was created such that there were five treatment groups 0.1-g/ml Mg(Mg), 316LSS, Control media, PE and Phenol for the assay. Cells were incubated with the elution media for 48- and 72-hours prior to being analyzed using the flow cytometry assay. Overall the addition of magnesium to the media during elution resulted in a decrease in cellular viability; however in most cases the effect was less toxic when compared to the phenol treated cells.

3.1 Introduction

The development of biodegradable/bioabsorbable implants is an active area in medical device design with particular interest in cardiovascular and orthopaedic devices.(1-7) An absorbable device would be advantageous for many reasons. For example, it would eliminate the risk of implant associated infections and chronic inflammatory reactions(3, 8) that can occur with permanent implants; the morbidity for retrieval surgeries would be avoided; and such implants would present an opportunity for enhancing the biological activity of cells near the device.(4) Magnesium (Mg) metal, whether pure or as an alloy, is considered to have potential use as a bioabsorbable device.(1, 4, 8) Mg has an anodic electromotive force potential; e^{o} = -2.372 (9) and rapidly corrodes in an electrolytic physiological environment following the general corrosion equation: $Mg(s) + 2H_2O \rightarrow Mg(OH)_2(s) + H2(g)$.(1, 10) In the presence of an activating anion (i.e. chloride) both magnesium and magnesium hydroxide can react further producing a magnesium salt.(1, 10)

Mg is also appealing as a device material because it is an inexpensive, lightweight and readily available metal; is an abundant cation (Mg^{2+}) in mammals, most of which is in bone; and is essential to many processes in eukaryotic cells.(1, 3, 4, 8, 11) When one considers the material properties of orthopaedic implants commonly used, none have physical and mechanical properties that closely resemble those of natural bone, whereas Mg does.(1) When addressing concerns for implant associated infections, Mg is interesting because of the recent characterization of some *in vitro* antibacterial properties.(12) Regardless of the mechanical or other properties, of paramount importance is the biocompatibility of a material. While a few studies have evaluated both the *in vivo* (2, 7, 13, 14) and *in vitro* (4, 5, 15) properties of magnesium alloys, even fewer have evaluated pure magnesium. Given the relative ease and minimal expense of *in vitro* studies they are arguably an essential first step in device design.

Thus, the objective of this study was to evaluate the cytotoxic effects of pure Mg metal on fibroblast and osteoblast-like cells via an elution test with both an MTT ((3-(4,5-Dimethylthiazol-2-yl)-2,5-diphenyltetrazolium bromide) colorimetric assay and propidium iodide staining flow cytometry viability assay.

3.2 Materials and methods

3.2.1 Cell culture

L929 (murine fibroblast cells) (ATCC CCL-1) and MC3T3-E1 Subclone 4 (murine pre-osteoblast cells) (ATCC CRL-259) were obtained from the American Type Culture Collection (American Type Culture Collection (ATCC), Manassas, VA, USA). The cells were cultivated according to the ATCC recommendations. The L929 cells were cultured in DMEM media (Invitrogen, Carlsbad, CA, USA) supplemented with 10% FBS (Invitrogen, Carlsbad, CA, USA), 100 U/ml penicillin (Invitrogen, Carlsbad, CA, USA), and 100 µg/ml streptomycin (Invitrogen, Carlsbad, CA, USA). The MC3T3 cells were cultured in custom Alpha MEM (A1049001, Invitrogen, Carlsbad, CA, USA) supplemented with 10% FBS and 0.6 g/L kanamycin sulfate (Invitrogen, Carlsbad, CA, USA). The cells were incubated at 37^{o}C in a 5% CO_2 incubator with the media changed every 3 days. A 0.25% trypsin solution, 0.5 mM EDTA solution was used to harvest confluent cells.

3.2.2 Materials

Magnesium turnings (Fisher Chemical, Pittsburgh, PA, USA) were used as the source of magnesium (Mg) metal. 316L stainless steel wires (316LSS) (Jorgensen Laboratories, Loveland, CO, USA) were used as the negative implant/metal control. Ultra high molecular weight polyethylene (PE) was used as the negative toxic control, 0.1% phenol solution was used as the positive toxic control and culture media was used as the negative control. The Mg, 316LSS and PE were cleaned and sterilized using steam sterilization prior to use for the elution testing.

3.2.3 Elution Media

Samples were added to the culture media such that there was 0.2 g of the sample material (SS, PE) per ml of culture media for elution.(16) Three amounts of Mg were tested (0.1 g/ml, 0.2 g/ml and 0.3 g/ml). DMEM culture media with additives was used for the L929 cells and Alpha MEM media with additives was used for the MC3T3 cells. The 1 day elution period was completed by adding the test material to the culture media with 10% FBS, whereas the 4, 5, 10 and 20 day elutions were completed using serum free culture media. All elutions were performed by incubation at 37^{o}C and 5% CO_2. At the end of the elution period 10% FBS was added to the serum free samples and all media samples were filter sterilized using a 0.22 μm filter. At this time the elution were ready to be added to cells for viability testing. In total there were seven treatment groups: 0.1 g/ml Mg, 0.2 g/ml Mg, 0.3 g/ml Mg, 316LSS, Control media, PE and Phenol for the MTT assay and five treatment groups 0.1 g/ml Mg (Mg), 316LSS, Control media, PE and Phenol for the flow cytometry viability assay.

3.2.4 MTT Assay

The L929 and MC3T3 cells were cultured to confluent layers as outlined above. Cells were collected and diluted such that there was approximately 10^6 cells/ml as determined by manual counts with a haemocytometer. 100 μl of cell suspension (equivalent to 10^5 cells) was seeded onto the well of a 96-well treated cell culture plate. The plates were then incubated at 37^{o}C and 5% CO_2 for 24 hours allowing the cells to reattached and form a near confluent layer. The formation of a monolayer was confirmed by microscopic evaluation of each well. For each treatment group there were 12 wells at each time point, 6 wells were for the elution test and the other 6 served as a blanks.

The cell culture media was removed and replaced with 100 μl of the test media. The plates were returned to the incubator and incubated at 37^{o}C and 5% CO_2 for 24, 48 or 72 hours, at which time the MTT assay was performed.

The MTT assay (MTT Cell Proliferation Assay, ATCC, Manassas, VA, USA) was performed according to the manufacturer's protocol. Specifically, at each time point 10 μl of the MTT reagent, containing the yellow tetrazolium MTT (3-(4, 5-dimethylthiazolyl-2)-2, 5-diphenyltetrazolium bromide), was added to each well. The plate was incubated at 37°C and 5% CO_2 for 4 hours at which time purple crystals could be visualized in the intracellular space of viable cells. At this time 100 μl of the detergent reagent was added and the plates gently swirled. The plate was then incubated at 37°C for 24 hours at which time the absorbance in each well was measured in a microtiter plate reader (FLUOstar OPTIMA, BMG Labtech Inc., Durham, NA, USA). The absorbance (A) was measured at 570 nm with measurements at 650 nm as a reference. The reference reading is used to correct for artifacts associated with the culture plate (i.e. scratches on the bottom of the plate).(17) The final absorbance was obtained using a modification of the manufacturer's protocol and the original description of the assay by Mosmann (18) using the following formula: [Sample A_{570nm} – Sample A_{650nm}] – [Blank A_{570nm} – Blank A_{650nm}]. The measurements of the blank were used to eliminate any background absorbance that may have occurred due to optical density differences in the elution media when compared to the control culture media.

3.2.5 Flow cytometry viability assay

The L929 and MC3T3 cells were cultured to confluent layers as outlined above. Cells were collected and diluted such that there was approximately 10^5 cells/ml as determined by manual counts with a haemocytometer. 2 ml of cell suspension (equivalent to ~10^5 cells) was seeded onto the well of a 6-well treated cell culture plate. The plates were then incubated at 37°C and 5% CO_2 for 48 hours allowing the cells to reattach and form a near confluent layer. The formation of a monolayer was confirmed by microscopic evaluation of each well. For each treatment group there was 1 well at each time point.

The cell culture media was removed and replaced with 2.0 ml of the test media. The plates were returned to the incubator and incubated at 37^{o}C and 5% CO_2 for 48 or 72 hours, at which time the viability assay was performed.

After each time point the media, with floating cells, was collected into a centrifuge tube on ice. The attached cells were then trypsinized and collected into the same tube. For each step any media or solution was collected into the same centrifuge tube to minimize loss of any cells. The sample was then centrifuged at 500 x g for 5 min at 4^{o}C. The result was a pellet of cells and cellular debris that had been collected. The supernatant was discarded. The pellet was gently resuspended in 1 ml of chilled DPBS without magnesium and calcium. The sample was again centrifuged at 500 x g for 5 min at 4^{o}C and the supernatant was discarded. The pellet was gently resuspended in 300 μl of FACS wash (3% FBS and 5 mM sodium azide in DPBS). Two tubes were labeled for each sample, one for propidium iodide (PI) staining and the other as a control. 3.0 μl of PI was added and the samples were incubated at 4^{o}C for 30 min in the dark. The samples were then counted using flow cytometry (BD FACSCanto, BD, Biosciences, San Jose, CA, USA). 20,000 events were counted for each sample and the results were analyzed in the forward scatter (FSC) versus the fluorochrome phycoerythrin output.(Figure 3.1) Using this, the data was gated such that the percentage of viable cells could be obtained. Each experiment was performed in triplicate.

3.2.6 Statistical analysis

For the flow cytometry assay the median % of viable cells is reported ± standard error (SE). The elution period (e.g. 1, 5, 10 and 20-days) for each incubation period (e.g. 24, 48 and 72 hours) was evaluated using Kruskal-Wallis one-way analysis of variance with significance set at $p < 0.05$. When the analysis revealed a statistically significant difference, each pair of sample groups (i.e. 316LSS, Mg, PE, phenol, control) was compared using an omnibus protected pairwise Wilcoxon rank sums test with significance set at $p < 0.05$.

3.3 Results

3.3.1 MTT Assay

After completion of this study, a manuscript was published by Fischer *et al.* regarding the influence of pH on the MTT assay. They specifically evaluated the corrosion products of Mg and found that it interferes with the chemical reaction in the MTT assay producing an inaccurate assessment of cell viability.(19) Given this finding the results of the MTT assay were unusable and will not be discussed.

3.3.2 Flow cytometry viability assay

A statistically significant difference was found across all groups with the L929 cell line (Mg, 316LSS, Control media, PE and Phenol) at the 48 hour incubation period for the 10 day and 20 day elution media and at 72 hour incubation period for the 1 day, 10 day and 20 day elution media.(Table 3.1) When the groups from these time points were compared in a pairwise manner, a statistically significant difference was not found in any of the comparisons.(Table 3.2 and 3.3) Overall the flow cytometry assay worked in that the phenol consistently resulted in a lower percentage of viable cells with the L929 cell line.(Figure 3.2) Similarly, the SS and PE consistently resulted in a percentage of viable cells that was comparable to the Control media in the L929 cell line. In general, the 0.1 g/ml Mg did not result in an appreciable decrease in cell viability but there did appear to be a negative trend associated with the longer elution and incubation periods.

A statistically significant difference was found across all groups with the MC3T3 cell line (Mg, SS, Control media, PE and Phenol) at the 48 and 72 hour incubation periods for the 4 day, 10 day and 20 day elution media.(Table 3.4) When the groups from these time points were compared in a pairwise manner, a statistically significant difference was not found in any of the

comparisons.(Table 3.5 and 3.6) Overall the flow cytometry assay worked for the MC3T3 cell line in that the phenol consistently resulted in a lower percentage of viable cells.(Figure 3.3) Additionally, the SS and PE consistently resulted in a percentage of viable cells that was similar to the Control media. Unlike the L929 cells, the 0.1 g/ml Mg did result in a substantial decrease in MC3T3 cell viability and there did appear to be a negative trend associated with the longer elution and incubation periods.

3.4 Discussion

Magnesium (Mg) has been a metal of interest in device design for some time. Its material properties(1), bioabsorbability(1, 4, 8) and apparent antimicrobial activity(12) are only a few reasons to support investigation into its use. The goal of the study presented here was to evaluate the cytotoxic effects of pure Mg metal on fibroblast and osteoblast-like cells via an elution test with both an MTT ((3-(4,5-Dimethylthiazol-2-yl)-2,5-diphenyltetrazolium bromide) colorimetric assay and propidium iodide staining flow cytometry viability assay. Overall the addition of Mg to the elution media did result in a decrease in cell viability. The degree of this effect however, appeared to depend on several factors. The MTT assay relies on the cleavage of the yellow tetrazolium salt MTT (3-(4, 5-dimethylthiazolyl-2)-2, 5-diphenyltetrazolium bromide), into formazan, a blue colored product by metabolically active cells.(17, 18) Thus this assay is useful because the presence of living cells is required for the formation of the formazan that which results in an increase in absorbance measured via spectrophotometry. In the study present here, the MTT assay was easy to perform and can be readily applied in many scenarios. Unfortunately, as discussed previously, the MTT assay is not viable when assessing Mg toxicity.(19) In their study, the authors noted that “corroded Mg converts tetrazolium salts to formazan, leading to a higher background and falsifying the results of cell viability.”(19) We were not aware of this limitation of the MTT assay when designing this study; nonetheless, it would be inappropriate to use the results from the MTT portion of our study.

The propidium iodide (PI) flow cytometry viability assay functions on different principles than the MTT test and is thus an alternative approach to assess viability. PI binds to DNA by intercalating between the nucleic acid bases and because PI cannot pass through semipermeable membranes and is generally excluded from viable cells, it can be used to identify cells that are dead or dying and thus have compromised membranes.(20) In this study, PI staining combined with flow cytometric analysis was used to assess cell viability. Unlike the MTT assay, the flow cytometry assay detected a difference in response between the L929 and MC3T3 cell lines. The addition of 0.1 g/ml of Mg to the elution media did not substantially alter L929 viability, however it did result in a marked decrease in MC3T3 cell viability and this decrease in viability was similar to that noted with exposure to phenol.

The trends towards decreased cell viability with both the longer elution time and longer incubation period were not surprising given that this was a closed system. In order to maintain an active cell culture in the laboratory, the media needs to be changed every 48 to 72 hours to eliminate waste products and potential toxins produced by the cells as they grow and divide. Thus, this could explain some of the decrease in viability we observed.

Of interest was the apparent greater sensitivity of the MC3T3 cells to the Mg elution media. Given that Mg ions are essential in the normal physiologic processes occurring within bone and that the majority of the total body Mg is in bone, this was surprising. It is known that Mg metal rapidly corrodes in an aqueous environment producing an alkaline pH.(1, 10) Perhaps this increase in alkalinity is also responsible for the loss of cell viability and it is not related to the concentration of Mg^{+2}. Regardless, we observed a considerable loss in cell viability with shorter elution (i.e. by the 4 day) and a more profound effect on viability (<10% viable in the 10 and 20 day elution media at 72 hours) in the MC3T3 cells compared to the L929 cells in the flow cytometry assay.

An important consideration for the flow cytometry assay is that an alteration in cell membrane permeability is all that is required for the PI to enter the cell and bind the nucleic acids resulting in a positively stained cell. Changes in cell membrane permeability can occur to varying degrees during cellular death and for reasons other than cellular death.(20, 21) It could therefore be argued that a cell that stains positive for PI is not necessarily a dead cell and instead it may just be injured and able to recover. Because we did not attempt to account for this ability to recover, we may have in fact overestimated the decrease in cell viability.

While other studies have evaluated magnesium, the emphasis has traditionally been on alloys because of the increased corrosion resistance and ability to enhance/alter other material properties.(2, 4, 5, 13, 15, 22) Li, L *et al.* (22) evaluated alkali-heat-treated magnesium; whereas Pietak *et al.* (4) and Gu *et al.* (15) evaluated the cytotoxicity of pure magnesium as a control group in alloy studies. Li, L *et al.* found that there was no evidence of morphological changes or inhibition of cell growth by the alkali-heat-treated magnesium on mouse marrow cells.(22) In agreement with Li, L *et al.* were the findings by Li, Z *et al*. where L929 cells demonstrated better growth in extraction media from a Mg-Ca alloy than in the control media.(5) A potential explanation for this finding was an enhanced cell viability associated with the increased concentration of Mg ions present in the media.(5) In their study Pietak *et al.* found that the alkaline phosphatase activity and total protein measurements for rat stromal cells cell cultures with Mg were equivalent to the controls.(4) They also de-emphasized the alterations in pH and ion concentration in their study arguing that these same findings would be less likely *in vivo* because of the local tissue circulation and buffering capacity of extracellular fluid.(4) Overall they concluded that “Mg based substrates support the adhesion and differentiation of stromal cells towards an osteoblast-like phenotype”.(4) In contrast, Gu *et al.* found a decrease in cell viability compared to controls after 7 days in culture for pure Mg with mouse fibroblasts (L929, NIH3T3), pre-osteoblasts (MC3T3), and rodent vascular smooth muscle cells.(15) The study presented

here evaluated pure magnesium, used immortalized cell lines to eliminate individual animal/cellular variability that is likely to occur when isolating cells from animals, and did not rely on subjective evaluation of morphology as an indication of viability. Nonetheless there is no clear consensus on the cytotoxic effect of Mg on cells in *in vitro* studies.

In vivo studies have primarily evaluated magnesium alloys, their corrosion rates and influence on bone response. Witte *et al.* found that when compared to a polymeric implant, a magnesium alloy resulted in enhanced bone formation around an implant that had been placed in a guinea pig femur.(2) In the authors' opinion, this enhanced bone formation was an indication of enhanced osteoblastic activity that may have been associated with the presence of magnesium ions generated during degradation.(2) Li, Z *et al*. had similar experience with a Mg-Ca alloy that was implanted into rabbit femoral shafts.(5) Enhanced osteoblastic activity was noted around the implant which gradually degraded over a 90-day period with new bone formation being evident 3-months after implantation.(5) Zhang *et al*. evaluated a Mg-Zn-Mn alloy that was implanted in the femur of a rat.(23) The goal of their study was not only to assess the *in vivo* degradation and bone response but also the systemic effects of degradation by-products.(23) Similar to previous studies, the implants were associated with new bone production. Interestingly, these in vivo studies suggest that magnesium is associated with increased bone formation; this is in contrast with what one might expect given the decreased viability that we found.

3.5 Conclusion

In this study we have characterized the *in vitro* response of L929 fibroblasts and MC3T3 osteoblast-like cells to elution media from pure magnesium metal. Cellular viability was assessed with a PI staining flow cytometry viability assay. Overall the addition of magnesium to the media during elution resulted in a decrease in cellular viability, however in most cases the effect was

much less than the toxic control phenol. In general cell viability decreased with longer elution and incubation times.

Figure 3.1: Output from the flow cytometry analysis. The debris was not included in the analysis. The outer (pink) gate was used to mark off the total cell count and then the dashed gate was used to determine the percent of viable cells. The PI stained cells were considered non-viable.

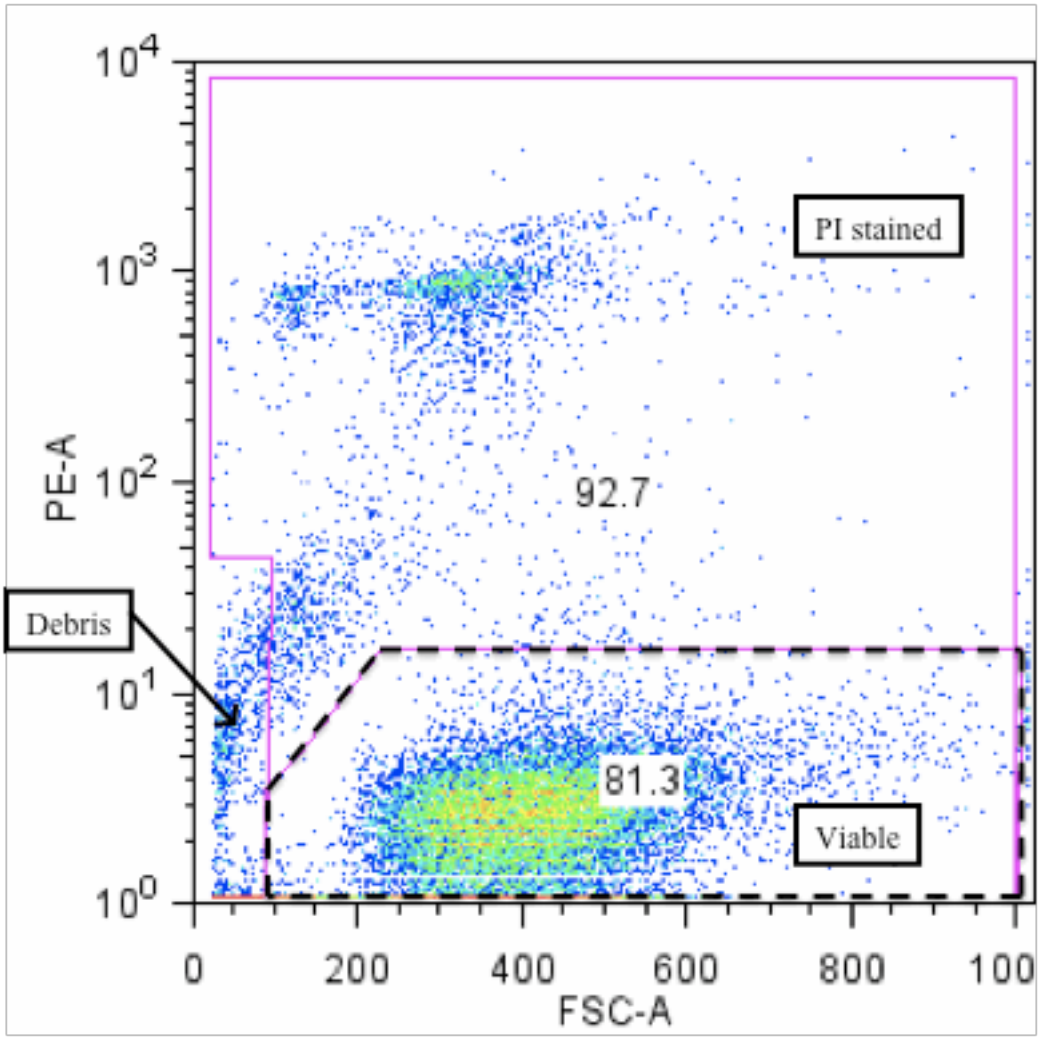

Figure 3.2: Mean ± SE percent cell viability for the L929 cells after 48 (a) and 72 hour (b) incubation.

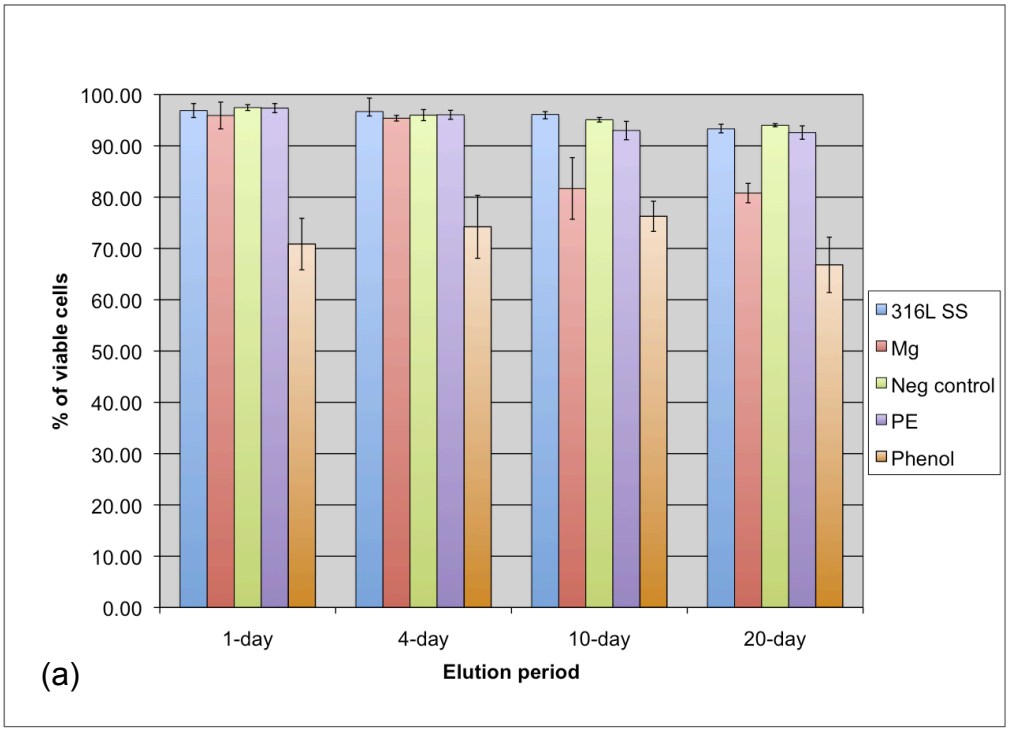

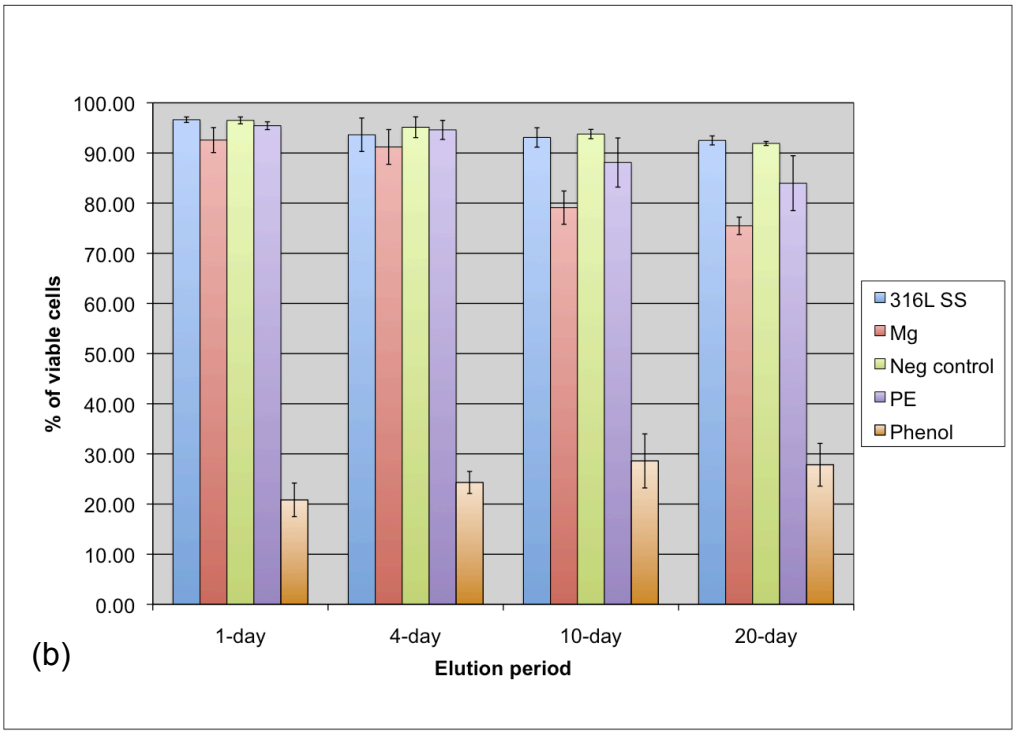

Figure 3.3: Mean ± SE percent cell viability for the MC3T3 cells after 48 (a) and 72 hour (b) incubation.

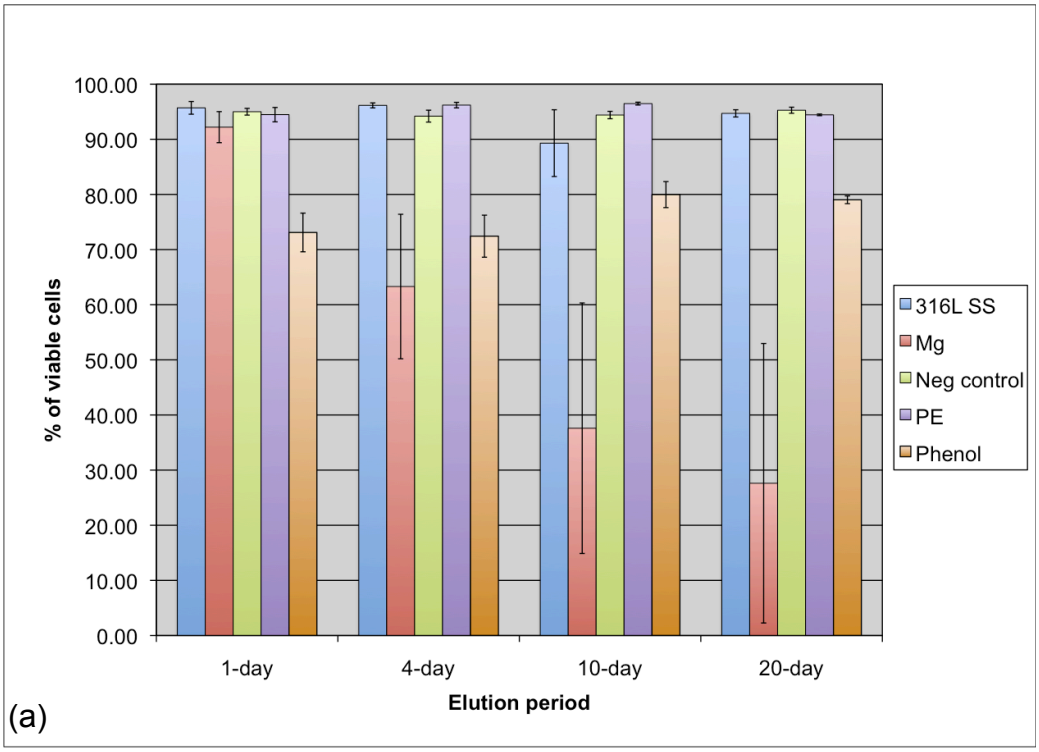

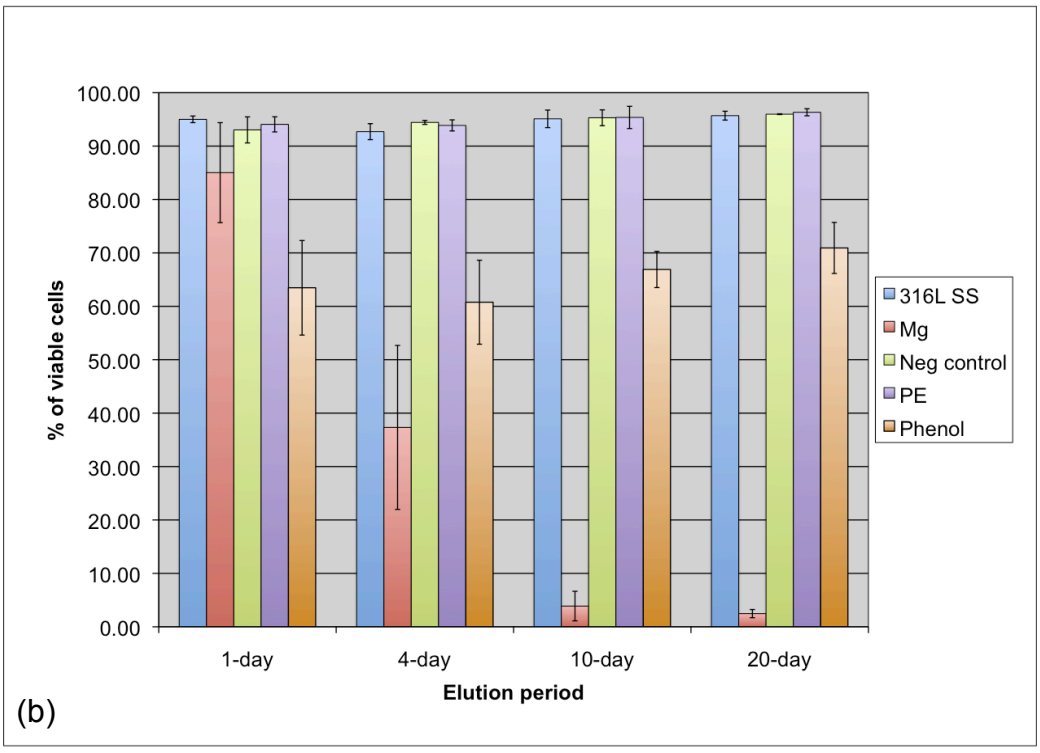

Table 3.1: P-values from the Kruskal-Wallis one-way analysis of variance for the L929 cells. The ★ indicates a statistically significant difference.

Incubation	Elution period	P-value
48-hours	1-day	0.1450
48-hours	4-days	0.1600
48-hours	10-days	0.0206★
48-hours	20-days	0.0285★
72-hours	1-day	0.0433★
72-hours	4-days	0.8120
72-hours	10-days	0.0293★
72-hours	20-days	0.0310★

Table 3.2: P-values for comparison of each pair of sample groups (i.e. 316LSS, Mg, PE, phenol, control) for the L929 cells at 48 hour incubation that had a P-value < 0.05 in Table 3.1.

	Mg	PE	316LSS	Phenol
PE	0.0765			
316LSS	0.0765	0.0809		
Phenol	0.6579	0.0809	0.0809	
Neg control	0.7650	0.8248	0.3827	0.0809

(a) 48-hours with 10-day elution

	Mg	PE	316LSS	Phenol
PE	0.0809			
316LSS	0.0809	0.6625		
Phenol	0.1904	0.0809	0.0809	
Neg control	0.0809	0.6625	0.6625	0.0809

(b) 48-hours with 20-day elution

Table 3.3: P-values for comparison of each pair of sample groups (i.e. 316LSS, Mg, PE, phenol, control) for the L929 cells at 72 hour incubation that had a P-value < 0.05 in Table 3.1.

	Mg	PE	316LSS	Phenol
PE	0.3827			
316LSS	0.0809	0.6625		
Phenol	0.0809	0.0809	0.0809	
Neg control	0.1904	0.3827	1.0000	0.0809

(a) 72-hours with 1-day elution

	Mg	PE	316LSS	Phenol
PE	0.1904			
316LSS	0.0809	0.6625		
Phenol	0.0809	0.0809	0.0809	
Neg control	0.0809	0.3827	1.0000	0.0809

(b) 72-hours with 10-day elution

	Mg	PE	316LSS	Phenol
PE	0.1904			
316LSS	0.0809	0.6625		
Phenol	0.0809	0.0809	0.0809	
Neg control	0.0809	0.6625	0.6625	0.0809

(c) 72-hours with 20-day elution

Table 3.4: P-values from the Kruskal-Wallis one-way analysis of variance for the MC3T3 cells. The ★ indicates a statistically significant difference.

Incubation	Elution period	P-value
48-hours	1-day	0.0788
48-hours	4-days	0.0356★
48-hours	10-days	0.0258★
48-hours	20-days	0.0253★
72-hours	1-day	0.1507
72-hours	4-days	0.0335★
72-hours	10-days	0.0266★
72-hours	20-days	0.0239★

Table 3.5: P-values for comparison of each pair of sample groups (i.e. 316LSS, Mg, PE, phenol, control) for the MC3T3 cells at 48 hour incubation that had a P-value < 0.05 in Table 3.4.

	Mg	PE	316LSS	Phenol
PE	0.0809			
316LSS	0.1489	1.0000		
Phenol	0.6625	0.0809	0.1489	
Neg control	0.0809	0.3827	0.3865	0.0809

(a) 48-hours with 4-day elution

	Mg	PE	316LSS	Phenol
PE	0.0809			
316LSS	0.1904	0.0809		
Phenol	0.1904	0.0809	0.3827	
Neg control	0.0809	0.6625	1.0000	0.0809

(b) 48-hours with 10-day elution

	Mg	PE	316LSS	Phenol
PE	0.0809			
316LSS	0.0809	0.6625		
Phenol	0.1904	0.0809	0.0809	
Neg control	0.0809	0.2683	1.0000	0.0809

(c) 48-hours with 20-day elution

Table 3.6: P-values for comparison of each pair of sample groups (i.e. 316LSS, Mg, PE, phenol, control) for the MC3T3 cells at 72 hour incubation that had a P-value < 0.05 in Table 3.4.

	Mg	PE	316LSS	Phenol
PE	0.0809			
316LSS	0.1489	0.7728		
Phenol	0.1904	0.0809	0.1489	
Neg control	0.0809	1.0000	0.3865	0.0809

(a) 72-hours with 4-day elution

	Mg	PE	316LSS	Phenol
PE	0.0809			
316LSS	0.0809	0.6625		
Phenol	0.0809	0.0809	0.0809	
Neg control	0.0809	1.0000	0.8248	0.0809

(b) 72-hours with 10-day elution

	Mg	PE	316LSS	Phenol
PE	0.0809			
316LSS	0.0809	0.3827		
Phenol	0.0809	0.0809	0.0809	
Neg control	0.0765	1.0000	0.6579	0.0765

(c) 72-hours with 20-day elution

3.6 Chapter references

1. Staiger MP, Pietak AM, Huadmai J, Dias G. Magnesium and its alloys as orthopedic biomaterials: a review. Biomaterials 2006 Mar;27(9):1728-34.
2. Witte F, Kaese V, Haferkamp H, Switzer E, Meyer-Lindenberg A, Wirth CJ, et al. *In vivo* corrosion of four magnesium alloys and the associated bone response. Biomaterials 2005 Jun;26(17):3557-63.
3. Song G, Song S. A Possible Biodegradable Magnesium Implant Material. Advanced Engineering Materials 2007;9(4):298-302.
4. Pietak A, Mahoney P, Dias GJ, Staiger MP. Bone-like matrix formation on magnesium and magnesium alloys. J Mater Sci Mater Med 2008 Jan;19(1):407-15.
5. Li Z, Gu X, Lou S, Zheng Y. The development of binary Mg-Ca alloys for use as biodegradable materials within bone. Biomaterials 2008 Apr;29(10):1329-44.
6. Di Mario C, Griffiths H, Goktekin O, Peeters N, Verbist J, Bosiers M, et al. Drug-eluting bioabsorbable magnesium stent. J Interv Cardiol 2004 Dec;17(6):391-5.
7. Heublein B, Rohde R, Kaese V, Niemeyer M, Hartung W, Haverich A. Biocorrosion of magnesium alloys: a new principle in cardiovascular implant technology? Heart 2003 Jun;89(6):651-6.
8. Hanzi AC, Gunde P, Schinhammer M, Uggowitzer PJ. On the biodegradation performance of an Mg–Y–RE alloy with various surface conditions in simulated body fluid Acta Biomaterialia 2009;5:162-71.
9. Jones D. Thermodynamics and Electrode Potential. In: Principles and prevention of corrosion. Second ed. Upper Sadle River, NJ: Prentice Hall; 1996. p.40-74.
10. Makar GL, Kruger J. Corrosion of magnesium. Int Mat Rev 1993;38(3):138-53.
11. Romani AM, Maguire ME. Hormonal regulation of Mg^{2+} transport and homeostasis in eukaryotic cells. Biometals 2002 Sep;15(3):271-83.

12. Robinson DA, Griffith RW, Shechtman D, Evans RB, Conzemius MG. *In vitro* antibacterial properties of magnesium metal against *Escherichia coli, Pseudomonas aeruginosa* and *Staphylococcus aureus*. Acta Biomater 2010 Oct 7;6(5):1869-77.
13. Witte F, Fischer J, Nellesen J, Crostack HA, Kaese V, Pisch A, et al. *In vitro* and *in vivo* corrosion measurements of magnesium alloys. Biomaterials 2006 Mar;27(7):1013-8.
14. Waksman R, Pakala R, Kuchulakanti PK, Baffour R, Hellinga D, Seabron R, et al. Safety and efficacy of bioabsorbable magnesium alloy stents in porcine coronary arteries. Catheter Cardiovasc Interv 2006 Oct;68(4):607,17; discussion 618-9.
15. Gu X, Zheng Y, Cheng Y, Zhong S, Xi T. *In vitro* corrosion and biocompatibility of binary magnesium alloys. Biomaterials 2009 Feb;30(4):484-98.
16. Northup SJ. Cytotoxicity tests of plastics and elastomers. Pharmacopeial Forum 1987;13:2939-42.
17. Denizot F, Lang R. Rapid colorimetric assay for cell growth and survival. Modifications to the tetrazolium dye procedure giving improved sensitivity and reliability. J Immunol Methods 1986 May 22;89(2):271-7.
18. Mosmann T. Rapid colorimetric assay for cellular growth and survival: application to proliferation and cytotoxicity assays. J Immunol Methods 1983 Dec 16;65(1-2):55-63.
19. Fischer J, Prosenc MH, Wolff M, Hort N, Willumeit R, Feyerabend F. Interference of magnesium corrosion with tetrazolium-based cytotoxicity assays. Acta Biomater 2010 May;6(5):1813-23.
20. Krysko DV, Vanden Berghe T, D'Herde K, Vandenabeele P. Apoptosis and necrosis: detection, discrimination and phagocytosis. Methods 2008 Mar;44(3):205-21.
21. Lodish H, Berk A, Kaiser CA, Krieger M, Scott MP, Bretscher A, et al. Transmembrane Transport of Ions and Small Molecules. In: Molecular Cell Biology. Sixth ed. New York, NY: W. H. Freeman and Company; 2008. p.437-76.
22. Li L, Gao J, Wand Y. Evaluation of cyto-toxicity and corrosion behavior of alkali-heat-treated magnesium in simulated body fluid. Surf Coat Technol 2004;185(1):92-8.

23. Zhang E, Xu L, Yu G, Pan F, Yang K. In vivo evaluation of biodegradable magnesium alloy bone implant in the first 6 months implantation. J Biomed Mater Res A 2008 Jul 10.

Chapter 4

In vitro evaluation of the antimicrobial and anti-biofilm effects of nano-magnesium oxide (nMgO)

Research into the use of nanomaterials is a rapidly expanding field and not surprisingly, they are materials being evaluated for their antimicrobial properties. The effect of the addition of nMgO, nZnO and Mg-mesh on the pH of tryptic soy broth was investigated. These materials were also evaluated for their effect on the growth of Gram-negative and Gram-positive bacteria that were from both clinical and laboratory strains. Supernatants were created for each of the materials and the influence of the supernatant was evaluated on both the planktonic growth and ability to produce a biofilm. nMgO caused a rapid increase in the pH of the bacterial growth media. nZnO also caused an increase in pH, but to a lesser degree. No bacteria were recovered from any of the culture vials where nMgO or its supernatant was added. Some Gram-postiive *Staphylococcus* were recovered from the nZnO vials and supernatant. When this occurred, the CFU/ml was 10^4 to 10^5 less than the Control. Supernatant from the nMgO, nZnO and Mg-mesh prevented a biofilm formation for the bacterial strains that produced a biofilm in the control wells. Although the mechanism is not clear, nMgO appears to have antimicrobial properties on both the planktonic forms and biofilm production for the organisms evaluated.

4.1 Introduction

As methodologies have improved and engineering techniques developed further, nanomaterials have become an area of great interest over many disciplines due in large part to their very high surface area to volume ratio. On one hand implant colonization may be prevented via "nano-functionalization" surface techniques(1), while on another the ability to produce particles of any shape and size contributes to their use as biocides(2). As research continues to work towards devices that have anti-fouling properties it seems logical that nanomaterials would be investigated.

Many metals have been evaluated for antibacterial potential when used on a nanoscale. In some cases these metals are used alone (e.g. silver nanoparticles (3, 4)), as oxides (e.g. ZnO, TiO_2, Al_2O_3, CuO, CeO_2, MgO (2)) and in combination with halogens(1, 5). Magnesium based nanoparticles are attractive for a number of reasons. The antimicrobial properties of this inexpensive bioabsorbable metal have been described(6) and unlike many of the other metal oxides, magnesium has very little inherent risk of toxicity. The antimicrobial efficacy of magnesium oxide nanoparticles has been investigated previously and the results appear to be dependent on the bacterial species studied. Dong *et al.* demonstrated activity against both *Escherichia coli* and *Burkholderia phytofirmans* (a Gram-negative organism found in soil) in suspension and when incorporated into paper sheets.(7) In contrast Jones *et al.* found that nMgO in a colloidal suspension had no significant inhibition on the growth of a clinical *Staphylococcus aureus* isolate.(2) Given the variation in resistance patters, cellular structure and virulence mechanisms this finding is not that surprising, especially when evaluating clinical isolates.

The goals of this study were: (1) to characterize the effects of the addition of nMgO on the pH of a microbial culture broth; (2) to evaluate the effects of the presence of nMgO on the *in vitro* growth of clinical and laboratory strains of *Staphylococcus aureus*, *Escherichia coli*, *Staphylococcus epidermidis* and *Pseudomonas aeruginosa*; and (3) to evaluate the effect of a supernatant produced from the nanoparticles on *in vitro* bacterial growth and biofilm production. The hypotheses were: (1) the addition of nMgO to a microbial culture broth will result in an increase in pH (i.e. make it more alkaline) that is similar to that noted when magnesium metal was added. This pH increase will also be greater than that noted with the addition of nZnO; (2) the addition of nMgO to a culture vial will result in a decrease in the CFU per ml recovered when compared to controls. This effect will be similar across all bacterial strains tested; (3) the addition of nMgO supernatant to a culture vial will result in a decrease in the CFU per ml recovered when compared to controls. This effect will be similar across all bacterial strains tested; and (4) the addition of nMgO supernatant will result in the prevention of biofilm formation in an *in vitro* microtiter biofilm model and this effect will be similar across all bacterial strains tested.

4.2 Materials and methods

4.2.1 Nano-magnesium oxide, nano-zinc oxide, magnesium metal mesh

To determine the reaction properties of nano-magnesium oxide (nMgO) ($\leq$ 8 nm; specific surface area (BET) $\geq$ 230 m^2/g)(nanoActive® Magnesium Oxide, NanoScale Corporation, Manhattan, KS, USA), nano-zinc oxide (nZnO) (< 100 nm; surface area 15-25 m^2/g) (Zinc oxide nanopowder, Aldrich, St. Louis, MO, USA) and magnesium metal mesh (Mg-mesh) (< 44 µm) (Mg metal powder, -325 mesh, American Elements, Los Angeles, CA, USA) in bacterial growth media 200 mg of each, were placed into 8.0-ml of sterile tryptic soy broth (TSB) (Beckton Dickinson Diagnostic Systems, MD, USA). The pH of the broth was serially measured over a 72 hour period using a pH meter (Denver Instruments, Boehmia, NY, USA).

4.2.2 Test materials

25 mg/ml of nMgO, nZnO and Mg-mesh were used as the source of nanoparticle. Although the Mg-mesh is not technically a nanoparticle, it was the smallest particle size commercially available at the time of this study. Enrofloxacin (Baytril Injectable, Bayer Animal Health, KS, USA) was used as a control for a bactericidal agent. A final concentration of enrofloxacin of 10 µg/ml was used in the culture vials. Finally, all bacteria were cultured with no additive to serve as a negative control.

4.2.3 Bacterial cultures

The bacterial inoculum consisted of one of the following organisms: *Escherichia coli* (ATCC 25922), *Pseudomonas aeruginosa* (ATCC 27853), *Pseudomonas aeruginosa* (MORF – isolated from an infected tibial implant), (which are Gram-negative organisms) and *Staphylococcus aureus* (ATCC 25923), *Staphylococcus aureus* (MORF 13G – isolated from an infected total hip arthroplasty), *Staphylococcus epidermidis* (RP62A) (which are Gram-positive organisms) (ATCC - American Type Culture Collection, VA, USA; MORF – Excelen Center of Bone and Joint Research and Education, Minneapolis, MN, USA; RP62A – Dr. Paul Fey, University of Nebraska Medical Center, Omaha, NE, USA). These bacterial strains were chosen to represent the spectrum of organisms encountered and because they are used as control strains in quality control susceptibility testing, for media testing and for susceptibility disc testing. Thus they are well-established cultures and strains in the *in vitro* setting. Pure cultures of all organisms were aerobically cultured for 24 hours at 37^{o}C on bovine blood agar plates. Samples of each of the pure cultures were collected using a sterile wooden applicator and suspended in 3 ml of TSB broth in 15 ml conical tubes. The tubes were incubated in the water bath at 37^{o}C with agitation at 220 rpm for approximately 2 hours.

4.2.4 Incubation of bacteria with test materials

Nanoparticles

Culture vials were prepared such that each contained 2 ml of sterile TSB broth. nMgO, nZnO, Mg-mesh or antibiotic (10.0 μg/ml of enrofloxacin) were added to the culture vials such that there were two vials of each material per bacteria to be tested.(Table 4.1) The vials were vortexed for 30 sec, sonicated (67 kHz) for 20 min and vortexed again to generate colloidal suspensions.(Figure 4.1) Inoculation suspensions for each organism were prepared such that OD_{595} was ~0.2 in 2 ml TSB. This resulted in ~10^8 CFU/ml. 20 µl of this suspension (~10^6 CFU/ml) was used to inoculate each vial. The culture vials were incubated aerobically in a water bath at 37^{o}C with agitation at 220 rpm for 24 hours after which time samples were collected and microtiter dilution was performed.(Figure 2.1)

Supernatant

A supernatant was generated for each material by adding the material to TSB such that there was 25 mg/ml of nMgO, nZnO or Mg-mesh. This was vortexed for 30 sec, sonicated for 20 min (67 kHz) and vortexed again to generate colloidal suspensions. They were then incubated in a vial for ~24 hours in a 37^{o}C waterbath with agitation at 200 rpm. After the incubation each suspension was filtered using a 0.22 µm syringe filter to generate a supernatant for further testing. Sterile vials were prepared by adding 1.5 ml of the supernatant (nMgO, nZnO or Mg-mesh) to each vial.(Table 4.1) An inoculation suspension for each bacteria was prepared as outlined above. Two vials were prepared for each bacteria and solution. The vials were incubated in a 37^{o}C waterbath with agitation at 200 rpm. At 24 hours, each vial was sampled and microtiter dilution was performed.(Figure 2.1)

96-well plates

Prior to addition to the wells in the 96-well plate, 5% sucrose was added to the supernatant, antibiotic suspension and TSB. The 96-well plate was prepared by adding 180 µl of the solution to each well. An inoculation suspension for each bacteria was prepared as outline above and was used to inoculate each well of the 96 well plate. The plates were then covered with sterile, breathable sealing tape (Thermo Scientific 241205, Fisher Scientific, Pittsburgh, PA, USA) and incubated in a dry incubator at 37^{o}C for 24 and 48 hours.(Table 4.2)

4.2.5 Bacterial counts and biofilm production

Microtiter dilution and viable bacterial counts (Figure 2.1)

Microtiter dilutions were performed using a modification of a previously described technique.(8, 9) The CFU in each tube were determined by aseptically collecting a sample from each tube at ~24hours post inoculation. Ten-fold dilutions were made (10^{-1} to 10^{-7}) using phosphate buffered saline (PBS) in 96-well round bottom microtiter plates. Twenty µl was collected from each well and streaked across a tryptic soy agar (TSA) (Beckton Dickinson Diagnostic Systems, MD, USA) plate in a uniform manner. The plates were incubated aerobically at 37^{o}C for 24 hours at which time the number of colonies were counted.

Biofilm staining

At 24 hours, the 96-well plates were stained for biofilm production.(1, 10, 11) At this time the planktonic suspension and nutrient solutions were gently aspirated and each well was washed three times with 200-250 µl sterile phosphate buffered saline (PBS) and dried in an inverted position for 15 min. 250 µl of 95% ethanol was added to each well and left for 15 min at room temperature. The plates were then emptied and left to dry. 200 µl of crystal violet (~0.4% solution) (Fisher Scientific, Pittsburgh, PA, USA) was added to each well and incubated for 10 min at room temperature. The unbound stain was removed and the wells were rinsed three times

with 300 µl PBS and dried in an inverted position for 30 min. The OD_{570} was then measured using an automated plate reader (FLUOstar OPTIMA, BMG Labtech Inc., Durham, NA, USA). The corrected OD_{570} was determined using the formula provided in Figure 4.2. This number was then used to classify biofilm formation as highly positive ($OD_{570} \geq 1$), low-grade positive ($0.1 \leq OD_{570} < 1$) or negative ($OD_{570} < 0.1$).(10)

4.2.6 Statistical analysis

Dilutions with up to 30 CFU present were used to calculate the median CFU/ml. Summary statistics were calculated and are presented as the median CFU/ml. The error bars in the figures represent the 25^{th} and 75^{th} percentiles.

4.3 Results

4.3.1 Reaction properties of nMgO, nZnO, and Mg-mesh

The addition of both nMgO and Mg-mesh resulted in a rapid increase in pH. After 1 hour it was 10.33 and 10.46 for the nMgO and Mg-mesh respectively. These results are similar to those noted for Mg metal turnings in Figure 2.2.(6) In the nZnO the pH reached a maximum of 8.36 after 72 hours.(Figure 4.3)

4.3.2 Incubation of bacteria with nanoparticles

The experimental conditions resulted in an expected growth pattern of all six bacterial organisms as indicated by the CFU/ml recovered from the control vials. There were no CFU recovered from either the nMgO or Mg-mesh vials after 24-hours of incubation. *Pseudomonas aeruginosa* was recovered from the enrofloxacin vials, although the amount recovered was ~10^5 times less than the CFU/ml in the control vials. CFU were recovered from the nZnO vials for each bacteria, with the exception of *Staphylococcus epidermidis* and *Staphylococcus aureus* ATCC where no CFU

were recovered. Even though CFU were recovered from the *Staphylococcus aureus* MORF incubated with the nZnO, there were ~10^5 less than the CFU/ml in the control vials.(Figure 4.4)

4.3.3 Incubation of bacteria with supernatant

The bacteria again grew as expected as indicated by the CFU/ml from the control vials. No bacteria were recovered from the vials containing the nMgO or Mg-mesh supernatant after 24-hours of incubation. *Pseudomonas aeruginosa* MORF was recovered from the enrofloxacin vials, although the amount recovered was ~10^4 times less than the CFU/ml in the control vials. CFU were recovered from the nZnO vials for each bacteria, with the exception of *Staphylococcus aureus ATCC* where no CFU were recovered. Even though CFU were recovered from the *Staphylococcus aureus* MORF and *Staphylococcus epidermidis* incubated with the nZnO supernatant, there were ~10^4 less than the CFU/ml in the control vials.(Figure 4.5)

4.3.4 Biofilm production

The *Staphylococcus epidermidis* (RP62A) was the only bacterial inoculum that produced a highly positive biofilm in the control wells. *Staphylococcus aureus* ATCC produced a low-grade positive at 24 hours.(Table 4.3) Evaluating these bacteria only, the nMgO, nZnO, Mg-mesh and enrofloxacin resulted in a negative biofilm at 24 hours. At 48 hours, only the nMgO, nZnO and enrofloxacin resulted in negative biofilm results with a low-grade positive for the Mg-mesh and the *S. epidermidis*.(Table 4.4)

4.4 Discussion

When one considers that the addition of MgO to water will result in the production of Mg(OH) it is not surprising that this material resulted in an increase in pH (i.e. a more alkaline environment) in this study. This is also the premise under which it is used as an antacid (i.e. Maalox®). The fact that this change in pH paralleled that of the magnesium metal powder confirms that the first

hypothesis was correct. As discussed previously, the *in vitro* antimicrobial activity appears to be related to this alkaline pH.(6) Although this was an interesting finding, the lack of facilities that work with pure magnesium coatings has limited further work with this material. The fact that nMgO may have a similar mechanism of activity is appealing because it is a much easier material to work with.

While others have demonstrated that nMgO has antimicrobial activity(2, 7), their methodologies were different and the results somewhat contradictory. With that in mind the goal of this study was to use methods that were familiar to our lab and to also evaluate the efficacy against both clinically relevant and laboratory strains of bacteria. When the nMgO and Mg-mesh were added to the bacterial culture media, no CFU were recovered. The addition of nZnO did not have a universal effect in that there were CFU recovered from 4 of the 6 bacterial strains evaluated. Interestingly, three of these were Gram-negative bacteria. Although many nanoparticles have demonstrated antimicrobial activity, a clear, universal mechanism is not apparent. Lellouche *et al.* evaluated nanosized magnesium fluoride and found that the nanoparticles had anti-biofilm activity against *E. coli* and *S. aureus* strains. They concluded that the MgF_2 nanoparticles penetrate the bacterial cells interfering with the membrane potential, bind DNA and enhance lipid peroxidation.(1) Penetration and resultant damage to cellular mechanisms has been noted by other researchers. $Mg(OH)_2$ nanoparticles were found to cause changes to the scanning electron microscopy (SEM) appearance of *E. coli* and resulted in an overall decrease in the number of bacteria recovered.(7) Similarly, MgO nanoparticles were found to disrupt the cell walls of Gram-negative and Gram-positive bacteria as well as bacterial spores. On transmission electron microscopy (TEM) nanoparticles were noted in the bacterial cells and remnants of cell wall pieces of the spores were also apparent.(5) Some form of cellular interaction undoubtedly plays a role in the antimicrobial activity of many nanoparticles but it also seems prudent to consider the role of the increasingly alkaline environment. Dong *et al*. present a mechanism whereby a thin water layer is formed around the nanoparticle and that the pH within this layer may be even higher than

that in an equilibrium solution. This layer will be highly concentrated with OH^- groups and interaction of the bacteria with these OH^- could damage the bacterial cell membrane.(7)

In an attempt to further evaluate the mechanism of antimicrobial activity in the model presented here a supernatant was created for each test material. By filtering each suspension, the goal was to remove as many of the particles as possible. Although the resultant supernatant was grossly clear for each material (compared to Figure 4.1) the pore size of the filter was 0.22 μm (220 nm) and thus nMgO and nZnO particles likely passed through. Nonetheless, there was a gross difference in the appearance meaning there were fewer nanoparticles present. The question of the minimum number of particles required for efficacy remains unknown. With this in mind the incubation of bacteria with the supernatant may just be an extension of a previous experiment (4.4.2 Incubation of bacteria with nanoparticles). Interestingly, the results for the nZnO were not the same. In the presence of the nZnO supernatant the *Staphylococcus epidermidis* grew whereas it did not grow in the presence of the nZnO nanoparticles. One explanation for this is that the pH after addition of nZnO only reached 8.36, a pH which allows for growth of some bacterial organisms.(6)(Figure 2.6) Another is that the nZnO nanoparticles are reported as < 100-nm thus some may have been retained by the 0.22 μm filter, especially nearing the end of the filtering process where more material could accumulate on the membrane. The other intriguing finding was that the nZnO had little if any effect on the Gram-negative organisms. Is it possible that the thick outer membrane/lipopolysaccharide layer (LPS) of these organisms interfered with the activity of the nZnO or is there another reason for this finding? Once again, this demonstrates the difficulties in dealing with microbial organisms in that there is tremendous variation in structure and virulence mechanisms.

While the ability of a material to inhibit bacterial growth in planktonic form is important, its influence on the production of a biofilm is arguably more relevant. Bacterial biofilms have and continue to be, a major barrier in the prevention and/or treatment of implant associated infections.

Thus the antibiofilm activity of a given material is often evaluated. Not all of bacteria used in this study produced a biofilm in the control wells, which is not surprising given that not all bacteria are able to produce a biofilm. *Staphylococcus epidermidis* RP62A produced a highly positive result at both 24 and 48 hours and *Staphylococcus aureus* ATCC produced a low-grade positive at 24 hours. For both of these organisms, the nMgO prevented biofilm formation in this *in vitro* model. To our knowledge this is a finding that has not been previously described for MgO or nMgO. The next logical experiment would be the incorporation of nMgO into a coating so that it could be evaluated in an *in vivo* model.

4.5 Conclusion

Based on the results of this study, nMgO appears to have similar antimicrobial properties to magnesium metal and a fluoroquinolone antibiotic. In general, the findings were consistent with the hypotheses except that the antibiofilm activity was only noted in two of the bacteria studied. The addition of nMgO to a bacterial growth media resulted in a rapid increase in pH and, like Mg metal, this may play a role in the results observed. It is important to note, however, that interaction of the nanoparticles with the bacteria cannot be ruled out as a mechanism of action. Nonetheless we have demonstrated the ability of the supernatant of this material to have an affect on both *in vitro* planktonic growth and biofilm formation.

Figure 4.1: Appearance of the bacterial broth after addition of the nMgO, nZnO and Mg-mesh.

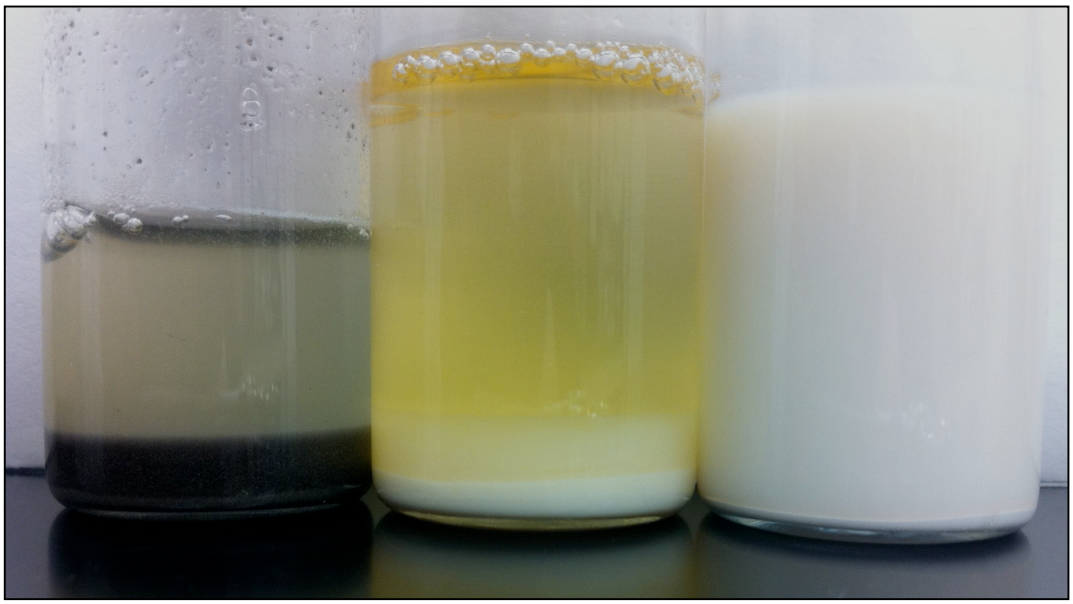

Mg-mesh nMgO nZnO

Figure 4.2: Appearance of the 96-well plate after staining for biofilm production. Explanation of the formula used to calculate the corrected OD_{570} for each pairing.

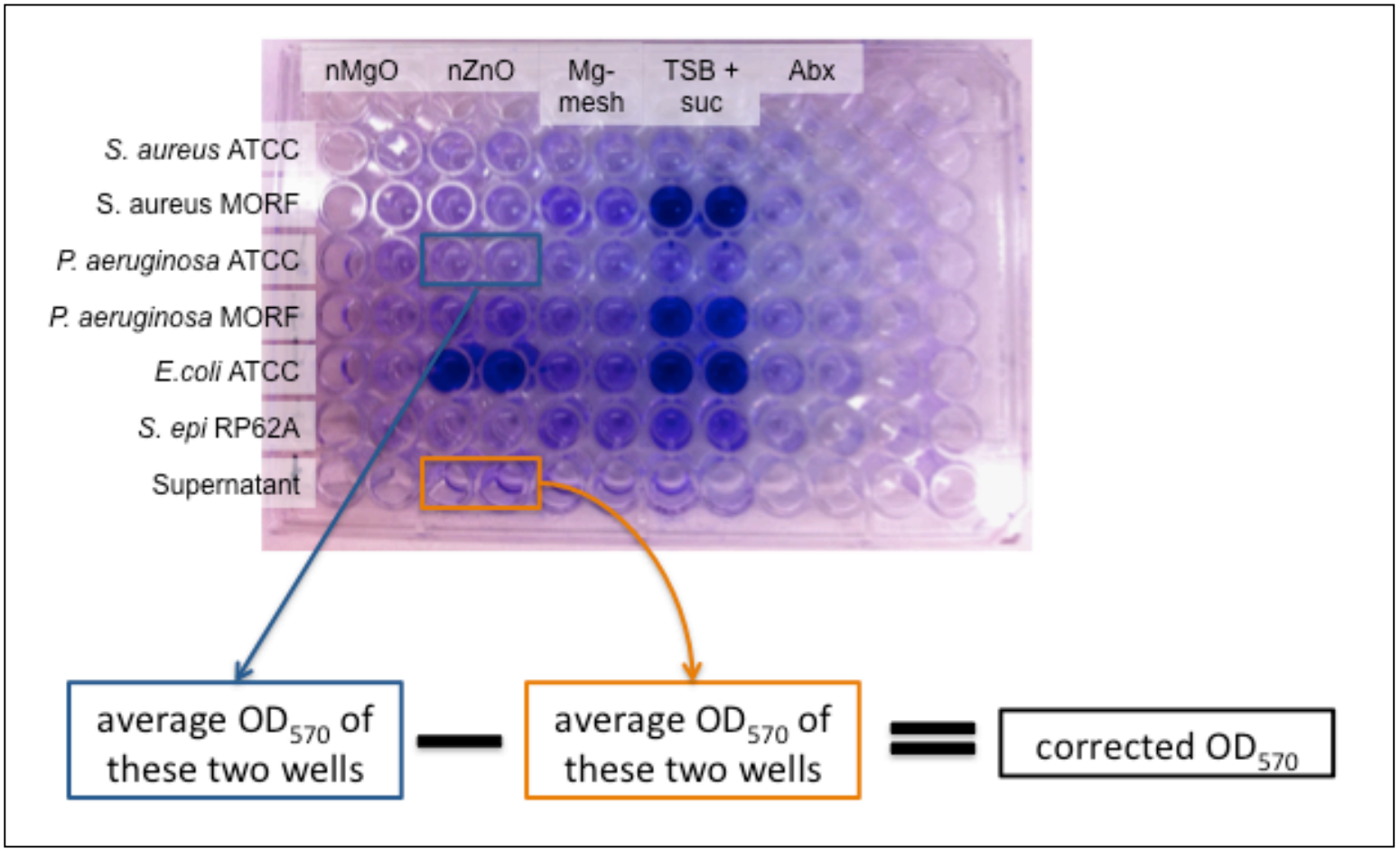

Figure 4.3: Results of pH measurement following the addition of nMgO, nZnO and Mg-mesh to bacterial culture broth.

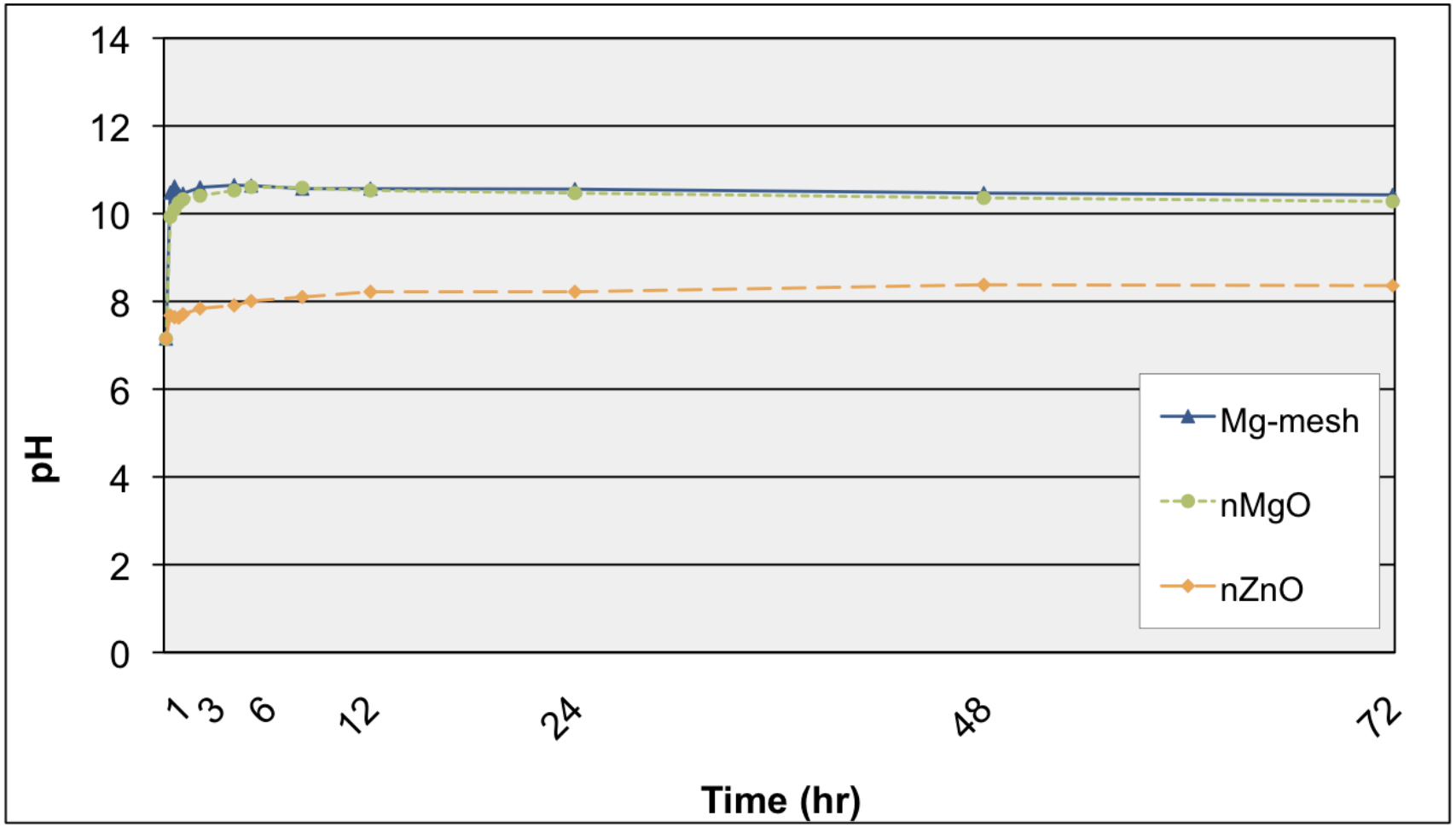

Figure 4.4: Median CFU/ml recovered from incubation with test material. Error bars represent the 25th and 75th percentiles.

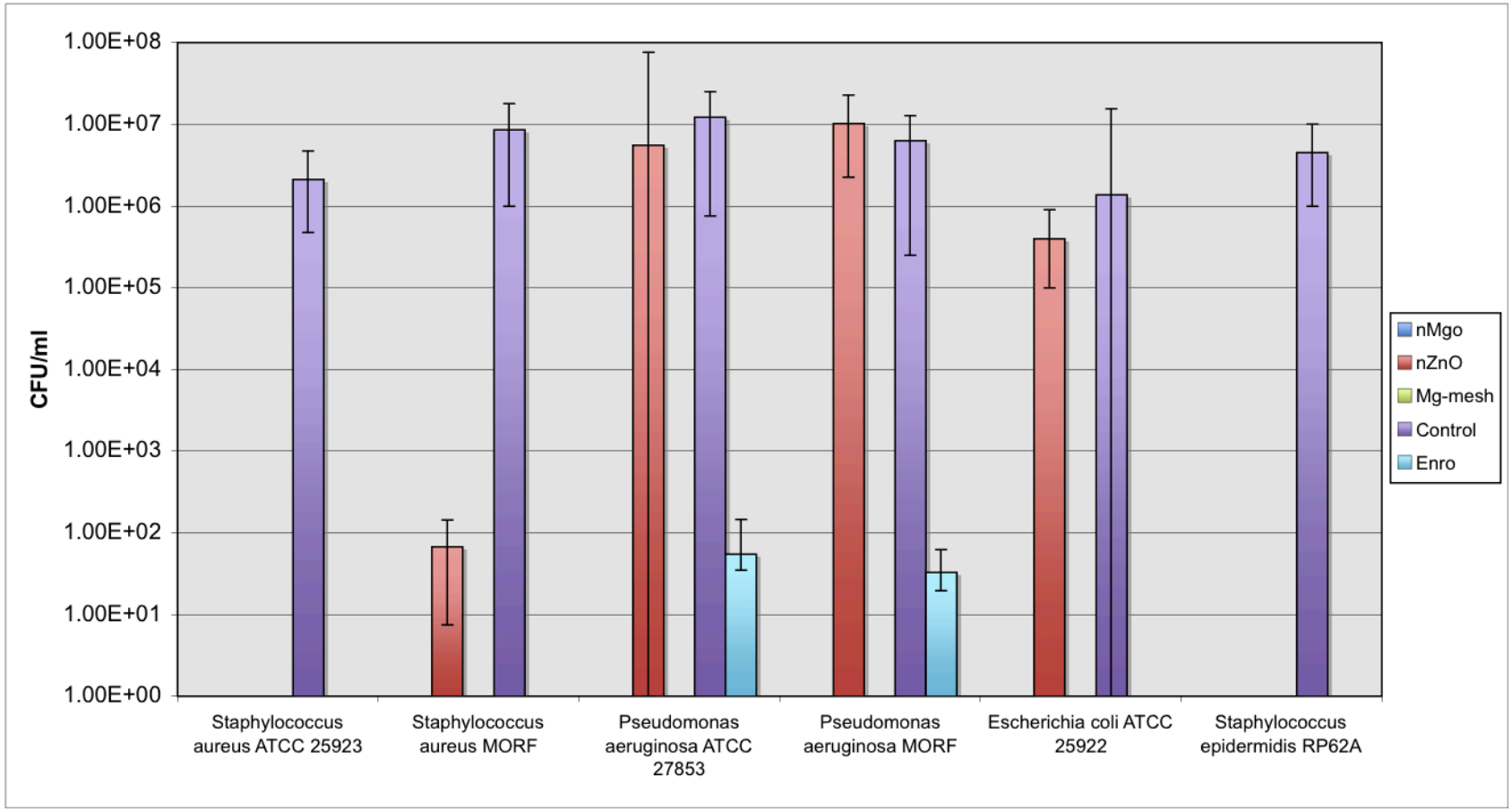

Figure 4.5: Median CFU/ml recovered from incubation with the supernatant from the test material. Error bars represent the 25th and 75th percentiles.

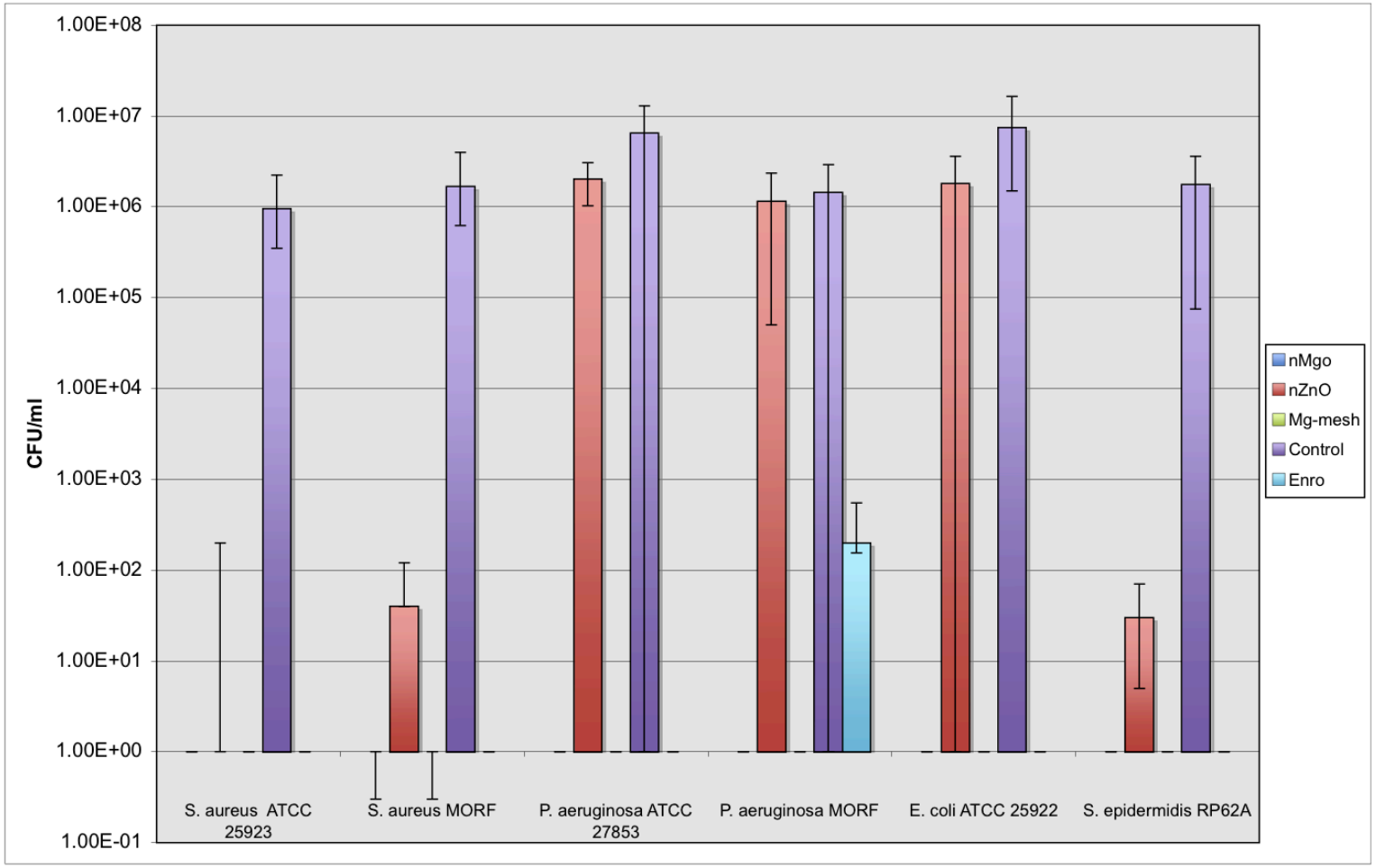

Table 4.1: Inoculation grouping for nanoparticle vials listing the number of vials used for each pairing of material and bacterium.

	nMgO	nZnO	Mg-mesh	Antibiotic	Control
Staphylococcus aureus ATCC	2	2	2	2	2
Staphylococcus aureus MORF	2	2	2	2	2
Pseudomonas aeruginosa ATCC	2	2	2	2	2
Pseudomonas aeruginosa MORF	2	2	2	2	2
Escherichia coli ATCC	2	2	2	2	2
Staphylococcus epidermidis RP62A	2	2	2	2	2

Table 4.2: Setup of 92-well plate for biofilm production. Two separate wells were used for each pairing. The supernatant row was not inoculated with bacteria and was used to control for background noise in the OD readings.

	nMgO	nZnO	Mg-mesh	Antibiotic	TSB + sucrose
Staphylococcus aureus ATCC	2	2	2	2	2
Staphylococcus aureus MORF	2	2	2	2	2
Pseudomonas aeruginosa ATCC	2	2	2	2	2
Pseudomonas aeruginosa MORF	2	2	2	2	2
Escherichia coli ATCC	2	2	2	2	2
Staphylococcus epidermidis RP62A	2	2	2	2	2
Supernatant	2	2	2	2	2

Table 4.3: Biofilm production 24 hours post inoculation. Corrected OD_{570} readings. ★Highly positive ($OD_{570} \geq 1$), §low-grade positive ($0.1 \leq OD_{570} < 1$) or negative ($OD_{570} < 0.1$).).(10) Antibiotic = enrofloxacin.

	nMgO	nZnO	Mg-mesh	Antibiotic	TSB + sucrose
Staphylococcus aureus ATCC	0.02455	0.02020	0.06300	0.01775	0.1192§
Staphylococcus aureus MORF	0.01425	0.00000	0.07110	0.00000	0.06855
Pseudomonas aeruginosa ATCC	0.00000	0.04525	0.00185	0.00545	0.08040
Pseudomonas aeruginosa MORF	0.00000	0.00000	0.02405	0.00000	0.02270
Escherichia coli ATCC	0.00010	0.00000	0.00440	0.00000	0.01185
Staphylococcus epidermidis RP62A	0.00460	0.00120	0.01045	0.02200	1.89005★

Table 4.4: Biofilm production 48 hours post inoculation. Corrected OD_{570} readings. ★Highly positive ($OD_{570} \geq 1$), §low-grade positive ($0.1 \leq OD_{570} < 1$) or negative ($OD_{570} < 0.1$).).(10) Antibiotic = enrofloxacin.

	nMgO	nZnO	Mg-mesh	Antibiotic	TSB + sucrose
Staphylococcus aureus ATCC	0.02985	0.03050	0.02930	0.01160	0.03675
Staphylococcus aureus MORF	0.04095	0.00000	0.03635	0.01425	0.07925
Pseudomonas aeruginosa ATCC	0.01365	0.02025	0.01585	0.01620	0.02325
Pseudomonas aeruginosa MORF	0.00335	0.00620	0.02290	0.01340	0.02215
Escherichia coli ATCC	0.01645	0.02250	0.01690	0.00180	0.01415
Staphylococcus epidermidis RP62A	0.01385	0.03855	0.2647§	0.01165	2.40275★

4.6 Chapter references

1. Lellouche J, Kahana E, Elias S, Gedanken A, Banin E. Antibiofilm activity of nanosized magnesium fluoride. Biomaterials 2009 Oct;30(30):5969-78.
2. Jones N, Ray B, Ranjit KT, Manna AC. Antibacterial activity of ZnO nanoparticle suspensions in a broad spectrum of microorganisms. FEMS Microbiol Lett 2008 Feb;279(1):71-6.
3. Jain J, Arora S, Rajwade JM, Omray P, Khandelwal S, Paknikar KM. Silver nanoparticles in therapeutics: development of an antimicrobial gel formulation for topical use. Mol Pharm 2009 Sep-Oct;6(5):1388-401.
4. Rai M, Yadav A, Gade A. Silver nanoparticles as a new generation of antimicrobials. Biotechnol Adv 2009 Jan-Feb;27(1):76-83.
5. Stoimenov PK, Klinger RL, Marchin GL, Klabunde KJ. Metal Oxide Nanoparticles as Bactericidal Agents. Langmuir 2002 08/01;18(17):6679-86.
6. Robinson DA, Griffith RW, Shechtman D, Evans RB, Conzemius MG. *In vitro* antibacterial properties of magnesium metal against *Escherichia coli, Pseudomonas aeruginosa* and *Staphylococcus aureus*. Acta Biomater 2010 Oct 7;6(5):1869-77.
7. Dong C, Cairney J, Sun Q, Maddan O, He G, Deng Y. Investigation of $Mg(OH)_2$ nanoparticles as an antibacterial agent. J Nanopart Res 2009.
8. Cutler SA, Rasmussen MA, Hensley MJ, Wilhelms KW, Griffith RW, Scanes CG. Effects of *Lactobacilli* and lactose on *Salmonella typhimurium* colonisation and microbial fermentation in the crop of the young turkey. Br Poult Sci 2005 Dec;46(6):708-16.
9. Johannsen SA, Griffith RW, Wesley IV, Scanes CG. *Salmonella enterica* serovar *typhimurium* colonization of the crop in the domestic turkey: influence of probiotic and prebiotic treatment (*Lactobacillus acidophilus* and lactose). Avian Dis 2004 Apr-Jun;48(2):279-86.
10. Zmantar T, Kouidhi B, Miladi H, Mahdouani K, Bakhrouf A. A microtiter plate assay for *Staphylococcus aureus* biofilm quantification at various pH levels and hydrogen peroxide supplementation. New Microbiol 2010 Apr;33(2):137-45.

11. Shakeri S, Kermanshahi RK, Moghaddam MM, Emtiazi G. Assessment of biofilm cell removal and killing and biocide efficacy using the microtiter plate test. Biofouling 2007;23(1-2):79-86.

Chapter 5

In vitro evaluation of the antimicrobial and anti-biofilm effects of nano-magnesium oxide (nMgO) when incorporated into a poly-ε-caprolactone (PCL)-based polymer

Polymeric composites are materials that are widely researched due in large part to the fact that they are bioabsorbable. As a means of preventing bacterial colonization and biofilm formation they can work by preventing bacterial attachment and/or by releasing an antimicrobial drug. With this in mind this study incorporated nMgO and Mg-mesh particles into a poly-ε-caprolactone (PCL) composite. This composite was applied to the surface of 316LSS orthopaedic screws and was also made into 4 mm discs. The *in vitro* antimicrobial activity of the composite was then evaluated against *Staphylococcus aureus* (MORF), *Escherichia coli* (ATCC 25922), *Pseudomonas aeruginosa* (MORF), and *Staphylococcus epidermidis* (RP62A). In all cases the bacteria grew as expected in the control vials. There was a statistically significant difference in the CFU/ml recovered across all treatment groups for all four bacteria in both the screw coatings and polymer disc experiments. For the coated screws when the CFU/ml in the PCL+nMgO group was compared independently to the PCL and no coating groups, a significant decrease in CFU/ml was only noted for *E. coli* and *P. aeruginosa*. For the discs a significant decrease in CFU/ml from the PCL+nMgO group was noted for all organisms except *S. epidermidis*. In this study both nMgO and Mg-mesh were easily added to a PCL polymer and this was then applied to a stainless steel screw. Thin discs of the same polymers were also easily prepared. In this *in vitro* application the nMgO+PCL did result in a significant decrease in some bacteria recovered but this result was not universal for all the organisms evaluated.

5.1 Introduction

The use of polymers, whether natural or synthetic, provide a unique opportunity to decrease bacterial adhesion to a biomaterial by increasing surface hydrophilicity.(1-3) The chemical or physical attachment of poly(ethylene oxide) or poly(ethylene glycol) to surfaces are two examples that have been proposed as a mechanism to create anti-adhesive surfaces. These polymers repel cells and bacteria from the surface by retention of a surrounding hydrous layer.(2) Poly-ε-caprolactone (PCL) is a biodegradable polyester that is degraded under physiologic conditions by hydrolysis of its ester linkages, a process that can be regulated by altering its crystal structure.(3, 4) The degradation process is known to be slower than other resorbable polymers, a feature that makes PCL ideal for use in application where prolonged degradation periods (i.e. > 1-year) are desired.(5) It has a low melting point (60^{o}C) and has ideal tensile properties that have generated interest in its use in tissue engineering applications.(3-5) Another intriguing characteristic is that PCL can be degraded by microorganisms, which are widely distributed in the environment(4, 6) a characteristic that may be advantageous in an infected environment. Degradation by the microorganisms, for example, could release an antimicrobial agent contained within the polymer. Its slow degradation process has lead to development/use in long term implantable devices and in drug delivery systems.(3, 7) It is currently approved by the Food and Drug Administration (FDA) as a component of suture material and other orthopaedic devices (i.e. Artelon® STT spacer, Capronor, Monocryl™ suture).(5, 8) The relative ease of use in processing and material characteristics are why PCL was chosen for further evaluation over other polymer compounds.

There were three main objectives of this study: (1) to determine if nMgO and Mg-mesh could be added to a poly-ε-caprolactone (PCL) based polymer; (2) to determine if this composite could be applied to orthopaedic screws and then evaluate the *in vitro* antimicrobial activity of said coating; and (3) to determine if thin films of the polymer composite could be made and then evaluate the *in vitro* antimicrobial activity of these discs. The hypotheses were: (1) The addition of nMgO and

Mg-mesh to a PCL based polymer will be possible using a chloroform-based emulsion/evaporation process; (2) the polymer composite will be applied to orthopaedic screws via a dip-coating process. Once applied to the orthopaedic screws, the nMgO and Mg-mesh coated screws will have less CFU per ml recovered than the uncoated controls; and (3) thin films will be readily made and the addition of these discs to culture vials will result in a decrease in the CFU per ml recovered when compared to controls.

5.2 Materials and methods

5.2.1 Nano-magnesium oxide, magnesium metal mesh, poly-ε-caprolactone

Commercially available nano-magnesium oxide (nMgO) (≤ 8 nm; specific surface area (BET) ≥ 230 m^2/g)(nanoActive® Magnesium Oxide, NanoScale Corporation, Manhattan, KS, USA) and magnesium metal mesh (Mg-mesh) (< 44 μm) (Mg metal powder, -325 mesh, American Elements, Los Angeles, CA, USA) were used. Poly-ε-caprolactone pellets (Mn= 80,000, Aldrich, St. Louis, MO, USA) were also a commercially available product.

5.2.2 Test materials

250 mg of nMgO or Mg-mesh were used as the source of nanoparticle. Although the Mg-mesh is not technically a nanoparticle, it was the smallest particle size commercially available at the time of this study. 316L stainless steel screws (316LSS) (Synthes Vet, West Chester, PA, USA) were used as the implant to be coated. Chloroform (≥ 99.8% purity, Burdick and Jackson, Muskegon, MI, USA) was used as the solvent for polymer emulsion. Enrofloxacin (Baytril Injectable, Bayer Animal Health, KS, USA) was used as a control for a bactericidal agent. A final concentration of enrofloxacin of 5 μg/disc was used and was added to a 4 mm disc of bibulous paper (Fisherbrand, Pittsburgh, PA, USA).

5.2.3 Bacterial cultures

The bacterial inoculum consisted of one of the following organisms: *Staphylococcus aureus* (MORF 13G – isolated from an infected total hip arthroplasty), *Escherichia coli* (ATCC 25922), *Pseudomonas aeruginosa* (MORF – isolated from an infected tibial implant), and *Staphylococcus epidermidis* (RP62A) (ATCC - American Type Culture Collection, VA, USA; MORF – Excelen Center of Bone and Joint Research and Education, Minneapolis, MN, USA; RP62A – Dr. Paul Fey, University of Nebraska Medical Center, Omaha, NE, USA). These bacterial strains were chosen to represent the spectrum of organisms encountered and because they have been used in other research projects. Thus they are well-established cultures and strains in the *in vitro* setting. Pure cultures of all organisms were aerobically cultured for 24 hours at 37^{o}C on bovine blood agar plates. Samples of each of the pure cultures were collected using a sterile wooden applicator and suspended in 3 ml of TSB broth in 15 ml conical tubes. The tubes were incubated in the water bath at 37^{o}C with agitation at 220 rpm for approximately 2-hours.

5.2.4 PCL composite

250 mg of nMgO or Mg-mesh were added to 15 ml of chloroform. For the control, nothing was added prior to the PCL. The mixture was sonicated at 67 kHz for 15 min to generate colloidal suspensions. 1 g of PCL pellets were added and the mixture was stirred for 24 hours.

Screws were coated by dipping them in the polymer composite for 5 min and allowing them to drain for 15 min between coatings. A total of three coats were applied.(Figure 5.1 and 5.2) They were then dried at room temperature for 24 hours followed by 24 hours at 37^{o}C. This allowed the chloroform to evaporate leaving the PCL composite behind. The uncoated screws were cleaned and rinsed in distilled water.

Films were created by pouring the polymer solution into trays and allowing it to sit for 24 hours at room temperature.(Figure 5.3) 4 mm discs were then cut from the films in areas that were 2-3 mm thick. Screws and discs were soaked in 75% ethanol for 15 minutes prior to use.(9)

5.2.5 Incubation of bacteria with test materials

Disc sensitivity plates

Sterile swabs were inserted into the concentrated broth cultures for each organism. The entire surface of the TSA and bovine blood agar plates were covered using the swab such that a confluent lawn of bacterial growth would occur. Once the plate was dry one of each disc was applied (i.e. PCL alone, PCL+nMgO, PCL+Mg-mesh, enrofloxacin).(Figure 5.4) The plates were incubated for 24-48 hours at 37^{o}C. At this time each plate was examined for a zone of inhibited bacterial growth around each disc.

Screws

Culture vials were prepared such that each contained 0.75 ml of sterile TSB + 5% sucrose. Screws were added to each – PCL, PCL+nMgO, PCL+Mg-mesh, no coating. Each was inoculated with ~10^4 of each organism. These were incubated in a 37^{o}C waterbath at 150 rpm for 48 hours.(Figure 5.5)

Discs

96-well round bottom plates were prepared such that each well contained 180 µl of TSB+5% sucrose. Discs were added to the wells so that there were 4 wells for each material (PCL, PCL+nMgO, PCL+Mg-mesh, enrofloxacin) per bacteria. Each well was inoculated with ~10^4 of each organism. The plates were then covered with sterile, breathable sealing tape (Thermo Scientific 241205, Fisher Scientific, Pittsburgh, PA, USA) and incubated in a dry incubator at 37^{o}C for ~84 hours.

5.2.6 Recovery of bacteria

The 316LSS screws or discs were aseptically retrieved from the culture vials/wells. Under sterile conditions, the screws/discs were rinsed in 1.0 ml sterile, chilled PBS. They were then placed in 1.0 ml of sterile, chilled PBS, and then sonicated (67 kHz) for a total of 40 min, vortexed, and centrifuged (~13,000 rpm) to dislodge adhered bacteria. Samples were then collected, in quadruplicate, for microtiter dilution and the results were used to calculate the CFU per screw/disc. Samples were also collected, in quadruplicate, from the media in the screw culture vials and the CFU/ml was determined.

Microtiter dilutions were performed using a modification of a previously described technique.(10, 11)(Figure 2.1) The CFU in each sample were determined by aseptically collecting a sample followed by ten-fold dilutions (10^{-1} to 10^{-7}) using phosphate buffered saline (PBS) in 96-well round bottom microtiter plates. Twenty μl was collected from each well and streaked across a tryptic soy agar (TSA) (Beckton Dickinson Diagnostic Systems, MD, USA) plate in a uniform manner. The plates were incubated aerobically at 37^{o}C for 24 hours at which time the number of colonies were counted.

5.2.7 Statistical analysis

Summary statistics were calculated and are presented as the median CFU/ml. The error bars in the figures represent the 25th and 75th percentiles. The distributions of CFU/ml were compared for each pair of groups using the least significant difference method to protect against Type I error inflation(12) followed by pairwise Wilcoxon rank sums test for nonparametric data. Statistical significance was set at $P<0.05$.

5.3 Results

5.3.1 Making the PCL composites

In general the process of adding the nMgO or Mg-mesh to the chloroform and then dissolving PCL in the suspension was straightforward. The PCL composite was easily applied to the screws and made into thin films. There were no major complications or processing issues encountered.

5.3.2 Disc sensitivity plates

All four bacteria grew as expected and formed confluent lawns on both the TSA and bovine blood agar plates. A zone of inhibition was only noted around the enrofloxacin discs. Thus neither the PCL+nMgO nor PCL+Mg-mesh inhibited bacterial growth in this model.(Figure 5.4)

5.3.3 Screws

In all cases the bacteria grew as expected in the control vials. There were statistically significant differences in the CFU/ml recovered across all treatment groups for all four bacteria. Grossly, there was a layer of slime/bacterial film noted on some of the screws.(Figure 5.6) Although specific evaluation was not done this presumably represents a biofilm. For the coated screws when the CFU/ml in the PCL+nMgO group was compared independently to the PCL and no coating groups, a significant decrease in CFU/ml was only noted for *E. coli* and *P. aeruginosa*.(Figure 5.7)

5.3.4 Planktonic growth from media the screw incubation media

In all cases the bacteria grew as expected in the control vials. There was a statistically significant difference in the CFU/ml recovered across all treatment groups for *Staphylococcus aureus* MORF, *Pseudomonas aeruginosa* MORF and *Staphylococcus epidermidis* RP62A. A significant difference was not detected for *Escherichia coli* ATCC. For the planktonic growth when the CFU/ml in the PCL+nMgO group was compared independently to the PCL and no coating

groups, significant differences in CFU/ml were noted for the *S. aureus* and *S. epidermidis* groups.(Figure 5.8) For the *P. aeruginosa* group the CFU from the PCL+nMgO vial was significantly higher than that in the no coating vial.(Figure 8) For the *E. coli* group, no significant difference was noted between the PCL+nMgO group and the PCL and no coating vials.(Figure 5.8)

5.3.5 Discs

In all cases the bacteria grew as expected in the control wells. There were statistically significant differences in the CFU/ml recovered across all treatment groups for all four bacteria. Grossly, there was a layer of slime/bacterial film noted on some of the discs and in the wells.(Figure 5.10) In some cases this slime made it difficult to sample the wells.(Figure 5.11) Much like the material on the screws, this most likely represents a biofilm. When the PCL+nMgO discs were compared to the control group, a significantly less CFU/ml were recovered for all organisms except *S. epidermidis*. A similar finding was noted for the PCL+Mg-mesh groups.

5.4 Discussion

In this study both nMgO and Mg-mesh were easily added to a PCL polymer and this was then applied to a stainless steel screw. Thin discs of the same polymer composites were also easily prepared. These are some of the characteristics that make poly-ε-caprolactone (PCL) an attractive polymer. The emulsion solvent/evaporation technique used in this study does present some issues in terms of toxicity of the solvents used. To address this concern attempts have been made to identify solvents for use with PCL that are less toxic.(13) Additionally, the low melting point (60^{o}C) makes it possible to use a hot melt/extrusion technique.(3, 5) Ultimately the technique used for processing this polymer will depend on what is being added to it as well as the targeted use of the end product.

The lack of growth inhibition on the sensitivity plate was not surprising. This methodology relies on elution of the test material from the disc into the surrounding agar creating a zone of inhibited growth. The slow degradation of the PCL may have contributed but the lack of a liquid phase to the environment was likely more of a limitation. Perhaps a thin layer of liquid media on top of the agar would have resulted in a different finding. Nonetheless, the methodology was a poor choice for evaluating the performance of the discs *in vitro*.

The effect of the PCL+nMgO coating on the *in vitro* growth of the *S. aureus*, *E. coli*, *S. epidermidis* and *P. aeruginosa* was unexpected. Mg metal, both as a macromaterial and a smaller particle (Mg-mesh) as well as nMgO have demonstrated antimicrobial properties against these same organisms when added directly to the culture media.(14) (Chapters 2, 4) Once incorporated into the PCL composite nMgO and Mg-mesh failed to have an effect on the CFU/ml of *S. aureus* and *S. epidermidis* while a significant decrease in CFU/ml did occur for the *E. coli* and *P. aeruginosa* strains. It is interesting to note that the organisms unaffected were Gram-positive while those affected were Gram-negative. Given the complex physiochemical relationship between the PCL and Mg particles within the composite and, in turn, the interaction of these with the microbial organisms, it is possible that the difference in cellular structure between a Gram-negative and Gram-positive organism played a role. The results from the planktonic growth in the vials with the screws are difficult to explain. The expectation was not that the coatings would have an effect on the growth of the bacteria within the media but rather only in the attachment and growth on the screws or in the microenvironment around the screw surface. Ideally, there would be no significant difference in any of the vials and in some cases a small difference would be considered an acceptable amount with the methodology used. In the end, this data can only be used to document planktonic bacterial growth within the vials and was not be interpreted any further.

In disc format the results were more consistent with the previous work. *Staphylococcus epidermidis* RP62A was the only case where the CFU/ml in the Mg particle groups was not significantly less than the control group. One possible explanation for the difference was the difficulty encountered in sampling the *S. epidermidis* wells given the propensity to form a slime. This occurred in the control wells and could conceivably have resulted in a lower CFU/ml count. Regardless, the overall finding was that the PCL+nMgO and PCL+Mg-mesh composites did result in a decrease in the bacteria recovered for three out of the four strains evaluated.

Although PCL appears to have worked in this model and is a polymer considered to be a valuable option in biomedical applications(3, 5) there are many factors that must be considered when attempting to produce and then evaluate a polymer based composite. The degradation process for the polymer is important. Does it undergo bulk degradation or surface erosion? In bulk degradation the water penetrates the polymer and hydrolysis can occur throughout the entire matrix. This results in random hydrolytic chain scission allowing monomers and oligomers to diffuse out.(5, 7) In the end the release kinetics of a material are very difficult to predict when bulk degradation occurs.(5, 7) Surface erosion results in a more predictable and controlled release of a drug.(7) In this case hydrolysis occurs on the surface of the polymer while the core remains essentially unchanged.(5, 7) In the case of PCL it appears that it undergoes bulk degradation, but in a two-stage process.(3, 5) Once it reaches a molecular weight of 3,000 or less, the polymer fragments are small enough to diffuse out of the bulk and undergo phagocytosis.(3, 5) Studies in rats have demonstrated intracellular polymer particles at the site of implantation and thus confirmed the role of phagocytosis in the elimination of PCL.(3) The fact the PCL undergoes bulk degradation may explain the results obtained in this study. If the nMgO and/or Mg-mesh were released in an unpredictable manner this may have contributed to the lack of efficacy noted. Another issue may have been the slow degradation process. While this may be ideal in an implant setting, it could have affected the results of this study. Cottam *et al.* report that when incubated in PBS PCL discs lost an average of 1% of their mass over a 13 month

period.(9) As a result, they added lipase derived from *Pseudomonas cepacia* to catalyze degradation.(9) In this study, the samples were incubated for 48-84 hours and therefore was not likely long enough for much, if any, polymer degradation to occur. The susceptibility of PCL to degradation by microbial lipase may present an advantage when used in an infected environment.

PCL has been evaluated for use in orthopaedic applications. In one study PCL coatings were used to control the corrosion of a magnesium alloy.(15) PCL coatings were applied to the surface of the implants using a custom designed spraying device. The implants were evaluated both *in vitro* and *in vivo*. Overall the addition of the PCL resulted in a decrease in the corrosion rate, did not result in any *in vitro* cellular toxicity or inflammation and appeared to increase the volume of new bone formation.(15) In another study Li *et al.* evaluated the incorporation of resveratrol (a drug that has been shown to decrease bone loss in ovariectomized rats) in PCL. The composite was implanted into calvarial defects and resulted in an increase in bone formation when compared to controls.(16) With regards to antimicrobial applications, PCL has been blended with chitosan. Unfortunately, it appeared to inhibit the antimicrobial activity owing to changes in surface topography.(4) A similar finding occurred when bone morphogenetic protein-2 (BMP-2) was incorporated into a PCL coating on an orthopaedic implant. In their *in vitro* studies, the authors identified PCL as a potential carrier for BMP-2 with a burst release followed by a plateau for 30 days. However, in the *in vivo* portion, the authors observed that the PCL layer appeared to act as a barrier and prevented new bone formation.(17) These studies demonstrate the inherent variability in polymer composites and why factors like PCL content, percent of drug loading, method of preparation all must be considered.(3)

The results of the study presented here, although inconclusive, represent an initial step in utilizing Mg nanoparticles in an implant coating. Further work in characterization of the polymer

composite, evaluation of the degree of adherence to the 316LSS, *in vitro* toxicity and release profile of the nanoparticles are some of the next steps in the process.

5.5 Conclusion

This work presents a relatively simple incorporation of a nanomaterial (nMgO) with antimicrobial properties into a biodegradable polymer (PCL). The *in vitro* application the PCL+nMgO did result in a significant decrease in some bacteria recovered but this result was not universal for all the bacteria evaluated. In and of itself, this result is not surprising as most bacteria respond differently to different therapeutics and have differing virulence mechanisms. This pilot work is encouraging and with refinement of the coating process the results may be improved.

Figure 5.1: 316LSS screws being coated with PCL composite. The image on the left is PCL alone and the right is PCL+Mg-mesh.

Figure 5.2: Images of the 316LSS screws after they have been coated. The right is coated with PCL+Mg-mesh, the middle is PCL alone and the right is PCL+nMgO.

Figure 5.3: Images of the PCL composite films that were used to generate the discs. On the left is a PCL+Mg-mesh film and on the right is PCL+nMgO.

Figure 5.4: Images of disc sensitivity plates. On the left is prior to incubation and the right is after incubation. Note that a zone of inhibited bacterial growth only occurred around the enrofloxacin (antibiotic) disc.

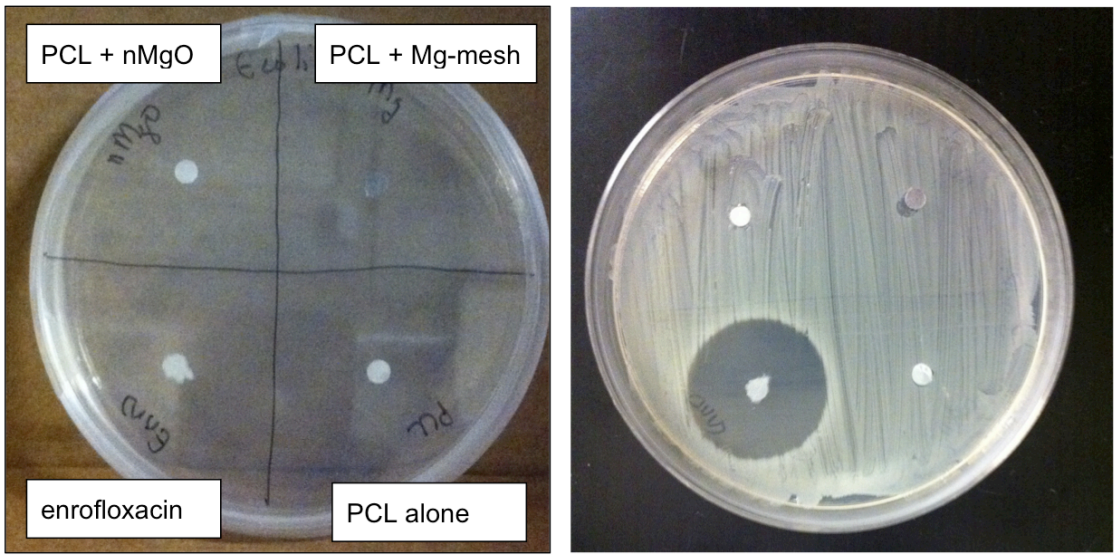

Figure 5.5: Images of the coated screws placed in the culture vials at the start of incubation. On the left is PCL+Mg-mesh, the middle is PCL+nMgO and on the right is an uncoated screw.

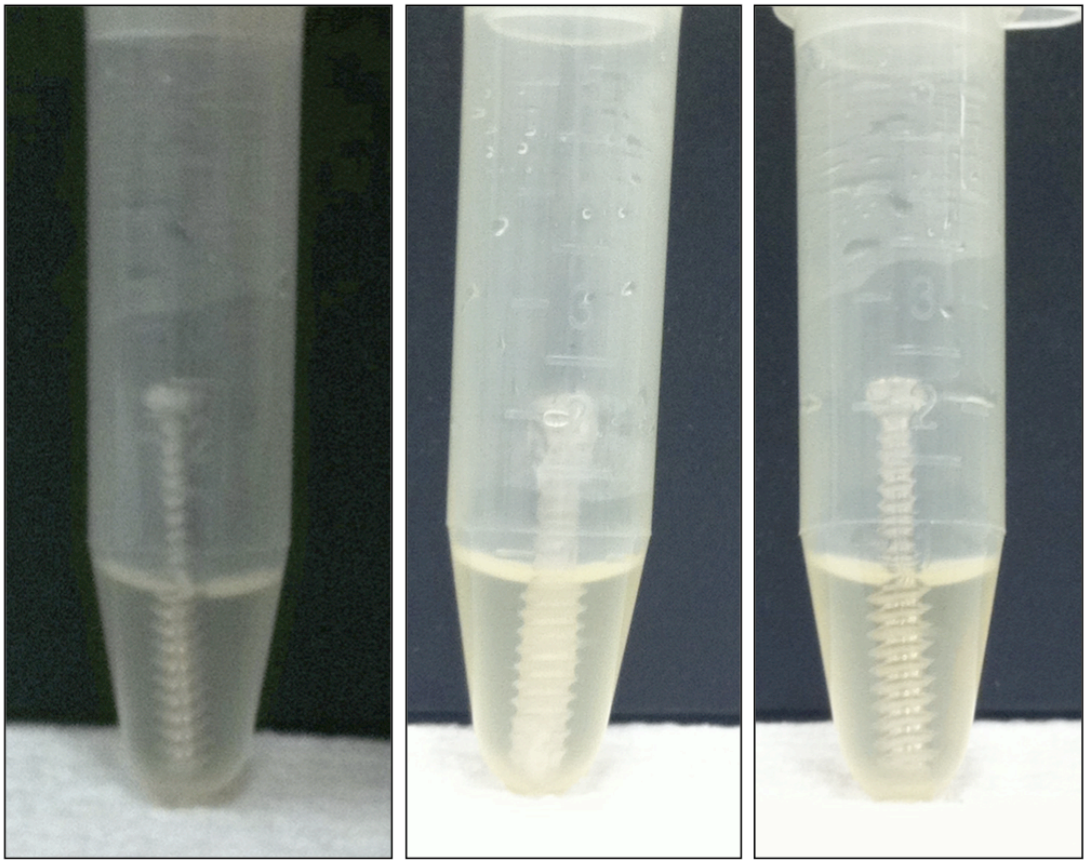

Figure 5.6: Image of a PCL+nMgO coated screw from the *Pseudomonas aeruginosa* MORF group. Not the change in color/slime layer that begins at the arrow and extends distally.

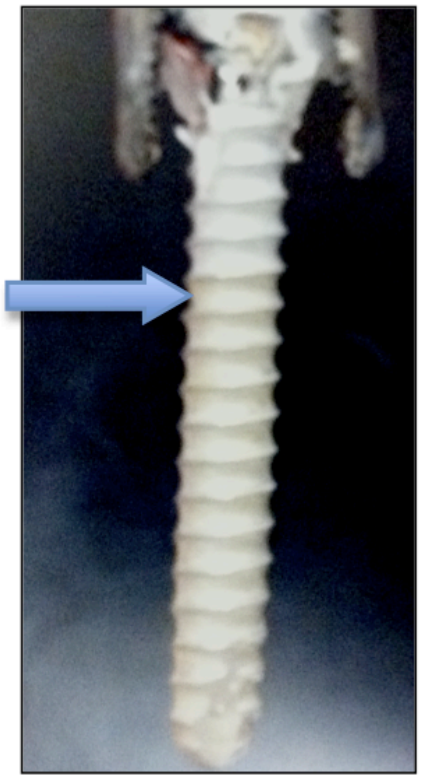

Figure 5.7: Median CFU/ml recovered from the coated screws. Error bars represent the 25th and 75th percentiles. Columns with the same letter **were not** significantly different.

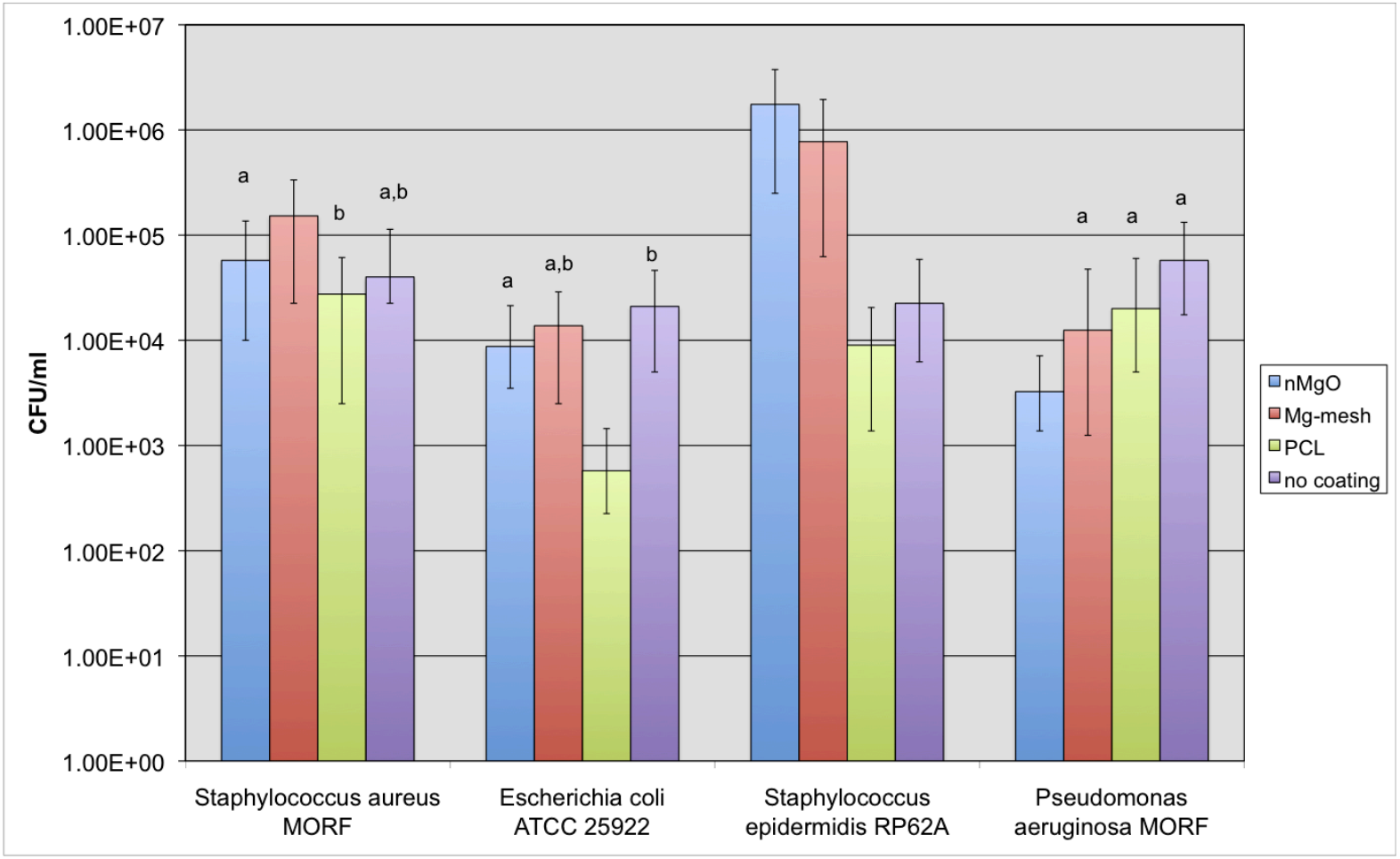

Figure 5.8: Median CFU/ml recovered from growth media that incubated the coated screws. Error bars represent the 25th and 75th percentiles. Columns with the same letter **were not** significantly different.

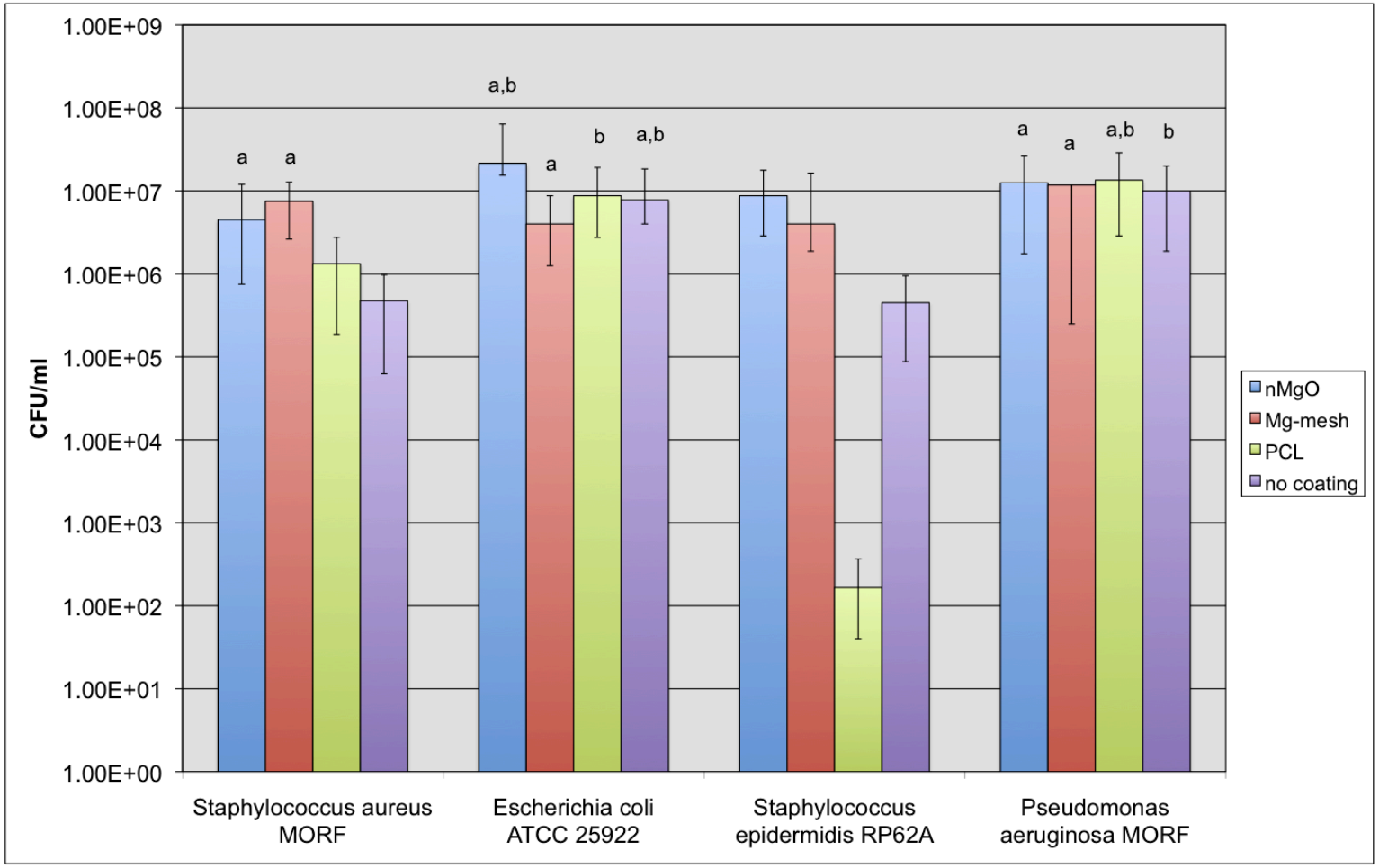

Figure 5.9: Median CFU/ml recovered from the discs. Error bars represent the 25th and 75th percentiles. Columns with the same letter **were not** significantly different.

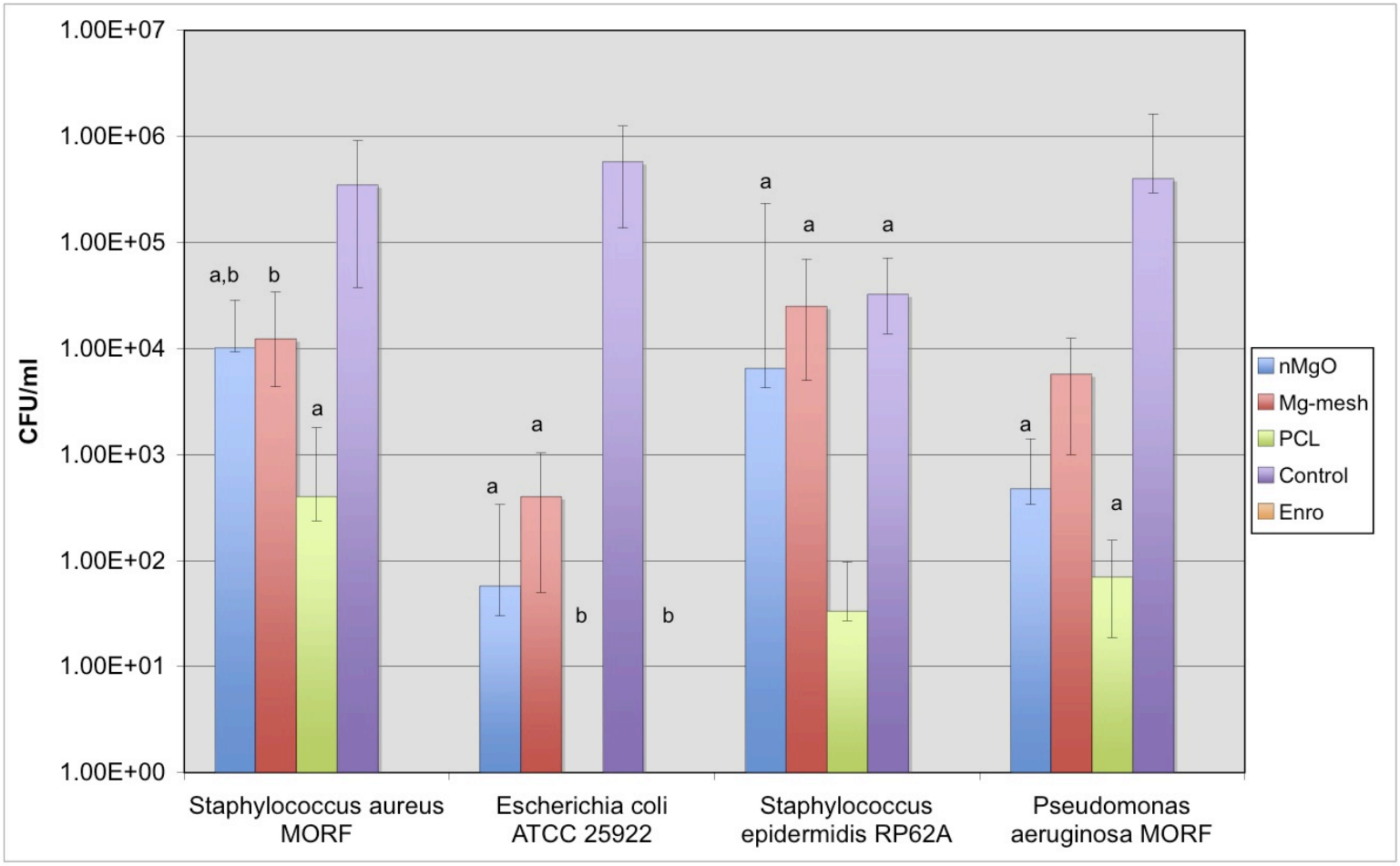

Figure 5.10: Images of the discs before and after incubation with the bacteria. Note the change in the appearance of the PCL+nMgO and PCL discs.

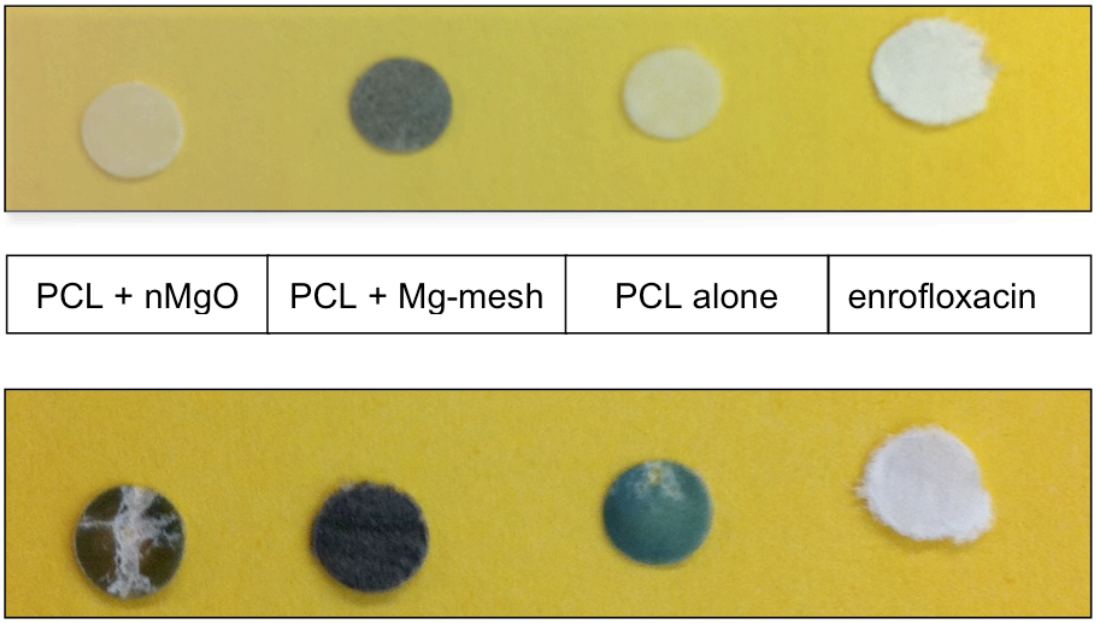

Figure 5.11: Image of the slime produced by *Pseudomonas aeruginosa* MORF (left) and *Staphylococcus epidermidis* RP62A (right) that made it difficult to sample from the well.

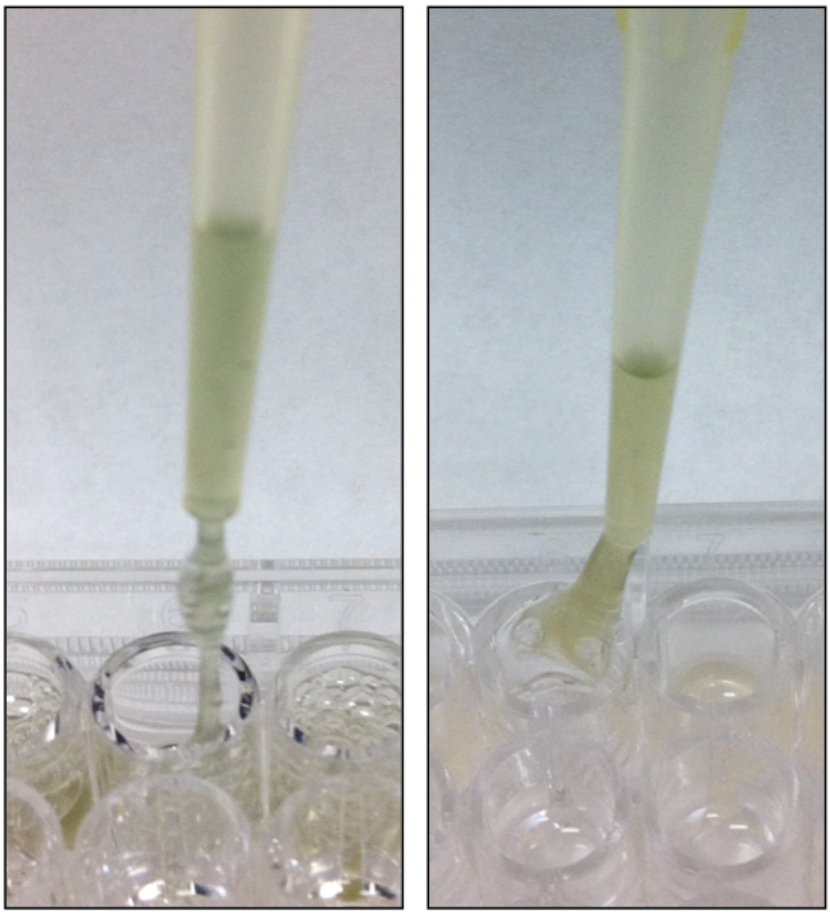

5.6 Chapter references

1. Arciola CR, Alvi FI, An YH, Campoccia D, Montanaro L. Implant infection and infection resistant materials: a mini review. Int J Artif Organs 2005 Nov;28(11):1119-25.
2. Qiu Y, Zhang N, An YH, Wen X. Biomaterial strategies to reduce implant-associated infections. Int J Artif Organs 2007 Sep;30(9):828-41.
3. Sinha VR, Bansal K, Kaushik R, Kumria R, Trehan A. Poly-epsilon-caprolactone microspheres and nanospheres: an overview. Int J Pharm 2004 Jun 18;278(1):1-23.
4. Sarasam AR, Krishnaswamy RK, Madihally SV. Blending chitosan with polycaprolactone: effects on physicochemical and antibacterial properties. Biomacromolecules 2006 Apr;7(4):1131-8.
5. Woodruff MA, Hutmacher DW. The return of a forgotten polymer-ε-polycaprolactone in the 21st century. Progress in Polymer Science 2010 10;35(10):1217-56.
6. Shimao M. Biodegradation of plastics. Curr Opin Biotechnol 2001 Jun;12(3):242-7.
7. Sinha VR, Khosla L. Bioabsorbable polymers for implantable therapeutic systems. Drug Dev Ind Pharm 1998 Dec;24(12):1129-38.
8. Food and Drug Administration. Search term: polycaprolactone. (http://www.fda.gov/default.htm)
9. Cottam E, Hukins DW, Lee K, Hewitt C, Jenkins MJ. Effect of sterilisation by gamma irradiation on the ability of polycaprolactone (PCL) to act as a scaffold material. Med Eng Phys 2009 Mar;31(2):221-6.
10. Cutler SA, Rasmussen MA, Hensley MJ, Wilhelms KW, Griffith RW, Scanes CG. Effects of Lactobacilli and lactose on *Salmonella typhimurium* colonisation and microbial fermentation in the crop of the young turkey. Br Poult Sci 2005 Dec;46(6):708-16.
11. Johannsen SA, Griffith RW, Wesley IV, Scanes CG. *Salmonella enterica* serovar *typhimurium* colonization of the crop in the domestic turkey: influence of probiotic and prebiotic treatment (*Lactobacillus acidophilus* and lactose). Avian Dis 2004 Apr-Jun;48(2):279-86.

12. Ramsey F, Schafer DF. The Statistical Sleuth: A Course in Methods of Data Analysis. 2nd ed. Florence, KY: Cengage Learning; 2002.
13. Bordes C, Freville V, Ruffin E, Marote P, Gauvrit JY, Briancon S, et al. Determination of poly(epsilon-caprolactone) solubility parameters: application to solvent substitution in a microencapsulation process. Int J Pharm 2010 Jan 4;383(1-2):236-43.
14. Robinson DA, Griffith RW, Shechtman D, Evans RB, Conzemius MG. *In vitro* antibacterial properties of magnesium metal against *Escherichia coli*, *Pseudomonas aeruginosa* and *Staphylococcus aureus*. Acta Biomater 2010 Oct 7;6(5):1869-77.
15. Wong HM, Yeung KW, Lam KO, Tam V, Chu PK, Luk KD, et al. A biodegradable polymer-based coating to control the performance of magnesium alloy orthopaedic implants. Biomaterials 2010 Mar;31(8):2084-96.
16. Li Y, Danmark S, Edlund U, Finne-Wistrand A, He X, Norgard M, et al. Resveratrol-conjugated poly-epsilon-caprolactone facilitates *in vitro* mineralization and *in vivo* bone regeneration. Acta Biomater 2011 Feb;7(2):751-8.
17. Niehaus AJ, Anderson DE, Samii VF, Weisbrode SE, Johnson JK, Noon MS, et al. Effects of orthopedic implants with a polycaprolactone polymer coating containing bone morphogenetic protein-2 on osseointegration in bones of sheep. Am J Vet Res 2009 Nov;70(11):1416-25.

Chapter 6

Development of a fracture osteomyelitis model in the rat femur

This chapter has been published as a single manuscript.

Robinson DA, Bechtold JE, Carlson CS, Evans RB, Conzemius MG. Development of a fracture osteomyelitis model in the rat femur. J Orthop 2011 29:131-137.

Osteomyelitis contributes significantly to fracture morbidity. The objective was to develop a model of induced implant-associated osteomyelitis following fracture repair by modifying an existing rat femur fracture model. Thirty male Sprague–Dawley rats were divided into three groups (Control, *Staphylococcus aureus*, *S. aureus* + ceftriaxone). The closed femur fracture model (right femur), stabilized with an intramedullary pin, was combined with inoculation of 10^4 colony-forming units (CFU) of *Staphylococcus aureus*. Radiographs were obtained immediately after surgery and at weeks 1, 2, and 3 and were evaluated by individuals blinded to treatment group. At necropsy the CFU of *S. aureus* per femur and pin were determined and synovial tissue and blood were cultured. The fractured femur from two rats in each group was evaluated histologically. A statistically significant difference in the CFU/femur and CFU/pin was found across treatment groups, with the highest CFU in the *S. aureus* group and the lowest in the Control group. Cultures of synovial tissue were positive in 11/19 of inoculated limbs. Osteomyelitis was present both radiographically and histopathologically in both *S. aureus* groups but not in the controls. No rats were systemically ill or had positive blood cultures at the study endpoint. This model will be useful for the evaluation of treatments or prophylactics designed for use in implant-associated osteomyelitis.

6.1 Introduction

In recent years the increasing use of implantable medical devices, both temporary and permanent, combined with the growing number of immunocompromised individuals being treated, has lead to a greater number of nosocomial infections.(1, 2) Several reports discuss device-associated infections in terms of economic and clinical consequences(3–5), and some studies suggest that *Staphylococcus* spp. can be isolated from deep wound infections in 70–90% of elective orthopaedic surgery patients.(6) This issue increases in importance as the recent rise in infections associated with methacillin/oxacillin-resistant organisms that respond poorly to traditional therapies is considered. Although advances in surgical technique, implant sterilization, and infection control have helped decrease the likelihood of implant-associated osteomyelitis, most would argue that bacterial contamination and infection still occur at an unacceptable level.

Bacterial biofilms have been ascribed a central role in implant-associated osteomyelitis due, in large part, to their resistance to antimicrobial therapy and clearance by the host immune system.(3, 7–9) The development of a biofilm is dependent on several bacterial, substrate, and host factors and is a process that is initiated by adherence of planktonic organisms.(4, 10) Regardless of their source or location, bacterial biofilms contribute significantly to increased morbidity and mortality, represent a therapeutic challenge, and are an area of tremendous interest in the research community. An important need in this area of research is an animal model that effectively mimics the clinical situation. While numerous implant-associated osteomyelitis models exist, most require creation of a bone defect(11), involve creation of an open fracture(12), result in chronic osteomyelitis(13) or require the use of a sclerosing agent to enhance infection(13). At the present time there is not a model that can be used to appropriately mimic implant-associated acute osteomyelitis following repair of closed fractures.

The use of an intramedullary pin or nail is a typical treatment method for many closed fractures.

Therefore, creating an animal model that mimics this clinical scenario would render the model useful for translational studies that are designed to evaluate methods to prevent and/or treat osteomyelitis and biofilm formation.

The objective of this study was to modify an existing femur fracture model in the rat to one that could be used as a model of osteomyelitis associated with a closed fracture. We hypothesized that an injection of 10^4 colony-forming units (CFU) of *Staphylococcus aureus* would result in acute osteomyelitis and impaired fracture healing in a rat femur fracture model. The development of osteomyelitis was verified by determining the number of CFU per femur, serial radiographic evaluations of osteomyelitic changes, and postmortem histopathological appearance of the tissues.

6.2 Materials and methods

6.2.1 Study design

Thirty male Sprague–Dawley rats (250–300-g) were randomly assigned into three groups (n=10/group): Control (pinned femur fracture); *S. aureus* (pinned femur fracture and bacteria); and *S. aureus* + ceftriaxone (pinned femur fracture and bacteria and antibiotics). The appetite, general attitude, and surgical sites of the rats were monitored every 12 hours for the first 7 days after surgery, after which they were monitored every 24 hours. The body weight of each rat was measured prior to surgery and every 7 days after surgery, until the end of the study. Opioid analgesia (buprenorphine 0.03 mg, Butler Animal Health, Dublin, OH, USA) was given via subcutaneous injection every 12 hours for the first 3 days after surgery. The rats were humanely euthanized when they developed radiographic evidence of severe osteomyelitis with systemic illness or 3 weeks after surgery, whichever occurred first. The development of osteomyelitis was documented via serial radiographs (all animals) and postmortem microbiologic (n = 8 per group)

and histopathologic (n = 2 per group) analyses. The study was approved by the Institutional Animal Care and Use Committee.

6.2.2 Bacterial culture

The organism used was a *Staphylococcus aureus* (MORF) strain that was isolated from a patient with an infected total hip arthroplasty, was known to have maintained virulence as assessed by its ability to cause osteomyelitis, and was known to have an in vitro sensitivity to ceftriaxone.(11, 14–16) Prior to use in the inoculation, a pure culture of the *S. aureus* was grown for 24 hours on blood agar plates. The bacterial inoculum was prepared such that there was 10^4 CFU in 50 µl of phosphate-buffered saline (PBS). Tryptic soy broth (TSB) was used as the culture media for the growth of the bacteria from harvested specimens. Tryptic soy agar (TSA) plates were used to grow and quantify organisms recovered from the implant and femora. All organisms and culture samples were incubated at 37^{o}C in ambient air.

6.2.3 Implants (Figure 6.1)

316L stainless steel pins (316LSS) (IMEX Veterinary Inc., Longview, TX, USA) (n = 30), 1.4 mm in diameter and 26 mm in length, were used to internally stabilize the femur fracture. One end of the pin was hand milled so it had a smaller diameter (0.8 mm) and could be easily seated in the proximal aspect of the femur. All pins were sterilized by steam autoclave sterilization before being used.

6.2.4 Surgical procedure

The surgical procedure was a modification of that outlined in detail in Skott *et al.*(17) Briefly, each rat was anesthetized using intraperitoneal injections of ketamine (100-200 mg/kg) and xylazine (2 - 4 mg/kg) and maintained using isoflurane delivered in oxygen via a mask. Breathing rate and depth, mucous membrane color, and jaw tone were used to measure the depth of anesthesia. The right femur was aseptically prepared and an approach to the distal femur was made via a

medial stifle arthrotomy.(Figure 6.2) An 18 gauge needle was used to create an entry port into the distal aspect of the medullary canal of the femur and ream the canal for placement of the intramedullary pin.(Figure 6.3) An inoculation dose of 50 µl of bacterial suspension was slowly injected into the medullary cavity via an 18 gauge polypropylene catheter that was left in place for 2 min following inoculation.(Figure 6.4) In the Control group PBS was injected instead of the bacterial suspension. After the bacteria or PBS were injected, the pin was inserted (narrow portion first) into the medullary canal and seated into the cortical bone in the proximal aspect of the femur.(Figure 6.5) The opening in the distal femur was sealed with bonewax (Ethicon, Somerville, NJ, USA) to prevent leakage of the bacterial inoculum from the medullary canal. The surgical site was lavaged with sterile saline and the soft tissues and skin were closed. A mid-shaft closed fracture of the right femur was then created using a specifically designed fracture apparatus.(17,18) (Figure 6.6) The femur was radiographed to document the fracture and the rat was recovered from anesthesia. Rats in the *S. aureus* + ceftriaxone group received ceftriaxone (50 mg/kg) every 24 hours, starting 4 hours after inoculation, via a subcutaneous injection for the duration of the study.

6.2.5 Radiographic assessment of osteomyelitis (Figure 6.7)

Lateral radiographs of the right hind limb were obtained immediately after surgery and at weeks 1, 2, and 3 postoperatively using a digital dental radiographic system (Scan X Digital Imaging System; Air Techniques, Inc., Melville, NY). Two individuals, blinded to study group, evaluated the radiographs focusing on three regions of interest (ROI): (a) proximal metaphyseal area where the implant was seated in cortical bone; (b) diaphyseal region involving the site of the fracture; and (c) distal metaphyseal area where access to the medullary canal was made. During each evaluation each radiograph was assessed based on a system described by Lucke *et al.*(6, 19) The following radiographic changes were evaluated for each ROI: (a) osteolysis; (b) soft tissue swelling; (c) periosteal reaction; (d) general impression; and (e) deformity. The changes were given a score corresponding to the following scale: 0 - absent; 1 - mild; 2 - moderate; or 3 -

severe. For the general impression evaluation a 0 represented a normal appearing femur/fracture and a 3 represented severe changes were present overall. In addition, sequestra formation (f) and spontaneous fracture (g) were evaluated for each femur as a whole and were given a score of 0 - absent or 1 - present. The scores were then summed, with highest possible total score being 47. The average of the scores from two evaluators were used for statistical evaluation.

6.2.6 Recovery of bacteria

Three weeks after surgery, the rats were sedated for radiographic evaluation of the operated femur after which a blood sample (approximately 2 ml) was collected aseptically and transferred to a blood culture container (BBL Septi-Chek TSB 20 ml, BD Company, Franklin Lakes, NJ, USA) for aerobic culture, according to the manufacturer's directions. After incubation for 7 days samples were aseptically retrieved from the blood culture container and streaked onto blood and MacConkey agar plates, which were then incubated for 48 hours at 37^{o}C, after which the plates were evaluated for bacterial growth (methods described below).

After euthanasia a sample of synovium was retrieved from both the operated (right) and unoperated (left) stifle joint from each animal for aerobic culture. The tissue samples were placed in 10 ml of TSB and incubated at 37^{o}C for 48 hours at which time each sample was classified as culture positive or negative based on the presence of turbidity in the culture vial. Both femurs were aseptically retrieved and used for bacterial quantification. The 316LSS pins were aseptically retrieved from the operated femurs prior to snap freezing. Under sterile conditions, the pins were placed in 1 ml of sterile, chilled PBS, and then sonicated (67 kHz), vortexed, and centrifuged (~11,000 rpm) to dislodge adhered bacteria. Samples were then collected for microtiter dilution and the results were used to calculate the CFU/pin (methods described below). Each femur was snap frozen and ground to a powder under sterile conditions.(11) The resulting

powder was suspended in 3 ml of chilled TSB, which was kept on ice until sampled (< 10 min) for microtiter dilutions and calculation of the CFU/femur (see methods below).

6.2.7 Microtiter dilution and viable bacterial counts (Figure 2.1)

Microtiter dilutions were performed using a modification of a previously described technique.(20, 21) The CFU in each tube was determined in quadruplicate by aseptically collecting a sample. Tenfold dilutions were made (10^{-1} to 10^{-6}) using PBS in 96-well round bottom microtiter plates. Twenty microliters was collected from each well and streaked across a TSA (Beckton Dickinson Diagnostic Systems, Sparks, MD) plate in a uniform manner. The plates were incubated aerobically at 37^{o}C for 24 hours at which time the number of colonies were counted. Dilutions with up to 30 colonies present were used to calculate the median CFU/pin or CFU/femur.

6.2.8 Histopathologic evaluation

The operated femurs from two rats in each group (n = 6 total) were used for histopathological evaluation. After removal of soft tissues, the intact femurs were fixed in 10% neutral buffered formalin for 48-h, after which they were transferred to 70% ethanol. After decalcification in 10% EDTA, the femurs were bisected midsagittally and the implant was removed. The bisected femurs were then processed for histology and embedded, longitudinally, with the cut surface down, in paraffin. Two 5 μm-thick sections were obtained from one block from each femur and were stained with hematoxylin and eosin. The sections were then evaluated by a veterinary pathologist who was blinded to treatment group. Histopathologic descriptions were provided for each section and then combined to provide a summary description for each of the three groups.

6.2.9 Statistical analysis

The results of the radiographic scoring across the three treatment groups were compared using one-way analysis of variance (ANOVA). The recovered CFU/pin and CFU/femur were reported as median CFU and were compared across all three groups using a Kruskal–Wallis one-way

analysis of variance (chi-square analysis), with significance set at $p<0.05$. The distributions of radiographic scores were compared for each pair of treatment groups using the Student's t-test with Bonferroni correction. The distributions of CFU/pin or CFU/femur were compared for each pair of treatment groups using the pairwise Wilcoxon rank sums test for nonparametric data with Bonferroni correction, with significance set at $p < 0.017$ (Bonferroni correction = 0.05/3 = 0.017).

6.3 Results

One rat in each of the Control and *S. aureus* + ceftriaxone groups had to be euthanized within 24 hours of surgery due to incisional dehiscence/self-mutilation. As a result of this, only seven rats were available for the culture-related outcome measures in both the Control and *S. aureus* + ceftriaxone groups versus eight rats in the *S. aureus* group. Similarly, only nine rats had radiographs available for evaluation in the Control and *S. aureus* + ceftriaxone groups versus 10 rats in the *S. aureus* group. No other rats had any obvious health issues and all remaining rats gained weight in a similar manner over the course of the study.

6.3.1 Radiographic assessment

Radiographs were available for all rats that survived the study period.(Figure 6.8) The fracture site was most evident in the *S. aureus* group, followed by the *S. aureus* + ceftriaxone group, but was only faintly evident in the Control group. The radiographs from the Control group were characterized by the formation of a normal bridging fracture callus and minimal periosteal reaction. There was a radiolucent area within the fracture callus that was typical of what would be expected at this stage of healing. The *S. aureus* group was characterized by a severe periosteal reaction extending along the entire length of the femur, accompanied by significant osteolysis. The periosteal new bone did not bridge the fracture site and osteolytic areas of radiolucency extended proximally and distally from the fracture site. The *S. aureus* + ceftriaxone group was characterized by a small amount of periosteal reaction and new bone formation. The

facture callus did not bridge the fracture site and the areas of radiolucency were present to a lesser degree when compared to the *S. aureus* group. The mean ± SE radiographic scores for the radiographs taken immediately postoperatively were similar in each of the three treatment groups (ANOVA, $p = 0.77$). The mean ± SE radiographic scores were significantly different at week 1 ($p = 0.02$), week 2 ($p < 0.0001$), week 3 ($p = 0.0005$). When the treatment groups were compared as pairs at all three time points, the radiographic scores for the *S. aureus* group were significantly higher than those in the Control group at each postoperative time point. The radiographic scores for the *S. aureus* + ceftriaxone group were significantly higher than those in the Control group at week 2 but not at week 1 or 3. The scores for the *S. aureus* group were also significantly higher than those of the *S. aureus* + ceftriaxone group at weeks 2 and 3, but not at week 1.(Table 6.1)

6.3.2 Recovery of bacteria

No bacteria were recovered from the left (unoperated) femur of any of the rats from any of the treatment groups or from the right (operated) femur in rats in the Control group. Chi-square analysis revealed a significant difference in the CFU/right femur ($p < 0.0001$) and CFU/pin ($p = 0.0002$) across all three-treatment groups. When the results were compared using the pairwise Wilcoxon rank sums test for nonparametric data, the CFU/right femur was significantly higher in the *S. aureus* ($p = 0.0006$) and the *S. aureus* + ceftriaxone ($p = 0.0008$) groups compared with the Control group; the CFU/right femur was significantly higher in the *S. aureus* group compared with the *S. aureus* + ceftriaxone group ($p = 0.0026$). The CFU/pin results followed an identical pattern to CFU/femur.(Figure 6.9 and 6.10)

Blood cultures were negative for all 28 rats. Stifle cultures were positive in 8/10 of the knees of rats that were in the *S. aureus* group, 3/9 of the knees of rats that were in the *S. aureus* + ceftriaxone group, and 0/9 of the knees of the rats in the Control group. None of the unoperated (left) knees had positive culture results.

6.3.3 Histopathology

Specimens within each treatment group were similar histologically. Specimens from the Control group were characterized by the presence of a callus that was composed of hyaline cartilage and periosteal new bone that bridged the fracture site in both specimens. No areas of inflammation were noted. In contrast, specimens from the *S. aureus* group were characterized by severe suppurative osteomyelitis with extension of the inflammation to the joint space and periosteum accompanied by extensive myelofibrosis. Although an extensive callus was present in both specimens, involving the diaphysis, metaphysis, and epiphysis, it contained extensive areas of fibrous connective tissue and inflammation (primarily composed of neutrophils) in the area of the fracture site, resulting in the lack of a bony bridge over the site. In both specimens, there also was nearly complete loss of cortical bone the majority of the diaphysis, with only necrotic fragments of this tissue remaining. Specimens from the *S. aureus* + ceftriaxone group contained a few small foci of suppurative inflammation; however, the marrow cavity, which in the specimens from the *S. aureus* group contained extensive areas of inflammation, was largely filled with fibrous connective tissue. Both specimens contained a bridging callus that was composed primarily of new bone but included a small component of hyaline cartilage.(Figure 6.11)

6.4 Discussion

Orthopaedic implants related infections occur in nearly 112,000 human patients annually and create an estimated $1.8-billion burden to the healthcare industry.(3) Among categories of orthopaedic implants, fracture fixation devices are particularly susceptible to infection as they are often used on devitalized tissue that may or may not have accompanying wounds that have been contaminated with bacteria.(3, 4) The physical and emotional consequences are more difficult to measure; however, infections also often result in revision surgeries, prolonged antibiotic therapy,

impaired functional outcome, and lengthy hospital stays.(6) The overall outcome is increased patient morbidity and in some cases mortality.(22)

An animal model that reproduces the salient features of the clinical situation is critical to advance scientific investigations in this field. While there are other implant associated infection models in the rat(11-13), none effectively mimic osteomyelitis that occurs following repair of closed fractures. The model presented here is based on a modification of a previously described fracture model, where a mid-diaphyseal closed fracture of the femur was created using a specifically designed fracture apparatus.(17, 18) In the present study, the femur was inoculated with a *S. aureus* strain that was known to be capable of producing osteomyelitis, as demonstrated by its use in other studies.(11, 14-16) Because the fracture site itself was not approached to insert the intramedullary nail, to inoculate the femur or to create the fracture, this model may better reflect the clinical situation of bacterial contamination of a closed fracture. The inoculation of this *S. aureus* strain at 10^4 CFU was effective in producing osteomyelitis without having untoward systemic effects on the rats. All the rats gained weight in a similar manner over the course of the study, none had positive blood cultures at the end of the study, and none of the unoperated femurs or synovial membrane samples had positive culture results.

In assessing an orthopaedic model, the use of a radiographic scoring system has several advantages. It is a noninvasive method of collecting data over the course of a study and mimics a diagnostic modality that is used in clinical practice. In our study we used a previously published system(6,19) where ROI were identified and scored using seven different parameters. Significant differences in the radiographic score for osteomyelitis were detected between the Control group and the *S. aureus* group by 1 week after surgery/inoculation. When the *S. aureus* group was compared to the *S. aureus* + ceftriaxone group a significant difference could also be found starting at week 2. These findings demonstrate that the model was representative of the clinical situation and differences between groups could be monitored noninvasively over time. However,

it is important to note that even though reviewers of the radiographs were blinded to group assignment, this remains a subjective outcome measure.

Osteomyelitis is often caused by bacterial infections making the recovery of bacteria an important characteristic of a proposed model. In our study, both the operated and unoperated femurs and pins from operated femurs were cultured and the bacteria recovered quantified as CFU per femur and pin. Blood and tissue cultures were also performed to determine if there was evidence of bacteremia or inoculation of the stifle during surgery. No bacteria were cultured from any of the blood samples or any of the unoperated femurs irrespective of the treatment group suggesting that in this model the infection remains localized to the contaminated femur. Bacteria were consistently retrieved from the inoculated femurs and none were retrieved from the Control group. Significant differences were found when the Control group was compared to both the *S. aureus* and *S. aureus* + ceftriaxone groups with respect to the CFU/right femur and CFU/pin. While antibiotic therapy did not eliminate the bacterial infection, significant treatment differences were noted, additional evidence that the model represents the clinical situation. However, one limitation of this model is that the knee (stifle joint) that was used to introduce bacteria into the femur was contaminated and a positive synovial tissue culture was found 3 weeks after surgery nearly 60% of the time. Additionally, this culture assessment did not evaluate the numbers of viable bacteria present, information that would be informative in treatment group comparisons. Because the possibility of septic arthritis exists, future investigations using this model must pay special attention to limiting contamination to the knee when introducing the bacteria, sealing the site where the pin is introduced into the femur and thoroughly lavaging the knee to further limit the contamination.

Although only two specimens/treatment groups were evaluated histologically, the results within each group were remarkably consistent; however, marked differences between the treatment groups were apparent. The marked inflammation present in the sections from the *S. aureus*

group was greatly attenuated in the *S. aureus* + ceftriaxone group. The quality of the callus was similar in the Control and *S. aureus* + ceftriaxone groups, but was poor in the *S. aureus* group. Grading schemes are available for use in these types of samples and would provide additional semiquantitative information in studies in which a larger sample size is available for evaluation.(6, 19, 23)

While there exist other models of implant-associated osteomyelitis(11-13, 24-26) the model presented here is unique in that it mimics implant-associated osteomyelitis in the setting of a closed fracture repair. Hematogenous models are excellent examples but they tend to be used to model seeding of an implant (e.g., seeding of an orthopedic implant after a dental procedure) and are thus not well suited for the "acute" setting without the use of trauma or additional foreign objects (e.g. sand).(24-26) Hematogenous models also run the risk of systemic consequences and often require higher amounts of inoculum, increasing the risk of morbidity and mortality. Hienz *et al.* reported that in order to achieve an infection rate of 100% an inoculum of 5×10^8 was required and that, without the use of the sclerosing agent, sodium morrhuate, osteomyelitis did not occur consistently.(27) Poultsides *et al.* reported that "variation between 1×10^8 and 4×10^8 CFU/ml induced reproducibly either no infection or acute infection and, consequently septic shock and death, respectively."(23) Thus, the advantages of our model are that it consistently produced osteomyelitis, did not have any obvious systemic effects and used a smaller inoculum (10^4 CFU) of bacteria.

6.5 Conclusion

The radiographic changes; bacterial isolation from infected femurs and implants; and histopathological changes document the reliable development of osteomyelitis after the inoculation with 10^4 CFU of *S. aureus* in this model. Thus, we can accept our hypothesis and

further suggest that this model has the potential to be used in evaluating anti-fouling/anti-biofilm implant coatings or other osteomyelitis studies.

Figure 6.1: Image of the 316LSS pin implant used. Note how one end of the pin is hand milled so it had a smaller diameter.

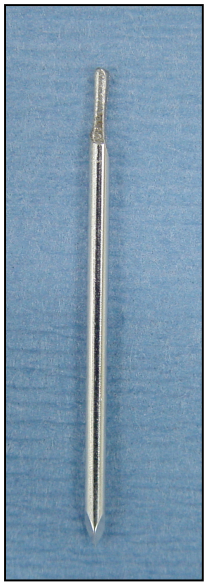

Figure 6.2: Medial stifle arthrotomy. The ★ indicates the distal aspect of the femur.

Figure 6.3: Preparation of the femoral canal.

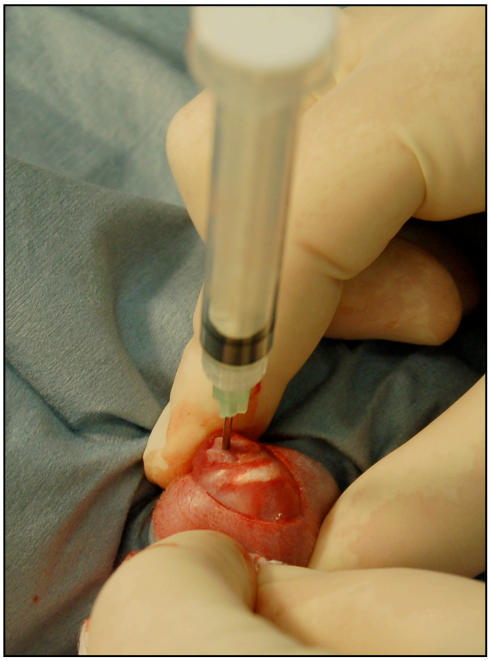

Figure 6.4: Inoculation of the femoral canal.

Figure 6.5: Insertion of the intramedullary pin.

Figure 6.6: Fracture apparatus. Note the load cell and weight. The grey figure represents the placement of the rat femur in the apparatus.

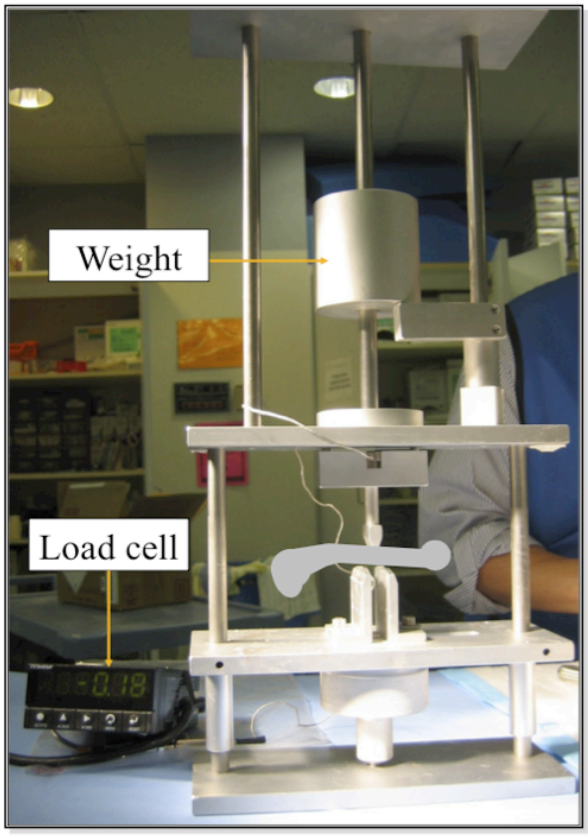

Figure 6.7: Diagrammatic representation of the system used to evaluate the radiographs.(19)

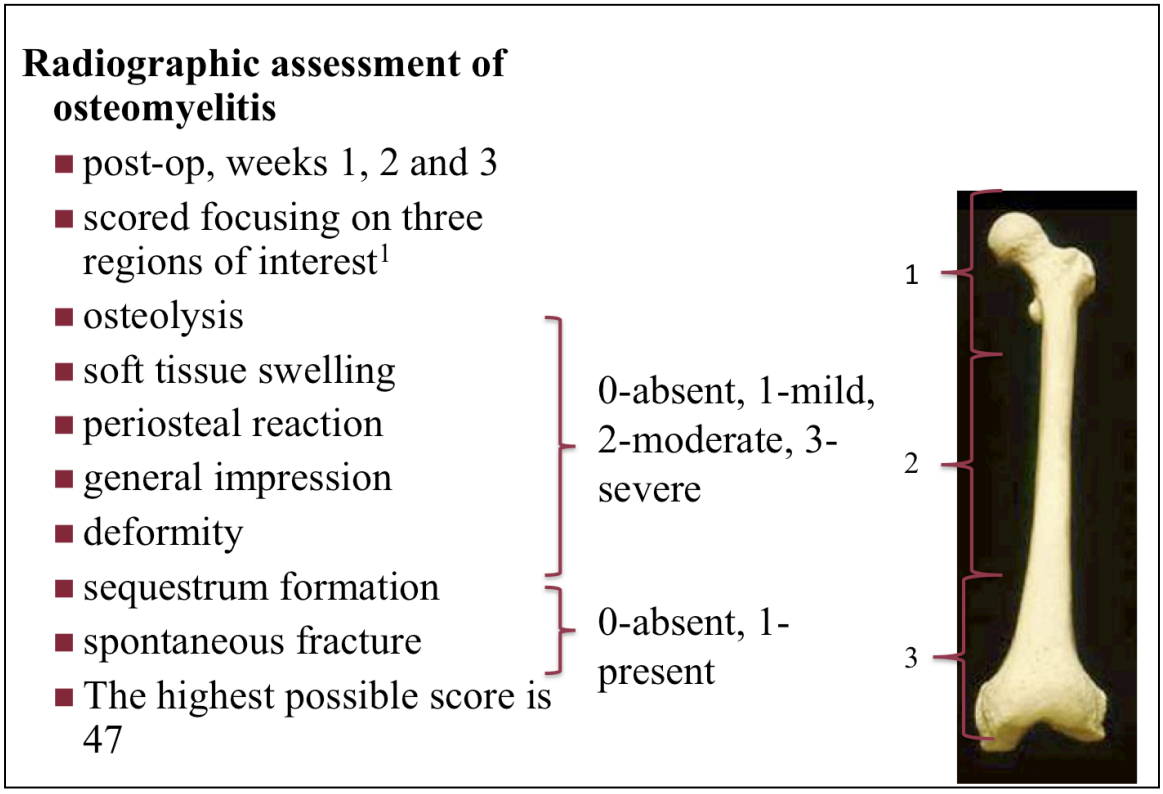

Figure 6.8: Representative radiographs from a rat in each group at 3 weeks after surgery. The solid black arrow indicates the fracture site in all three images. The Control group (A) was characterized by a slight periosteal reaction and new bone formation that is centered on the fracture site (black arrowhead). The *Staphylococcus aureus* group (B) was characterized by a severe periosteal reaction extending along the entire length of the femur (black arrowheads) with significant osteolysis. The *Staphylococcus aureus* + ceftriaxone group (C) was characterized by some periosteal reaction and new bone formation. Osteolysis is present but to a lesser degree when compared to the *S. aureus* group.

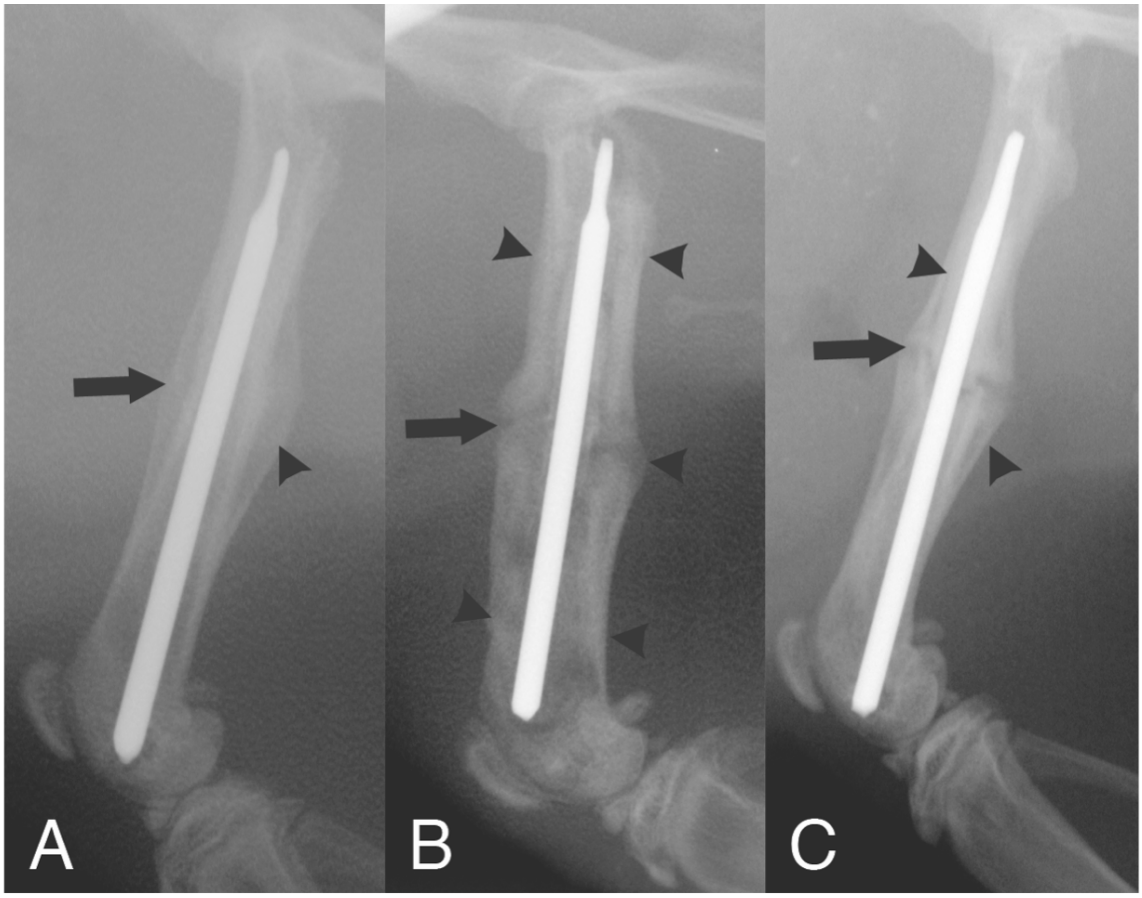

Figure 6.9: Colony forming units (CFU) recovered from each femur and the intramedullary pins. The data are presented as the median CFU/femur or pin with the error bars representing the 25th and 75th percentiles. Pairwise comparisons were made within the CFU groups and bars with a different letter were significantly different when a Bonferroni correction was applied ($p < 0.017$). No bacteria were cultured from any of the unoperated (left) femurs in any of the treatment groups.

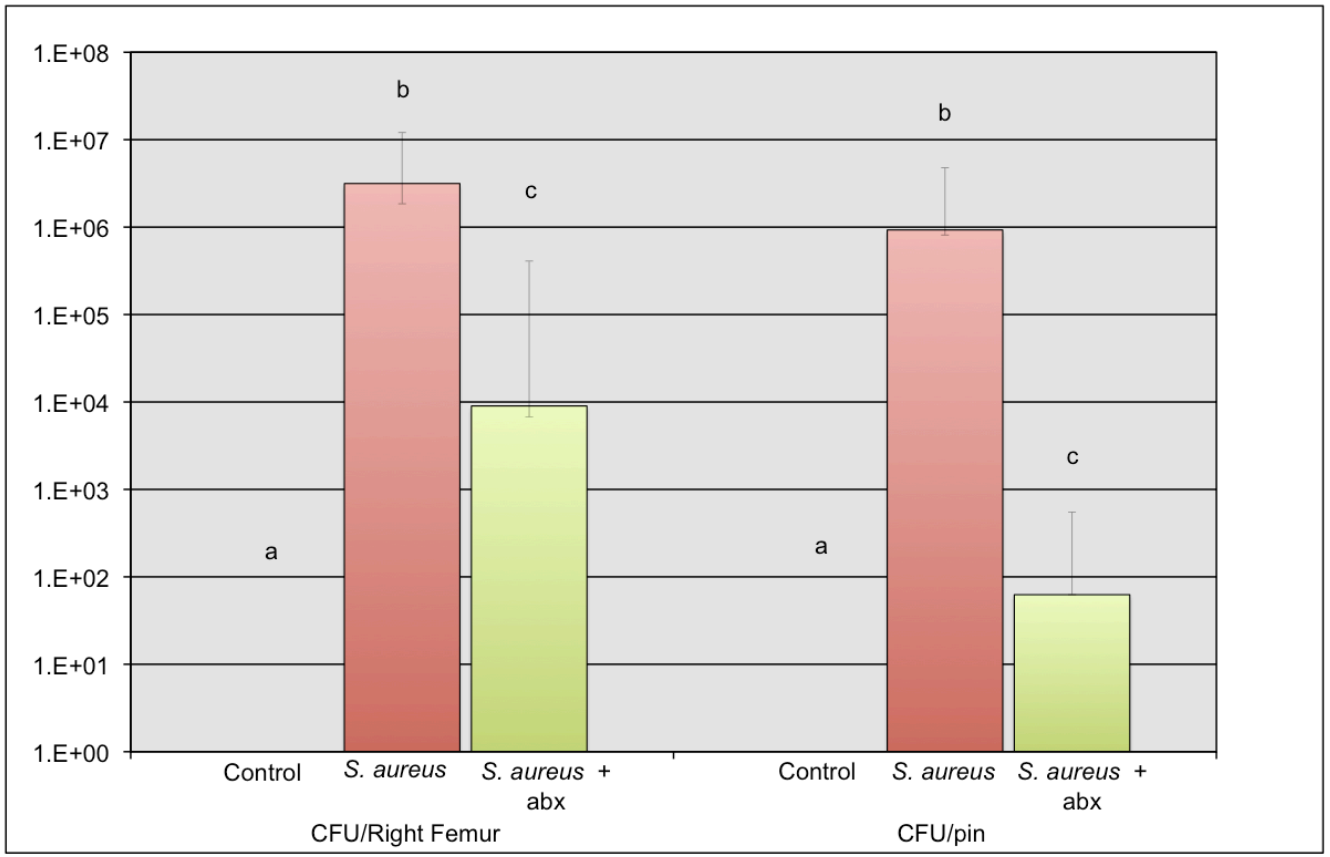

Figure 6.10: Images of operated femurs at removal. The arrow is pointing to the fracture site. Note the purulent material in the fracture site of the *S. aureus* group.

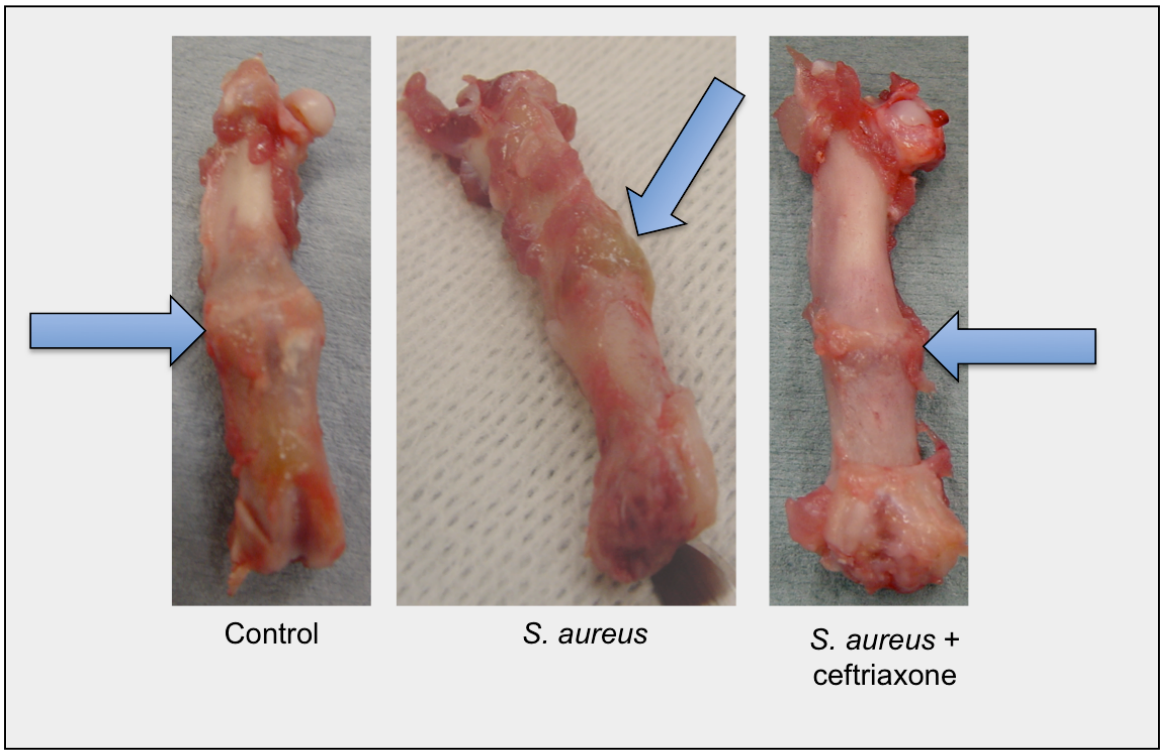

Figure 6.11: Demineralized histological sections of one cortex from the right femur from a representative rat in each group, stained with hematoxylin and eosin. (A) Control group; (B) *S. aureus* group; and (C) *S. aureus* + ceftriaxone group. The fracture site is not visible in (B) due to necrosis and lysis of the involved cortical bone. (1) Periosteal surface; (2) endosteal surface; (3) fracture site; (4) cortical bone; (5) periosteal new bone; (6) inflammation/necrosis.

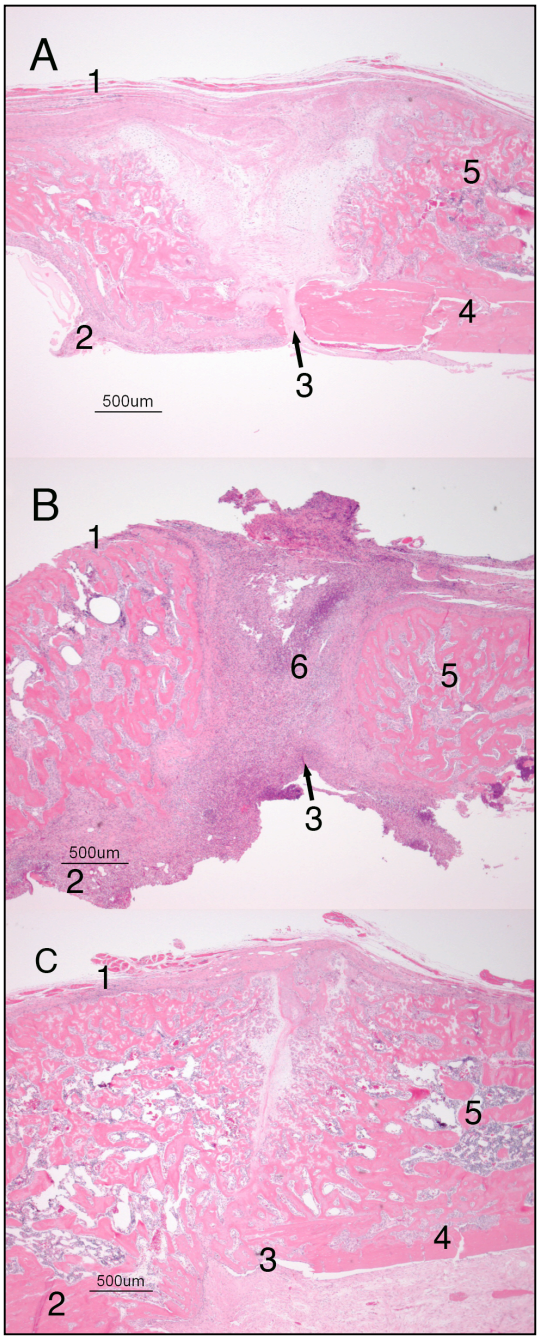

Table 6.1: Radiographic scores. Immediately and at 1, 2, and 3 weeks after surgery. Scores were compared at each time point (within each column). A lower score represents a radiograph that is more similar to normal healing without osteomyelitis. Cells (within a given column) with a different letter were significantly different when a Bonferroni correction was applied ($p < 0.017$).

	Mean ± SE radiographic score			
	Post-operative	Week 1	Week 2	Week 3
Control	1.17 ± 0.48^{a}	6.00 ± 2.23^{a}	9.05 ± 1.03^{a}	10.20 ± 1.55^{a}
S. aureus	0.75 ± 0.45^{a}	11.94 ± 0.89^{b}	21.86 ± 1.36^{b}	20.50 ± 1.67^{b}
S. aureus + ceftriaxone	0.78 ± 0.40^{a}	$12.60 \pm 1.52^{a,b}$	14.50 ± 0.96^{c}	12.20 ± 1.71^{a}

6.6 Chapter references

1. von Eiff C, Arciola CR, Montanaro L, Becker K, Campoccia D. Emerging *Staphylococcus* species as new pathogens in implant infections. Int J Artif Organs 2006 Apr;29(4):360-7.
2. Adams CS, Antoci V, Jr, Harrison G, Patal P, Freeman TA, Shapiro IM, et al. Controlled release of vancomycin from thin sol-gel films on implant surfaces successfully controls osteomyelitis. J Orthop Res 2008 Dec 2.
3. Darouiche RO. Treatment of infections associated with surgical implants. N Engl J Med 2004 Apr 1;350(14):1422-9.
4. Darouiche RO. Device-associated infections: a macroproblem that starts with microadherence. Clin Infect Dis 2001 Nov 1;33(9):1567-72.
5. Darouiche RO. Antimicrobial coating of devices for prevention of infection: principles and protection. Int J Artif Organs 2007 Sep;30(9):820-7.
6. Lucke M, Schmidmaier G, Sadoni S, Wildemann B, Schiller R, Stemberger A, et al. A new model of implant-related osteomyelitis in rats. J Biomed Mater Res B Appl Biomater 2003 Oct 15;67(1):593-602.
7. Donlan RM, Costerton JW. Biofilms: survival mechanisms of clinically relevant microorganisms. Clin Microbiol Rev 2002 Apr;15(2):167-93.
8. Costerton JW, Stewart PS, Greenberg EP. Bacterial biofilms: a common cause of persistent infections. Science 1999 May 21;284(5418):1318-22.
9. Fux CA, Costerton JW, Stewart PS, Stoodley P. Survival strategies of infectious biofilms. Trends Microbiol 2005 Jan;13(1):34-40.
10. Donlan RM. Biofilms and device-associated infections. Emerg Infect Dis 2001 Mar-Apr;7(2):277-81.
11. Chen X, Tsukayama DT, Kidder LS, Bourgeault CA, Schmidt AH, Lew WD. Characterization of a chronic infection in an internally-stabilized segmental defect in the rat femur. J Orthop Res 2005;23(4):816-23.

12. Darouiche RO, Farmer J, Chaput C, Mansouri M, Saleh G, Landon GC. Anti-Infective Efficacy of Antiseptic-Coated Intramedullary Nails. J Bone Joint Surg Am 1998 September 1;80(9):1336-40.
13. Monzon M, Garcia-Alvarez F, Lacleriga A, Amorena B. Evaluation of four experimental osteomyelitis infection models by using precolonized implants and bacterial suspensions. Acta Orthop Scand 2002 Jan;73(1):11-9.
14. Chen X, Kidder LS, Lew WD. Osteogenic protein-1 induced bone formation in an infected segmental defect in the rat femur. J Orthop Res 2002;20(1):142-50.
15. Chen X, Kidder LS, Schmidt AH, Lew WD. Osteogenic protein-1 induces bone formation in the presence of bacterial infection in a rat intramuscular osteoinduction model. J Orthop Trauma 2004 Aug;18(7):436-42.
16. Chen X, Schmidt AH, Tsukayama DT, Bourgeault CA, Lew WD. Recombinant human osteogenic protein-1 induces bone formation in a chronically infected, internally stabilized segmental defect in the rat femur. J Bone Joint Surg Am 2006 July 1;88(7):1510-23.
17. Skott M, Andreassen TT, Ulrich-Vinther M, Chen X, Keyler DE, LeSage MG, et al. Tobacco extract but not nicotine impairs the mechanical strength of fracture healing in rats. J Orthop Res 2006 Jul;24(7):1472-9.
18. Bonnarens F, Einhorn TA. Production of a standard closed fracture in laboratory animal bone. J Orthop Res 1984;2(1):97-101.
19. Lucke M, Schmidmaier G, Sadoni S, Wildemann B, Schiller R, Haas NP, et al. Gentamicin coating of metallic implants reduces implant-related osteomyelitis in rats. Bone 2003 May;32(5):521-31.
20. Cutler SA, Rasmussen MA, Hensley MJ, Wilhelms KW, Griffith RW, Scanes CG. Effects of *Lactobacilli* and lactose on *Salmonella typhimurium* colonisation and microbial fermentation in the crop of the young turkey. Br Poult Sci 2005 Dec;46(6):708-16.

21. Johannsen SA, Griffith RW, Wesley IV, Scanes CG. *Salmonella enterica* serovar *typhimurium* colonization of the crop in the domestic turkey: influence of probiotic and prebiotic treatment (*Lactobacillus acidophilus* and lactose). Avian Dis 2004 Apr-Jun;48(2):279-86.
22. Ryan TJ. Infection following soft tissue injury: its role in wound healing. Curr Opin Infect Dis 2007 Apr;20(2):124-8.
23. Poultsides LA, Papatheodorou LK, Karachalios TS, Khaldi L, Maniatis A, Petinaki E, et al. Novel model for studying hematogenous infection in an experimental setting of implant-related infection by a community-acquired methicillin-resistant *S. aureus* Strain. J Orthop Res 2008 Apr 18.
24. McPherson JC, Runner RR, Shapiro B, et al. An acute osteomyelitis model in traumatized rat tibiae involving sand as a foreign body, thermal injury, and bimicrobial contamination. Comp Med 2008;58:369–374.
25. Morrissy RT, Haynes DW. Acute hematogenous osteomyelitis: a model with trauma as an etiology. J Pediatr Orthop 1989;9:447–456.
26. An YH, Kang QK, Arciola CR. Animal models of osteomyelitis. Int J Artif Organs 2006;29:407–420.
27. Hienz SA, Sakamoto H, Flock JI, et al. Development and characterization of a new model of hematogenous osteomyelitis in the rat. J Infect Dis 1995;171:1230–1236.

Chapter 7

Summary and Future directions

7.1 Summary

Implant-associated infections continue to plague both human and veterinary medicine and research continues for methodologies that attempt to prevent/treat this enormous problem. To this end biomaterials-based research is an area of huge interest. The overall goals of this body of work were to characterize the antimicrobial properties of magnesium (Mg) metal and nano-magnesium oxide (nMgO) *in vitro*, to evaluate the *in vitro* cytotoxicity of Mg metal, and to incorporate MgO nanoparticles into a polymeric implant coating and evaluate its *in vitro* antimicrobial properties. These goals were accomplished to varying degrees through Specific Aims 1 through 4 (Chapters 2 through 5 respectively). As progress was made through the project it became apparent that an ideal *in vivo* model for evaluating the performance of a coated implant in a closed fracture setting did not exist. To address this issue the goals in Specific Aim 5 (Chapter 6) were accomplished and a model was developed.

In ***Specific Aim 1 (Chapter 2)*** the *in vitro* properties of Mg metal were evaluated.(1) When added to a bacterial culture broth Mg metal caused a rapid increase in pH (> 9) and a rise in Mg^{2+} (> 6 mmol/L) as the metal corroded. The overall increase was not unexpected given the predictable corrosion reaction of this metal. The next step evaluated the effect of this change on the *in vitro* growth of three common bacteria. In this experiment there were significantly less CFU/ml recovered from the Mg group compared to the Control and 316LSS groups. When compared to the bactericidal antibiotic enrofloxacin, there was also an overall trend towards no significant differences. Next were experiments that attempted to determine the mechanism for this antimicrobial activity. In the first the role of Mg^{2+} was evaluated. $MgCl_2$ was used to increase the Mg^{2+} concentration and was compared to NaCl. The result was that the increase in Mg^{2+} concentration, via the addition of $MgCl_2$, did not result in an appreciable effect on the CFU/ml for three bacteria evaluated when compared to controls or NaCl. The final experiment evaluated the role of increasing pH (i.e. more alkaline). Four groups were used based on varying the pH (i.e.

7.4(Control), 8.0, 9.0 and 10.0). When compared to the Control group, an increase in pH to $\geq$ 9 resulted in a significant decrease in the CFU/ml recovered in this *in vitro* model. In this aim the goals were achieved and the hypotheses accepted. While these results were exciting, further evaluation was necessary. In particular, toxicity, both *in vitro* and *in vivo* must be considered for any new biomaterial.

In ***Specific Aim 2 (Chapter 3)*** the cytotoxic effects of pure Mg metal on murine fibroblast and osteoblast-like cells was evaluated. Initially the plan was to use two outcome measures to evaluate this effect, the MTT colorimetric assay and a propidium iodide (PI) staining flow cytometry assay. Unfortunately, a manuscript published by Fischer *et al.* reported that the corrosion products of Mg interfere with the chemical reaction in the MTT assay producing an inaccurate assessment of cell viability.(19) Given this finding the results of the MTT assay were not used in the final analysis. Evaluation of the PI staining flow cytometry assay results revealed a difference depending on the cell line. The fibroblast cells, for example, were affected less than the osteoblast-like cells when incubated with the Mg elution media. The Mg elution media did not result in an appreciable decrease in viability of the fibroblast cells, but there did appear to be a negative trend associated with the longer elution and incubation periods. The osteoblast-like cells were affected to a greater degree. The Mg elution media did result in a decrease in cell viability and this decrease appears to be associated with the shorter elution and incubation periods. While the results of this experiment were disappointing in that Mg did appear to have a negative impact on the osteoblast-like cells, the mechanism and determinants of Mg corrosion are multifactorial and require *in vivo* evaluation when being considered for use in an implant.(2) In this aim the goal was partially achieved in that only one outcome measure was used and the hypothesis cannot be accepted because of the negative impact on the osteoblast-like cells.

Continued research into the use of Mg and coating options presented some difficulties. There are potential hazards in manufacturing processes with the pure metal and limitations in terms of the

availability of facilities that have dedicated coating equipment. This search led to publications on the use of nanoparticles and nanomaterials in implant coatings and as antimicrobial agents. In ***Specific Aim 3 (Chapter 4)*** the *in vitro* properties of nano-magnesium oxide (nMgO) were evaluated. When added to a microbial broth nMgO resulted in a rapid increase in pH (> 10) after 1 hour. This increase was similar to that noted with Mg metal mesh evaluated at the same time and to the Mg metal evaluated previously.(1) (Chapter 2) Next, the antimicrobial properties of nMgO and a supernatant generated by incubating the nMgO in growth media were evaluated for their effect on planktonic bacterial growth and biofilm formation. In this experiment the bacterial strains were well-established strains and were chosen to represent a spectrum of laboratory and clinical isolates. No bacteria were recovered from vials where either the nMgO was added or where the supernatant was used. For the biofilm experiment, not all of the organisms evaluated produced a positive biofilm in the control wells. *Staphylococcus epidermidis* (RP62A) and *Staphylococcus aureus* ATCC were the only organisms that were positive and thus were the only ones evaluated. For both organisms, the addition of the nMgO supernatant resulted in a negative biofilm at both 24- and 48-hours post inoculation. In this aim the goals were achieved and the hypotheses were accepted. Much like Specific Aim1, these results were exciting, especially since nMgO was a material that was easy to work with and had great potential for incorporation into a coating or other biomaterial.

When considering the options available for implant coatings, in particular bioabsorbable ones, polymers are ideal candidates. In ***Specific Aim 4 (Chapter 5)*** poly-ε-caprolactone (PCL) was evaluated as a carrier for nMgO and Mg-mesh. Using a chloroform emulsion/evaporation technique the composites were easily made and applied to the surface of 316LSS orthopaedic screws. Similarly, thin film discs were made of the composite for *in vitro* evaluation. Although the PCL+nMgO coating on the screws had an effect on the Gram-negative organisms, a significant decrease in CFU/ml recovered was not noted for the Gram-positive organisms. When the PCL+nMgO and PCL+Mg-mesh discs were compared to the Control group, a significantly less

CFU/ml were recovered from the PCL+nMgO group for all organisms except *S. epidermidis*. A possible explanation for this finding was that there was a very thick slime that formed in the *S. epidermidis* Control wells. Sampling of this was challenging and could have resulted in an underestimation of the CFU/ml in this group. Overall the goals of this aim were achieved. The first hypothesis was accepted; the second was accepted for Gram-negative organisms only; and the third was accepted for all organisms with the exception of *S. epidermidis*. Polymer manufacturing is challenging and as discussed in Chapter 5, there are many components to consider. Nonetheless, this initial work represents some intriguing results and further investigation is warranted.

With a long-term goal of developing a technique that could be commercially applied in the prevention of implant-associated infections and in particular osteomyelitis an applicable *in vivo* model is required. In ***Specific Aim 5 (Chapter 6)*** an existing femur fracture model in the rat was developed into a closed-fracture osteomyelitis model. A clinical isolate of *Staphylococcus aureus* was used to inoculate the femur followed by an intramedullary pin and generation of a mid-diaphyseal fracture. Radiographic, CFU/femur, CFU/pin and histopathology were used as outcome measures and these documented the consistent development of osteomyelitis in this model. The goal of this aim was achieved and the hypothesis was accepted. In the future, this model has the potential to be used in evaluating anti-fouling/anti-biofilm implant coatings or other osteomyelitis studies.

On the whole, the results from this body of work are compelling. Magnesium, a readily available and inexpensive metal was shown to have antimicrobial properties that appear to be related to its corrosion products. Nano-magnesium oxide was found to have similar effects when used alone although the mechanisms in this case remain to be elucidated. When the nano-magnesium oxide was incorporated into a poly-ε-caprolactone composite, similar, although not identical, results were achieved. Finally, a new model of a closed fracture osteomyelitis was developed in the rat.

Together this provides a foundation for further investigation in the attempt to address this remarkable clinical issue.

7.2 Future directions

7.2.1 PCL composite biofilm evaluation

While the potential for future projects is immense there are some that would appear to be a logical next step. Evaluating the effect of the PCL composite discs on biofilm production (as outlined in Section 5.3) would provide some interesting information. Especially since the prevention of a biofilm is arguably more important in the clinical setting of implant-associated infections. (3-7) The methodology used in Chapter 5 could easily be applied to the PCL discs. In addition, confocal laser scanning microscopy (CLSM)(8), electron microscopy and other direct culture techniques could be employed.

7.2.2 Characterize the PCL in terms of distribution of nMgO, strength, adherence to the pin, surface charge and rheologic properties.

The material properties of a polymeric coating are important determinants in how the coating will perform its intended function. When developing a coating that contains a pharmaceutical or other chemical that has a specific purpose the distribution of that chemical is important. Similarly, cellular interaction is often key in performance and thus surface characteristics such as charge, roughness and porosity are also important.(9-11) The first step would be to work with a coating facility to standardize the emulsion/evaporation as well as the coating process. Once that is achieved the rheologic properties (material behavior such as yield stress, kinetic properties, complex viscosity, modulus, creep, and recovery) of the polymeric coating could be evaluated. SEM and TEM could be used to visualize the distribution of the nMgO within the polymer and atomic force microscopy (AFM) could be utilized to image the three-dimensional topography of the polymer and determine the surface roughness and charge. Finally, the adherence of the

polymer to the metal substrate could be evaluated using the “tape peel test” according to the American Society for Testing and Materials (ASTM 3359 B). The coatings could also be evaluated for pull-off strength according to ASTM D4541-02, indentation hardness, shear force and with scratch testing according to the appropriate standards.

7.2.3 Determine the optimal polymer coating thickness and concentration of nMgO required to prevent in vitro colonization of the implant

Before embarking on any animal modeling it is prudent to have supporting *in vitro* data to support the *in vivo* design. The data presented in this body of work has demonstrated that nMgO can be incorporated in a PCL based coating and that this coating can be applied to a stainless steel screw using a “dip coating” method. Coating thickness and uniformity are key factors in determining the lifespan of the coating and thus its ability to prevent colonization. This is an important consideration because the coating needs to be absorbed slowly and consistently in order to adequately prevent colonization. To this end, different coating thicknesses and nMgO concentrations within the coating could be explored and the ideal coating thickness and concentration of nMgO established. This could be accomplished using the *in vitro* methods presented in this project (Chapter 5) as well as those discussed in section 7.2.1.

7.2.4 Evaluate the antimicrobial properties of PCL+nMgO coatings in an in vivo fracture osteomyelitis model

An *in vivo* evaluation is a logical step in evaluating any technique that has potential clinical usage. In choosing an animal model careful consideration must be given to the pros and cons of a given model and if it accurately reflects the clinical situation you wish to model. The femur fracture osteomyelitis model in the rat that was developed as part of this work(12) (Chapter 6) could be used to evaluate the PCL+nMgO implant coating. This model would allow assessment using objective outcome measures in the form of CFU per implant and inoculated femur; radiographic evaluation for signs consistent with osteomyelitis; and histological evaluation of harvested

specimens. A coating that prevents implant colonization should result in statistically significant differences in these outcome measures when compared to an infected but not treated Control group.

7.2.5 Poloxamer coatings/gels

Poloxamer solutions are easily prepared using cold mixing methods and the % weight is easily adjusted by changing the amount of polymer added. It is difficult to make mixtures at concentrations above 30-35% (F 127) however, because of the increased viscosity of the solution. As discussed in Chapter 1, poloxamers are difunctional block copolymer surfactants that are nonionic and bioabsorbable.(10) The sol-gel transition of these polymers tends to be just below the normal body temperature, meaning that they become a solid or gel at body temperature.(13, 14) This feature has prompted research into their use as antibiotic carriers in wounds and thermal burns.(13, 15, 16) Commercially available Pluronic® F 68 and F 127 were purchased for use in some preliminary work. A 35% weight solution of Pluronic® F 127 was made using a modification of the cold technique(13) and nMgO was added to this mixture. A 316LSS pin was dipped in the resulting solution and allowed to dry overnight at room temperature.(Figure 7.1) To evaluate the ability of the Pluronic® F 127 + nMgO to prevent bacterial growth, the coated pin and 1 ml of the polymer suspension were evaluated using the *in vitro* methods described in previous chapters. A vial with a 316LSS pin was used as a Control and the culture vials were inoculated with 10^4 CFU of *Staphylococcus aureus* (MORF). After 24 hours the CFU/pin, CFU/ml were determined.(Figure 7.2) No CFU were recovered from either of the Pluronic® F 127 + nMgO samples compared to the SS control.

To investigate the ability of the Pluronic® F 127 + nMgO gel to prevent bacterial growth in a simulated topical setting, the polymer was added to the surface of a blood agar plate after the plate was inoculated with a lawn of 10^4 CFU of *S. aureus*. Pluronic® F 127 + nMgO and Pluronic® F 127 with no additive were added to the surface of the plate which was then incubated

at 37^{o}C for 48 hours.(Section 5.3.5 – Disc sensitivity plates) The Pluronic® F 127 + nMgO had a zone of inhibition around the gel on the plate whereas the Pluronic® F 127 with no additive did not.(Figure 7.3) A sample was collected from the "zone of inhibition" and inoculated on a blood agar plate which was then incubated at 37^{o}C for 24 hours. No growth occurred.

This preliminary data with the Pluronic® F 127 show promise for its use as an antimicrobial carrier. One key advantage is that, much like PCL, it is bioabsorbable. Because of the low sol-gel transition temperature it is challenging to work with, but this is not an insurmountable issue. Further steps would involve standardizing the process of adding nMgO to the polymer followed by characterization of the rheologic properties, as discussed in 7.2.2. Once this is achieved, the composite could be easily used in any/all of the methodologies discussed in this body of work whereby its effect on relevant bacterial strains could be evaluated.

This is by no means an exhaustive list of the future possibilities for this research but does provide a foundation for further investigation.

Figure 7.1: Image of a Pluronic® F 127 coated 316LSS pin.

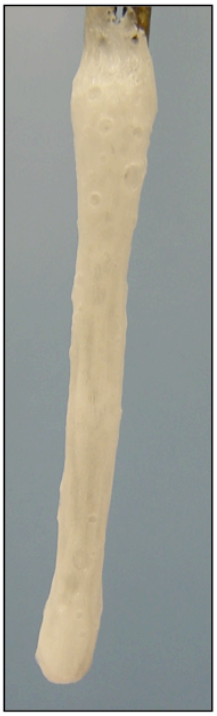

Figure 7.2: CFU recovered from Pluronic® F 127 cultures.

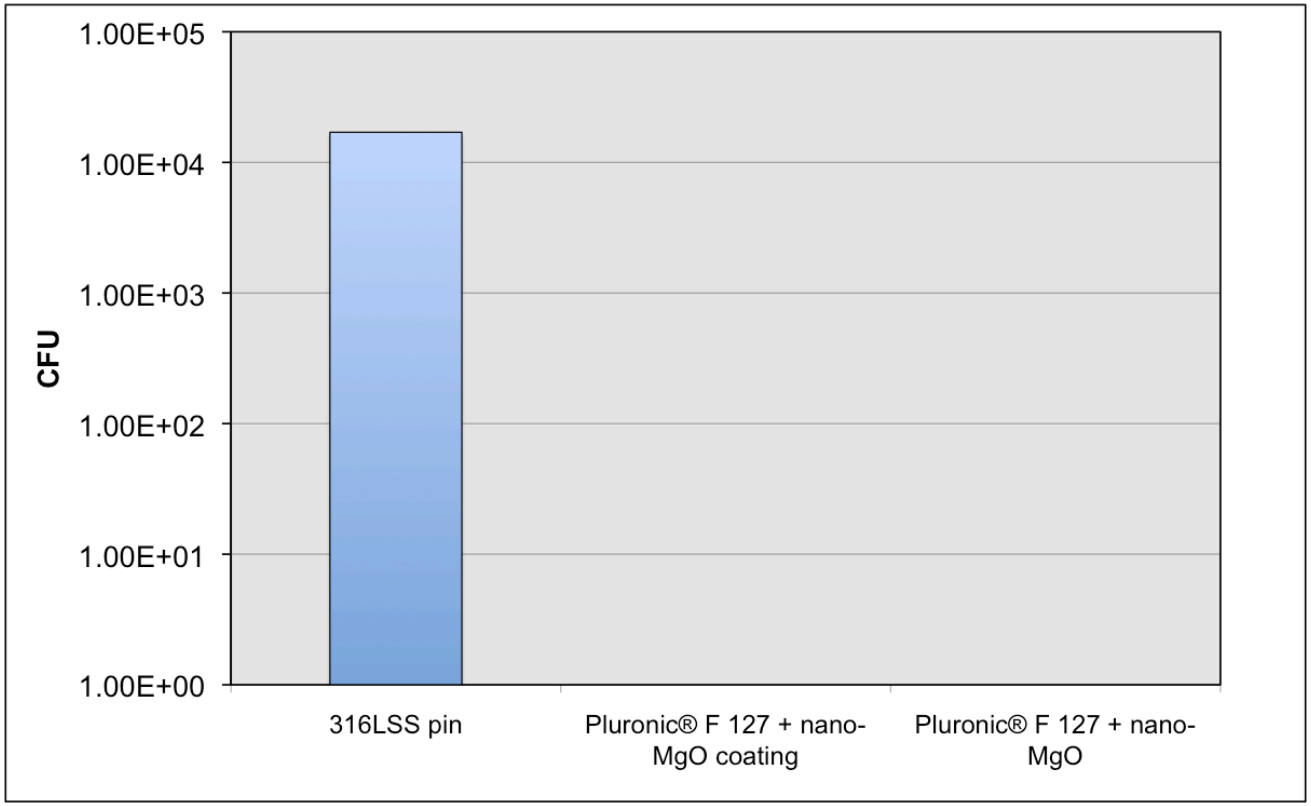

Figure 7.3: Blood agar plates with Pluronic® F 127 placed on surface of bacterial lawn.

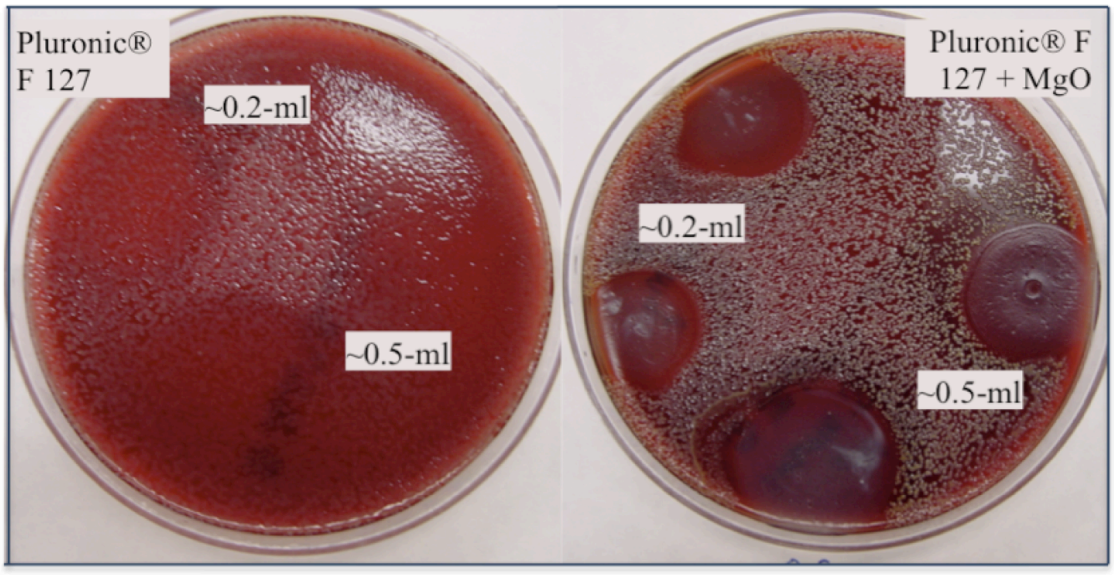

7.3 Chapter references

1. Robinson DA, Griffith RW, Shechtman D, Evans RB, Conzemius MG. *In vitro* antibacterial properties of magnesium metal against *Escherichia coli*, *Pseudomonas aeruginosa* and *Staphylococcus aureus*. Acta Biomater 2010 Oct 7;6(5):1869-77.
2. Witte F, Fischer J, Nellesen J, Crostack HA, Kaese V, Pisch A, et al. *In vitro* and *in vivo* corrosion measurements of magnesium alloys. Biomaterials 2006 Mar;27(7):1013-8.
3. Darouiche RO. Treatment of infections associated with surgical implants. N Engl J Med 2004 Apr 1;350(14):1422-9.
4. Darouiche RO. Antimicrobial approaches for preventing infections associated with surgical implants. Clin Infect Dis 2003 May 15;36(10):1284-9.
5. Costerton JW, Stewart PS, Greenberg EP. Bacterial biofilms: a common cause of persistent infections. Science 1999 May 21;284(5418):1318-22.
6. Fux CA, Costerton JW, Stewart PS, Stoodley P. Survival strategies of infectious biofilms. Trends Microbiol 2005 Jan;13(1):34-40.
7. Donlan RM, Costerton JW. Biofilms: survival mechanisms of clinically relevant microorganisms. Clin Microbiol Rev 2002 Apr;15(2):167-93.
8. Stoodley P, Kathju S, Hu FZ, Erdos G, Levenson JE, Mehta N, et al. Molecular and imaging techniques for bacterial biofilms in joint arthroplasty infections. Clin Orthop Rel Res 2005 Aug;(437)(437):31-40.
9. Woodruff MA, Hutmacher DW. The return of a forgotten polymer-epsilon-Polycaprolactone in the 21st century. Progress in Polymer Science 2010 10;35(10):1217-56.
10. Sinha VR, Khosla L. Bioabsorbable polymers for implantable therapeutic systems. Drug Dev Ind Pharm 1998 Dec;24(12):1129-38.
11. Sinha VR, Bansal K, Kaushik R, Kumria R, Trehan A. Poly-epsilon-caprolactone microspheres and nanospheres: an overview. Int J Pharm 2004 Jun 18;278(1):1-23.

12. Robinson DA, Bechtold JE, Carlson CS, Evans RB, Conzemius MG. Development of a fracture osteomyelitis model in the rat femur. J Orthop Res 2011 Jan;29(1):131-7.
13. Schmolka IR. Artificial skin. I. Preparation and properties of pluronic F-127 gels for treatment of burns. J Biomed Mater Res 1972 Nov;6(6):571-82.
14. Oh SH, Kim JK, Song KS, Noh SM, Ghil SH, Yuk SH, et al. Prevention of postsurgical tissue adhesion by anti-inflammatory drug-loaded pluronic mixtures with sol-gel transition behavior. J Biomed Mater Res A 2005 Mar 1;72(3):306-16.
15. Nalbandian RM, Henry RL, Wilks HS. Artificial skin. II. Pluronic F-127 Silver nitrate or silver lactate gel in the treatment of thermal burns. J Biomed Mater Res 1972 Nov;6(6):583-90.
16. Faulkner DM, Sutton ST, Hesford JD, Faulkner BC, Major DA, Hellewell TB, et al. A new stable pluronic F68 gel carrier for antibiotics in contaminated wound treatment. Am J Emerg Med 1997 Jan;15(1):20-4.

References

Adams CS, Antoci V Jr, Harrison G, Patal P, Freeman TA, Shapiro IM, et al. Controlled release of vancomycin from thin sol-gel films on implant surfaces successfully controls osteomyelitis. J Orthop Res 2008 Dec 2.

Allan I, Newman H, Wilson M. Antibacterial activity of particulate bioglass against supra- and subgingival bacteria. Biomaterials 2001 Jun;22(12):1683-7.

An YH, Stuart GW, McDowell SJ, McDaniel SE, Kang Q, Friedman RJ. Prevention of bacterial adherence to implant surfaces with a crosslinked albumin coating *in vitro*. J Orthop Res 1996 Sep;14(5):846-9.

An YH, Kang QK, Arciola CR. Animal models of osteomyelitis. Int J Artif Organs 2006;29:407–420.

Arciola CR, Bustanji Y, Conti M, Campoccia D, Baldassarri L, Samorì B, *et al. Staphylococcus epidermidis*–fibronectin binding and its inhibition by heparin. Biomaterials, 2003 8;24(18):3013-9.

Arciola CR, Alvi FI, An YH, Campoccia D, Montanaro L. Implant infection and infection resistant materials: a mini review. Int J Artif Organs 2005 Nov;28(11):1119-25.

Arens S, Schlegel U, Printzen G, Ziegler WJ, Perren SM, Hansis M. Influence of materials for fixation implants on local infection. An experimental study of steel versus titanium DCP in rabbits. J Bone Joint Surg Br 1996 Jul;78(4):647-51.

Auckenthaler R, Michea-Hamzehpour M, Pechere JC. *In vitro* activity of newer quinolones against aerobic bacteria. J Antimicrob Chemother 1986 Apr;17 Suppl B:29-39.

Baena MI, Marquez MC, Matres V, Botella J, Ventosa A. Bactericidal activity of copper and niobium-alloyed austenitic stainless steel. Curr Microbiol 2006 Dec;53(6):491-5.

Barie PS. No pay for no performance. Surg Infect (Larchmt) 2007 Aug;8(4):421-33.

Belinda Ostrowsky. Epidemiology of Healthcare-Assocaited Infections. In: Jarvis WR, editor. Bennett and Brachman's Hosptial Infections. 5th ed. Philadelphia: Wolters Kluwer Health/Lippincott Williams & Wilkins; 2007. p.3.

Bonnarens F, Einhorn TA. Production of a standard closed fracture in laboratory animal bone. J Orthop Res 1984;2(1):97-101.

Bordes C, Freville V, Ruffin E, Marote P, Gauvrit JY, Briancon S, et al. Determination of poly(epsilon-caprolactone) solubility parameters: application to solvent substitution in a microencapsulation process. Int J Pharm 2010 Jan 4;383(1-2):236-43.

Borkow G, Gabbay J. Putting copper into action: copper-impregnated products with potent biocidal activities. FASEB J 2004 Nov;18(14):1728-30.

Borkow G, Gabbay J. Copper as a biocidal tool. Curr Med Chem 2005;12(18):2163-75.

Bose D, Eggebrecht H, Erbel R. Absorbable metal stent in human coronary arteries: imaging with intravascular ultrasound. Heart 2006 Jul;92(7):892.

Brown DC, Conzemius MG, Shofer F, Swann H. Epidemiologic evaluation of postoperative wound infections in dogs and cats. J Am Vet Med Assoc 1997 May 1;210(9):1302-6.

Bryers JD, Jarvis RA, Lebo J, Prudencio A, Kyriakides TR, Uhrich K. Biodegradation of poly(anhydride-esters) into non-steroidal anti-inflammatory drugs and their effect on *Pseudomonas aeruginosa* biofilms *in vitro* and on the foreign-body response *in vivo*. Biomaterials 2006 Oct;27(29):5039-48.

Carmen JC, Roeder BL, Nelson JL, Robison Ogilvie RL, Robison RA, Schaalje GB, *et al.* Treatment of biofilm infections on implants with low-frequency ultrasound and antibiotics. American Journal of Infection Control, 2005 3;33(2):78-82.

Castelli P, Caronno R, Ferrarese S, Mantovani V, Piffaretti G, Tozzi M, *et al.* New trends in prosthesis infection in cardiovascular surgery. Surg Infect (Larchmt) 2006;7 Suppl 2:S45-7.

Centers for Disease Control and Prevention, National Center for Emerging and Zoonotic Infectious Diseases (NCEZID), Division of Healthcare Quality Promotion (DHQP). Surgical Site Infection (SSI). 2011 (http://www.cdc.gov/HAI/ssi/ssi.html).

Chen X, Kidder LS, Lew WD. Osteogenic protein-1 induced bone formation in an infected segmental defect in the rat femur. Journal of Orthopaedic Research 2002;20(1):142-50.

Chen X, Kidder LS, Schmidt AH, Lew WD. Osteogenic protein-1 induces bone formation in the presence of bacterial infection in a rat intramuscular osteoinduction model. J Orthop Trauma 2004 Aug;18(7):436-42.

Chen X, Tsukayama DT, Kidder LS, Bourgeault CA, Schmidt AH, Lew WD. Characterization of a chronic infection in an internally-stabilized segmental defect in the rat femur. Journal of Orthopaedic Research 2005;23(4):816-23.

Chen X, Schmidt AH, Tsukayama DT, Bourgeault CA, Lew WD. Recombinant human osteogenic protein-1 induces bone formation in a chronically infected, internally stabilized segmental defect in the rat femur. J Bone Joint Surg Am 2006 July 1;88(7):1510-23.

Cho YH, Lee SJ, Lee JY, Kim SW, Lee CB, Lee WY, et al. Antibacterial effect of intraprostatic zinc injection in a rat model of chronic bacterial prostatitis. Int J Antimicrob Agents 2002 Jun;19(6):576-82.

Chopra I. The increasing use of silver-based products as antimicrobial agents: a useful development or a cause for concern? J Antimicrob Chemother 2007 Apr;59(4):587-90.

Clutterbuck AL, Cochrane CA, Dolman J, Percival SL. Evaluating antibiotics for use in medicine using a poloxamer biofilm model. Ann Clin Microbiol Antimicrob 2007 Feb 15;6:2.

Costerton JW, Geesey GG, Cheng KJ. How bacteria stick. Sci Am 1978 Jan;238(1):86-95.

Costerton JW. Introduction to biofilm. Int J Antimicrob Agents 1999 May;11(3-4):217,21; discussion 237-9.

Costerton JW, Stewart PS, Greenberg EP. Bacterial biofilms: a common cause of persistent infections. Science 1999 May 21;284(5418):1318-22.

Costerton JW, Montanaro L, Arciola CR. Biofilm in implant infections: its production and regulation. Int J Artif Organs 2005 Nov;28(11):1062-8.

Cottam E, Hukins DW, Lee K, Hewitt C, Jenkins MJ. Effect of sterilisation by gamma irradiation on the ability of polycaprolactone (PCL) to act as a scaffold material. Med Eng Phys 2009 Mar;31(2):221-6.

Curtin JJ, Donlan RM. Using bacteriophages to reduce formation of catheter-associated biofilms by *Staphylococcus epidermidis*. Antimicrob Agents Chemother 2006 Apr;50(4):1268-75.

Cutler SA, Rasmussen MA, Hensley MJ, Wilhelms KW, Griffith RW, Scanes CG. Effects of *Lactobacilli* and lactose on *Salmonella typhimurium* colonisation and microbial fermentation in the crop of the young turkey. Br Poult Sci 2005 Dec;46(6):708-16.

Daniels R, Vanderleyden J, Michiels J. Quorum sensing and swarming migration in bacteria. FEMS Microbiol Rev 2004;28:261-89.

Darouiche RO, Farmer J, Chaput C, Mansouri M, Saleh G, Landon GC. Anti-infective efficacy of antiseptic-coated intramedullary nails. J Bone Joint Surg Am 1998 September 1;80(9):1336-40.

Darouiche RO. Device-associated infections: a macroproblem that starts with microadherence. Clin Infect Dis 2001 Nov 1;33(9):1567-72.

Darouiche RO. Antimicrobial approaches for preventing infections associated with surgical implants. Clin Infect Dis 2003 May 15;36(10):1284-9.

Darouiche RO. Treatment of infections associated with surgical implants. N Engl J Med 2004 Apr 1;350(14):1422-9.

Darouiche RO. Antimicrobial coating of devices for prevention of infection: principles and protection. Int J Artif Organs 2007 Sep;30(9):820-7.

Davis KA, Moran KA, McAllister CK, Gray PJ. Multidrug-resistant *Acinetobacter* extremity infections in soldiers. Emerg Infect Dis 2005 Aug;11(8):1218-24.

Denizot F, Lang R. Rapid colorimetric assay for cell growth and survival. Modifications to the tetrazolium dye procedure giving improved sensitivity and reliability. J Immunol Methods 1986 May 22;89(2):271-7.

Di Mario C, Griffiths H, Goktekin O, Peeters N, Verbist J, Bosiers M, et al. Drug-eluting bioabsorbable magnesium stent. J Interv Cardiol 2004 Dec;17(6):391-5.

Dong C, Cairney J, Sun Q, Maddan O, He G, Deng Y. Investigation of Mg(OH)2 nanoparticles as an antibacterial agent. J Nanopart Res 2009.

Donlan RM. Biofilms and device-associated infections. Emerg Infect Dis 2001 Mar-Apr;7(2):277-81.

Donlan RM, Costerton JW. Biofilms: survival mechanisms of clinically relevant microorganisms. Clin Microbiol Rev 2002 Apr;15(2):167-93.

de Lissovoy G, Fraeman K, Hutchins V, Murphy D, Song D, Vaughn BB. Surgical site infection: incidence and impact on hospital utilization and treatment costs. Am J Infect Control 2009 Jun;37(5):387-97.

del Pozo JL, Serrera A, Martinez-Cuesta A, Leiva J, Penades J, Lasa I. Biofilm related infections: is there a place for conservative treatment of port-related bloodstream infections? Int J Artif Organs 2006 Apr;29(4):379-86.

Department of Health and Human Services. Medicare Program; Changes to the Hospital Inpatient Prospective Payment Systems and Fiscal Year 2008 Rates. Federal Register 2007 08/22/2007;72(162):47200-18.

Dimick JB, Weeks WB, Karia RJ, Das S, Campbell DA,Jr. Who pays for poor surgical quality? Building a business case for quality improvement. J Am Coll Surg 2006 Jun;202(6):933-7.

Eagye KJ, Kim A, Laohavaleeson S, Kuti JL, Nicolau DP. Surgical site infections: does inadequate antibiotic therapy affect patient outcomes? Surg Infect (Larchmt) 2009 Aug;10(4):323-31.

Elemam A, Rahimian J, Mandell W. Infection with panresistant *Klebsiella pneumoniae*: a report of 2 cases and a brief review of the literature. Clin Infect Dis 2009 Jul 15;49(2):271-4.

Eugster S, Schawalder P, Gaschen F, Boerlin P. A prospective study of postoperative surgical site infections in dogs and cats. Vet Surg 2004 Sep-Oct;33(5):542-50.

Faulkner DM, Sutton ST, Hesford JD, Faulkner BC, Major DA, Hellewell TB, *et al.* A new stable pluronic F68 gel carrier for antibiotics in contaminated wound treatment. Am J Emerg Med 1997 Jan;15(1):20-4.

Federle MJ, Bassler BL. Interspecies communication in bacteria. J Clin Invest 2003 Nov;112(9):1291-9.

Ferrando WA. Review of corrosion and corrosion control of magnesium alloys and composites. J Mater Eng 1989;11(4):299-313.

Fischer J, Prosenc MH, Wolff M, Hort N, Willumeit R, Feyerabend F. Interference of magnesium corrosion with tetrazolium-based cytotoxicity assays. Acta Biomater 2010 May;6(5):1813-23.

Food and Drug Administration. Search term: polycaprolactone. (http://www.fda.gov/default.htm).

Frey TN, Hoelzler MG, Scavelli TD, Fulcher RP, Bastian RP. Risk factors for surgical site infection-inflammation in dogs undergoing surgery for rupture of the cranial cruciate ligament: 902 cases (2005-2006). J Am Vet Med Assoc 2010 Jan 1;236(1):88-94.

Fux CA, Costerton JW, Stewart PS, Stoodley P. Survival strategies of infectious biofilms. Trends Microbiol 2005 Jan;13(1):34-40.

Garcia Vescovi E, Soncini FC, Groisman EA. Mg^{2+} as an extracellular signal: environmental regulation of *Salmonella* virulence. Cell 1996 Jan 12;84(1):165-74.

Gosheger G, Hardes J, Ahrens H, Streitburger A, Buerger H, Erren M, *et al.* Silver-coated megaendoprostheses in a rabbit model--an analysis of the infection rate and toxicological side effects. Biomaterials 2004 Nov;25(24):5547-56.

Gu X, Zheng Y, Cheng Y, Zhong S, Xi T. *In vitro* corrosion and biocompatibility of binary magnesium alloys. Biomaterials 2009 Feb;30(4):484-98.

Hanzi AC, Gunde P, Schinhammer M, Uggowitzer PJ. On the biodegradation performance of an Mg–Y–RE alloy with various surface conditions in simulated body fluid Acta Biomaterialia 2009;5:162-71.

Harris LG, Richards RG. *Staphylococcus aureus* adhesion to different treated titanium surfaces. J Mater Sci Mater Med 2004 Apr;15(4):311-4.

Heublein B, Rohde R, Kaese V, Niemeyer M, Hartung W, Haverich A. Biocorrosion of magnesium alloys: a new principle in cardiovascular implant technology? Heart 2003 Jun;89(6):651-6.

Hienz SA, Sakamoto H, Flock JI, et al. Development and characterization of a new model of hematogenous osteomyelitis in the rat. J Infect Dis 1995;171:1230–1236.

Ho D, Lynch RJ, Ranney DN, Magar A, Kubus J, Englesbe MJ. Financial impact of surgical site infection after kidney transplantation: implications for quality improvement initiative design. J Am Coll Surg 2010 Jul;211(1):99-104.

Hu S, Chang J, Liu M, Ning C. Study on antibacterial effect of 45S5 Bioglass. J Mater Sci Mater Med 2009 Jan;20(1):281-6.

Huang L, Li DQ, Lin YJ, Wei M, Evans DG, Duan X. Controllable preparation of Nano-MgO and investigation of its bactericidal properties. J Inorg Biochem 2005 May;99(5):986-93.

Isiklar ZU, Darouiche RO, Landon GC, Beck T. Efficacy of antibiotics alone for orthopaedic device related infections. Clin Orthop Relat Res 1996 Nov;(332)(332):184-9.

Jain J, Arora S, Rajwade JM, Omray P, Khandelwal S, Paknikar KM. Silver nanoparticles in therapeutics: development of an antimicrobial gel formulation for topical use. Mol Pharm 2009 Sep-Oct;6(5):1388-401.

Johansen C, Falholt P, Gram L. Enzymatic removal and disinfection of bacterial biofilms. Appl Environ Microbiol 1997 Sep;63(9):3724-8.

Johannsen SA, Griffith RW, Wesley IV, Scanes CG. *Salmonella enterica* serovar *typhimurium* colonization of the crop in the domestic turkey: influence of probiotic and prebiotic treatment (*Lactobacillus acidophilus* and lactose). Avian Dis 2004 Apr-Jun;48(2):279-86.

Jones D. Thermodynamics and Electrode Potential. In: Principles and prevention of corrosion. Second ed. Upper Sadle River, NJ: Prentice Hall; 1996. p.40-74.

Jones D. Galvanic and concentration cell corrosion. In: Principles and prevention of corrosion. Second ed. Upper Sadle River, NJ: Prentice Hall; 1996. p.168-98.

Jones N, Ray B, Ranjit KT, Manna AC. Antibacterial activity of ZnO nanoparticle suspensions on a broad spectrum of microorganisms. FEMS Microbiol Lett 2008 Feb;279(1):71-6.

Krysko DV, Vanden Berghe T, D'Herde K, Vandenabeele P. Apoptosis and necrosis: detection, discrimination and phagocytosis. Methods 2008 Mar;44(3):205-21.

Kurtz S, Ong K, Lau E, Mowat F, Halpern M. Projections of primary and revision hip and knee arthroplasty in the United States from 2005 to 2030. J Bone Joint Surg Am 2007 Apr;89(4):780-5.

Kurtz SM, Ong KL, Schmier J, Mowat F, Saleh K, Dybvik E, *et al.* Future clinical and economic impact of revision total hip and knee arthroplasty. J Bone Joint Surg Am 2007 Oct;89 Suppl 3:144-51.

Lellouche J, Kahana E, Elias S, Gedanken A, Banin E. Antibiofilm activity of nanosized magnesium fluoride. Biomaterials 2009 Oct;30(30):5969-78.

Li L, Gao J, Wand Y. Evaluation of cyto-toxicity and corrosion behavior of alkali-heat-treated magnesium in simulated body fluid. Surf Coat Technol 2004;185(1):92-8.

Li Y, Danmark S, Edlund U, Finne-Wistrand A, He X, Norgard M, et al. Resveratrol-conjugated poly-epsilon-caprolactone facilitates *in vitro* mineralization and *in vivo* bone regeneration. Acta Biomater 2011 Feb;7(2):751-8.

Li Z, Gu X, Lou S, Zheng Y. The development of binary Mg-Ca alloys for use as biodegradable materials within bone. Biomaterials 2008 Apr;29(10):1329-44.

Lodish H, Berk A, Kaiser CA, Krieger M, Scott MP, Bretscher A, et al. Transmembrane Transport of Ions and Small Molecules. In: Molecular Cell Biology. Sixth ed. New York, NY: W. H. Freeman and Company; 2008. p.437-76.

Lucas E, Decker S, Khaleel A, Seitz A, Fultz S, Ponce A, *et al.* Nanocrystalline metal oxides as unique chemical reagents/sorbents. Chemistry 2001 Jun 18;7(12):2505-10.

Lucke M, Schmidmaier G, Sadoni S, Wildemann B, Schiller R, Haas NP, et al. Gentamicin coating of metallic implants reduces implant-related osteomyelitis in rats. Bone 2003 May;32(5):521-31.

Lucke M, Schmidmaier G, Sadoni S, Wildemann B, Schiller R, Stemberger A, et al. A new model of implant-related osteomyelitis in rats. J Biomed Mater Res B Appl Biomater 2003 Oct 15;67(1):593-602.

Lusk JE, Williams RJP, Kennedy EP. Magnesium and the Growth of *Escherichia coli*. J Biol Chem 1968 May 25;243(10):2618-24.

Makar GL, Kruger J. Corrosion of magnesium. Int Mat Rev 1993;38(3):138-53.

Mann CK, Yoe JH. Spectrophotometric determination of magnesium with sodium-1-azo-2-hydroxy-3-(2,4-dimethylcarboxanilido)-naphthalene-10 -(2- hydroxybenzene-5-sulfonate). Anal Chem 1956;28:202–5.

McPherson JC, Runner RR, Shapiro B, et al. An acute osteomyelitis model in traumatized rat tibiae involving sand as a foreign body, thermal injury, and bimicrobial contamination. Comp Med 2008;58:369–374.

Monzon M, Garcia-Alvarez F, Lacleriga A, Amorena B. Evaluation of four experimental osteomyelitis infection models by using precolonized implants and bacterial suspensions. Acta Orthop Scand 2002 Jan;73(1):11-9.

Morrissy RT, Haynes DW. Acute hematogenous osteomyelitis: a model with trauma as an etiology. J Pediatr Orthop 1989;9:447–456.

Mosmann T. Rapid colorimetric assay for cellular growth and survival: application to proliferation and cytotoxicity assays. J Immunol Methods 1983 Dec 16;65(1-2):55-63.

Mousain-Bosc M, Roche M, Polge A, Pradal-Prat D, Rapin J, Bali JP. Improvement of neurobehavioral disorders in children supplemented with magnesium-vitamin B6. I. Attention deficit hyperactivity disorders. Magnes Res 2006 Mar;19(1):46-52.

Mousain-Bosc M, Roche M, Polge A, Pradal-Prat D, Rapin J, Bali JP. Improvement of neurobehavioral disorders in children supplemented with magnesium-vitamin B6. II. Pervasive developmental disorder-autism. Magnes Res 2006 Mar;19(1):53-62.

Murray CK, Roop SA, Hospenthal DR, Dooley DP, Wenner K, Hammock J, *et al.* Bacteriology of war wounds at the time of injury. Mil Med 2006 Sep;171(9):826-9.

Nablo BJ, Rothrock AR, Schoenfisch MH. Nitric oxide-releasing sol-gels as antibacterial coatings for orthopedic implants. Biomaterials 2005 Mar;26(8):917-24.

Nablo BJ, Prichard HL, Butler RD, Klitzman B, Schoenfisch MH. Inhibition of implant-associated infections via nitric oxide release. Biomaterials 2005 Dec;26(34):6984-90.

Nalbandian RM, Henry RL, Wilks HS. Artificial skin. II. Pluronic F-127 Silver nitrate or silver lactate gel in the treatment of thermal burns. J Biomed Mater Res 1972 Nov;6(6):583-90.

Neel EA, Ahmed I, Pratten J, Nazhat SN, Knowles JC. Characterisation of antibacterial copper releasing degradable phosphate glass fibres. Biomaterials 2005 May;26(15):2247-54.

Nelson DL, Kennedy EP. Transport of magnesium by a repressible and a nonrepressible system in *Escherichia coli.* Proc Natl Acad Sci U S A 1972 May;69(5):1091-3.

Niehaus AJ, Anderson DE, Samii VF, Weisbrode SE, Johnson JK, Noon MS, et al. Effects of orthopedic implants with a polycaprolactone polymer coating containing bone morphogenetic protein-2 on osseointegration in bones of sheep. Am J Vet Res 2009 Nov;70(11):1416-25.

Niemela SM, Ikaheimo I, Koskela M, Veiranto M, Suokas E, Tormala P, *et al.* Ciprofloxacin-releasing bioabsorbable polymer is superior to titanium in preventing *Staphylococcus epidermidis* attachment and biofilm formation *in vitro*. J Biomed Mater Res B Appl Biomater 2006 Jan;76(1):8-14.

Northup SJ. Cytotoxicity tests of plastics and elastomers. Pharmacopeial Forum 1987;13:2939-42.

Oh SH, Kim JK, Song KS, Noh SM, Ghil SH, Yuk SH, *et al.* Prevention of postsurgical tissue adhesion by anti-inflammatory drug-loaded pluronic mixtures with sol-gel transition behavior. J Biomed Mater Res A 2005 Mar 1;72(3):306-16.

Pacchiana PD, Morris E, Gillings SL, Jessen CR, Lipowitz AJ. Surgical and postoperative complications associated with tibial plateau leveling osteotomy in dogs with cranial cruciate ligament rupture: 397 cases (1998-2001). J Am Vet Med Assoc 2003 Jan 15;222(2):184-93.

Petrini P, Arciola CR, Pezzali I, Bozzini S, Montanaro L, Tanzi MC, *et al.* Antibacterial activity of zinc modified titanium oxide surface. Int J Artif Organs 2006 Apr;29(4):434-42.

Pietak A, Mahoney P, Dias GJ, Staiger MP. Bone-like matrix formation on magnesium and magnesium alloys. J Mater Sci Mater Med 2008 Jan;19(1):407-15.

Poultsides LA, Papatheodorou LK, Karachalios TS, Khaldi L, Maniatis A, Petinaki E, et al. Novel model for studying hematogenous infection in an experimental setting of implant-related infection by a community-acquired methicillin-resistant *S. aureus* Strain. J Orthop Res 2008 Apr 18.

Priddy NH,2nd, Tomlinson JL, Dodam JR, Hornbostel JE. Complications with and owner assessment of the outcome of tibial plateau leveling osteotomy for treatment of cranial cruciate ligament rupture in dogs: 193 cases (1997-2001). J Am Vet Med Assoc 2003 Jun 15;222(12):1726-32.

Poon VK, Burd A. *In vitro* cytotoxity of silver: implication for clinical wound care. Burns 2004 Mar;30(2):140-7.

Qiu Y, Zhang N, An YH, Wen X. Biomaterial strategies to reduce implant-associated infections. Int J Artif Organs 2007 Sep;30(9):828-41.

Rai M, Yadav A, Gade A. Silver nanoparticles as a new generation of antimicrobials. Biotechnol Adv 2009 Jan-Feb;27(1):76-83.

Ramsey F, Schafer DF. The Statistical Sleuth: A Course in Methods of Data Analysis. 2nd ed. Florence, KY: Cengage Learning; 2002.

Reading NC, Sperandio V. Quorum sensing: the many languages of bacteria. FEMS Microbiol Lett 2006 Jan;254(1):1-11.

Robinson DA, Griffith RW, Shechtman D, Evans RB, Conzemius MG. *In vitro* antibacterial properties of magnesium metal against *Escherichia coli, Pseudomonas aeruginosa* and *Staphylococcus aureus*. Acta Biomater 2010 Oct 7;6(5):1869-77.

Robinson DA, Bechtold JE, Carlson CS, Evans RB, Conzemius MG. Development of a fracture osteomyelitis model in the rat femur. J Orthop Res 2011 Jan;29(1):131-7.

Romani AM, Maguire ME. Hormonal regulation of Mg^{2+} transport and homeostasis in eukaryotic cells. Biometals 2002 Sep;15(3):271-83.

Rossier P, van Erven S, Wade DT. The effect of magnesium oral therapy on spasticity in a patient with multiple sclerosis. Eur J Neurol 2000 Nov;7(6):741-4.

Ryan TJ. Infection following soft tissue injury: its role in wound healing. Curr Opin Infect Dis 2007 Apr;20(2):124-8.

Sarasam AR, Krishnaswamy RK, Madihally SV. Blending chitosan with polycaprolactone: effects on physicochemical and antibacterial properties. Biomacromolecules 2006 Apr;7(4):1131-8.

Saris NL, Mervaala E, Karppanen H, Khawaja JA, Lewenstam A. Magnesium: An update on physiological, clinical and analytical aspects. Clinica Chimica Acta 2000/4;294(1-2):1-26.

Sawai J, Kojima H, Igarashi H, Hashimoto A, Shoji S, Sawaki T, *et al.* Antibacterial characteristics of magnesium oxide powder. World Journal of Microbiology and Biotechnology 2000 03/01;16(2):187-94.

Schierholz JM, Lucas LJ, Rump A, Pulverer G. Efficacy of silver-coated medical devices. J Hosp Infect 1998 Dec;40(4):257-62.

Schildhauer TA, Robie B, Muhr G, Koller M. Bacterial adherence to tantalum versus commonly used orthopedic metallic implant materials. J Orthop Trauma 2006 Jul;20(7):476-84.

Schmolka IR. Artificial skin. I. Preparation and properties of pluronic F-127 gels for treatment of burns. J Biomed Mater Res 1972 Nov;6(6):571-82.

Scott III RD. The Direct medical costs of Healthcare-Associated Infections in US Hospitals and the Benefits of Prevention. 2009 (http://www.cdc.gov/ncidod/dhqp/pdf/Scott_CostPaper.pdf).

Shakeri S, Kermanshahi RK, Moghaddam MM, Emtiazi G. Assessment of biofilm cell removal and killing and biocide efficacy using the microtiter plate test. Biofouling 2007;23(1-2):79-86.

Sheng J, Nguyen PT, Marquis RE. Multi-target antimicrobial actions of zinc against oral anaerobes. Arch Oral Biol 2005 Aug;50(8):747-57.

Shimao M. Biodegradation of plastics. Curr Opin Biotechnol 2001 Jun;12(3):242-7.

Silver S, Phung le T, Silver G. Silver as biocides in burn and wound dressings and bacterial resistance to silver compounds. J Ind Microbiol Biotechnol 2006 Jul;33(7):627-34.

Sinha VR, Khosla L. Bioabsorbable polymers for implantable therapeutic systems. Drug Dev Ind Pharm 1998 Dec;24(12):1129-38.

Sinha VR, Bansal K, Kaushik R, Kumria R, Trehan A. Poly-epsilon-caprolactone microspheres and nanospheres: an overview. Int J Pharm 2004 Jun 18;278(1):1-23.

Skott M, Andreassen TT, Ulrich-Vinther M, Chen X, Keyler DE, LeSage MG, et al. Tobacco extract but not nicotine impairs the mechanical strength of fracture healing in rats. J Orthop Res 2006 Jul;24(7):1472-9.

Sparling KW, Ryckman FC, Schoettker PJ, Byczkowski TL, Helpling A, Mandel K, *et al.* Financial impact of failing to prevent surgical site infections. Qual Manag Health Care 2007 Jul-Sep;16(3):219-25.

Smith AW. Biofilms and antibiotic therapy: is there a role for combating bacterial resistance by the use of novel drug delivery systems? Adv Drug Deliv Rev 2005 Jul 29;57(10):1539-50.

Song G, Song S. A possible biodegradable magnesium implant material. Advanced Engineering Materials 2007;9(4):298-302.

Staiger MP, Pietak AM, Huadmai J, Dias G. Magnesium and its alloys as orthopedic biomaterials: a review. Biomaterials 2006 Mar;27(9):1728-34.

Stauffer KD, Tuttle TA, Elkins AD, Wehrenberg AP, Character BJ. Complications associated with 696 tibial plateau leveling osteotomies (2001-2003). J Am Anim Hosp Assoc 2006 Jan-Feb;42(1):44-50.

Stoimenov PK, Klinger RL, Marchin GL, Klabunde KJ. Metal oxide nanoparticles as bactericidal agents. Langmuir 2002 08/01;18(17):6679-86.

Stoodley P, Kathju S, Hu FZ, Erdos G, Levenson JE, Mehta N, et al. Molecular and imaging techniques for bacterial biofilms in joint arthroplasty infections. Clin Orthop Relat Res 2005 Aug;(437)(437):31-40.

Stoor P, Soderling E, Salonen JI. Antibacterial effects of a bioactive glass paste on oral microorganisms. Acta Odontol Scand 1998 Jun;56(3):161-5.

Tiller JC, Liao CJ, Lewis K, Klibanov AM. Designing surfaces that kill bacteria on contact. Proc Natl Acad Sci U S A 2001 May 22;98(11):5981-5.

Tsioutis C, Kritsotakis EI, Maraki S, Gikas A. Infections by pandrug-resistant gram-negative bacteria: clinical profile, therapeutic management, and outcome in a series of 21 patients. Eur J Clin Microbiol Infect Dis 2010 Mar;29(3):301-5.

Ueberrueck T, Zippel R, Tautenhahn J, Gastinger I, Lippert H, Wahlers T. Vascular graft infections: *in vitro* and *in vivo* investigations of a new vascular graft with long-term protection. J Biomed Mater Res B Appl Biomater 2005 Jul;74(1):601-7.

van de Belt H, Neut D, Schenk W, van Horn JR, van der Mei HC, Busscher HJ. Gentamicin release from polymethylmethacrylate bone cements and *Staphylococcus aureus* biofilm formation. Acta Orthop Scand 2000 Dec;71(6):625-9.

van de Belt H, Neut D, Schenk W, van Horn JR, van Der Mei HC, Busscher HJ. *Staphylococcus aureus* biofilm formation on different gentamicin-loaded polymethylmethacrylate bone cements. Biomaterials 2001 Jun;22(12):1607-11.

Vasseur PB, Levy J, Dowd E, Eliot J. Surgical wound infection rates in dogs and cats. Data from a teaching hospital. Vet Surg 1988 Mar-Apr;17(2):60-4.

von Eiff C, Arciola CR, Montanaro L, Becker K, Campoccia D. Emerging *Staphylococcus* species as new pathogens in implant infections. Int J Artif Organs 2006 Apr;29(4):360-7.

Waksman R, Pakala R, Kuchulakanti PK, Baffour R, Hellinga D, Seabron R, et al. Safety and efficacy of bioabsorbable magnesium alloy stents in porcine coronary arteries. Catheter Cardiovasc Interv 2006 Oct;68(4):607,17; discussion 618-9.

Weese JS. A review of post-operative infections in veterinary orthopaedic surgery. Vet Comp Orthop Traumatol 2008;21(2):99-105.

White D. Membrane Bioenergetics: The Proton Potential. In: The Physiology and Biochemistry of Prokaryotes. 3rd ed. New York: Oxford University Press; 2007. p.83-119.

White RJ, Cutting K, Kingsley A. Topical antimicrobials in the control of wound bioburden. Ostomy Wound Manage 2006 Aug;52(8):26-58.

Witte F, Kaese V, Haferkamp H, Switzer E, Meyer-Lindenberg A, Wirth CJ, et al. *In vivo* corrosion of four magnesium alloys and the associated bone response. Biomaterials 2005 Jun;26(17):3557-63.

Witte F, Fischer J, Nellesen J, Crostack HA, Kaese V, Pisch A, et al. *In vitro* and *in vivo* corrosion measurements of magnesium alloys. Biomaterials 2006 Mar;27(7):1013-8.

Wong HM, Yeung KW, Lam KO, Tam V, Chu PK, Luk KD, et al. A biodegradable polymer-based coating to control the performance of magnesium alloy orthopaedic implants. Biomaterials 2010 Mar;31(8):2084-96.

Woodruff MA, Hutmacher DW. The return of a forgotten polymer- ε-Polycaprolactone in the 21st century. Progress in Polymer Science 2010 10;35(10):1217-56.

Yates AA, Schlicker SA, Suitor CW. Dietary Reference Intakes: the new basis for recommendations for calcium and related nutrients, B vitamins, and choline. J Am Diet Assoc 1998 Jun;98(6):699-706.

Yun HC, Murray CK, Roop SA, Hospenthal DR, Gourdine E, Dooley DP. Bacteria recovered from patients admitted to a deployed U.S. military hospital in Baghdad, Iraq. Mil Med 2006 Sep;171(9):821-5.

Zhang E, Xu L, Yu G, Pan F, Yang K. *In vivo* evaluation of biodegradable magnesium alloy bone implant in the first 6 months implantation. J Biomed Mater Res A 2008 Jul 10.

Zips A, Schaule G, Flemming HC. Ultrasound as a means of detaching biofilms. Biofouling 1990;2:323-33.

Zmantar T, Kouidhi B, Miladi H, Mahdouani K, Bakhrouf A. A microtiter plate assay for *Staphylococcus aureus* biofilm quantification at various pH levels and hydrogen peroxide supplementation. New Microbiol 2010 Apr;33(2):137-45.